

Article

Perception, Planning, Control, and Coordination for Autonomous Vehicles

Scott Drew Pendleton ^{1*}, Hans Andersen ¹, Xinxin Du ², Xiaotong Shen ², Malika Meghjani ², You Hong Eng ², Daniela Rus ³, and Marcelo H. Ang Jr. ¹

¹ Department of Mechanical Engineering, National University of Singapore; {scott.pendleton01, hans.andersen}@u.nus.edu, mpeangh@nus.edu.sg

² Singapore-MIT Alliance for Research and Technology; {xinxin, xiaotong, malika, youhong}@smart.mit.edu

³ Massachusetts Institute of Technology; rus@csail.mit.edu

* Correspondence: scott.pendleton01@u.nus.edu

Academic Editor: name

Version February 2, 2017 submitted to *Machines*; Typeset by L^AT_EX using class file mdpi.cls

Abstract: Autonomous vehicles are expected to play a key role in the future of urban transportation system, as they offer potential for additional safety, increased productivity, greater accessibility, better road efficiency, and positive impact to the environment. Research in autonomous systems has seen dramatic advances in recent years, due to the increases in available computing power and reduced cost in sensing and computing technologies, resulting in maturing technological readiness level of fully autonomous vehicles. The objective of this paper is to provide a general overview of the recent developments in the realm of autonomous vehicle software systems. Fundamental components of autonomous vehicle software are reviewed, and recent developments in each area are discussed.

Keywords: Autonomous Vehicles; Localization; Perception; Planning; Automotive Control; Multi-Vehicle Cooperation

1. Introduction

Autonomous Vehicles (AVs) are widely anticipated to alleviate road congestion through higher throughput, improve road safety by eliminating human error, and free drivers from the burden of driving, allowing greater productivity and/or time for rest, along with myriad other foreseen benefits. The past three decades have seen steadily increasing research efforts in developing self-driving vehicle technology, in part fueled by advances in sensing and computing technologies which have resulted in reduced size and price of necessary hardware. Furthermore, the perceived societal benefits continue to grow in scale along with the rapid global increase of vehicle ownership. As of 2010, the number of vehicles in use in the world was estimated to be 1.015 billion [1], while the world population was estimated to be 6.916 billion [2]. This translates to one vehicle for every seven persons. The societal cost of traffic crashes in the United States was approximately 300 billion USD in 2009 [3]. The financial cost of congestion is continually increasing each year, with the cost estimate for United States reaching as high as 160 billion USD in 2014 [4]. The associated health cost of congestions in United States was estimated to be over 20 billion USD in 2010 from premature deaths resulting from pollution inhalation [5]. While it is uncertain just how much these ongoing costs can be reduced through autonomous vehicle deployment, attempting to curtail the massive scale of these numbers serves as great motivation for the research.

A future with self-driving cars was first envisioned as early as 1918 [6], with the idea even broadcasted over television as early as 1958 [7]. By 1988, Carnegie Mellon's NAVLAB vehicle

31 was being demonstrated to perform lane-following using camera images [8]. Development was
32 accelerated when several research teams later developed more advanced driverless vehicles to
33 traverse desert terrain in the 2004 and 2005 DARPA Grand Challenges [9], and then urban roads in
34 the 2007 DARPA Urban Challenge (DUC) [10]. Research related to self-driving has since continued at
35 a fast pace in academic settings, but furthermore is now receiving considerable attention in industry
36 as well.

37 As research in the field of autonomous vehicles has matured, a wide variety of impressive
38 demonstrations have been made on full-scale vehicle platforms. Recent studies have also
39 been conducted to model and anticipate the social impact of implementing autonomous
40 Mobility-on-Demand (MoD) [11]. The case studies have shown that MoD system would make access
41 to mobility more affordable and convenient compared to traditional mobility system characterized
42 by extensive private vehicle ownership.

43 Autonomous driving on urban roads has seen tremendous progress in recent years, with several
44 commercial entities pushing the bounds alongside academia. Google has perhaps the most experience
45 in the area, having tested its fleet of autonomous vehicles for more than 2 million miles, with
46 expectation to soon launch a pilot MoD service project using 100 self-driving vehicles [12]. Tesla
47 is early to market their work, having already provided an autopilot feature in their 2016 Model S
48 cars [13]. Uber's mobility service has grown to upset the taxi markets in numerous cities worldwide,
49 and has furthermore recently indicated plans to eventually replace all their human driven fleet with
50 self-driving cars [14], with their first self-driving vehicle pilot program already underway [15].

51 There are several places where automated road shuttles are in commercial operations. Examples
52 include deployments at Rivium Business Park, Masdar City, and Heathrow Airport [16,17]. The
53 common feature of these operations is that road vehicles are certified as a rail system meaning
54 that vehicles operate in a segregated space [17]. This approach has been necessary due to legal
55 uncertainty around liability in the event of an accident involving an autonomous vehicle. To address
56 this, governments around the world are reviewing and implementing new laws. Part of this process
57 has involved extended public trials of automated shuttles, with CityMobil and CityMobil2 being
58 among the largest of such projects [17].

59 While the majority of the research contributions discussed in the remaining sections of this
60 article are from academic institutions, it is worth noting that the industrial market interest is also
61 largely responsible for research investigations into certification and validations processes, especially
62 in regards to autonomous car manufacturability and services [18,19]. These topics are however left
63 out of the scope of this survey paper.

64 Driving in urban environments has been of great interest to researchers due in part to the high
65 density of vehicles and various area-specific traffic rules that must be obeyed. The DARPA Urban
66 Challenge[20], and more recently the V-Charge Project [21] catalyzed the launch of research efforts
67 into autonomous driving on urban road for numerous organizations. Referring to Fig.1, the problem
68 of urban driving is both interesting and difficult because it pushes the research direction to address
69 both increased operating speeds of autonomous vehicles as well increased environmental complexity.

70 The core competencies of an autonomous vehicle software system can be broadly categorized
71 into three categories, namely *perception*, *planning*, and *control*, with the interactions between these
72 competencies and the vehicle's interactions with the environment depicted in Fig. 2. Also,
73 Vehicle-to-Vehicle (V2V) communications can be leveraged to achieve further improvements in areas
74 of perception and/or planning through *vehicle cooperation*.

75 Perception refers to the ability of an autonomous system to collect information and extract
76 relevant knowledge from the environment. *Environmental perception* refers to developing a contextual
77 understanding of environment, such as where obstacles are located, detection of road signs/markings,
78 and categorizing data by their semantic meaning. *Localization* refers to the ability of the robot to
79 determine its position with respect to the environment.

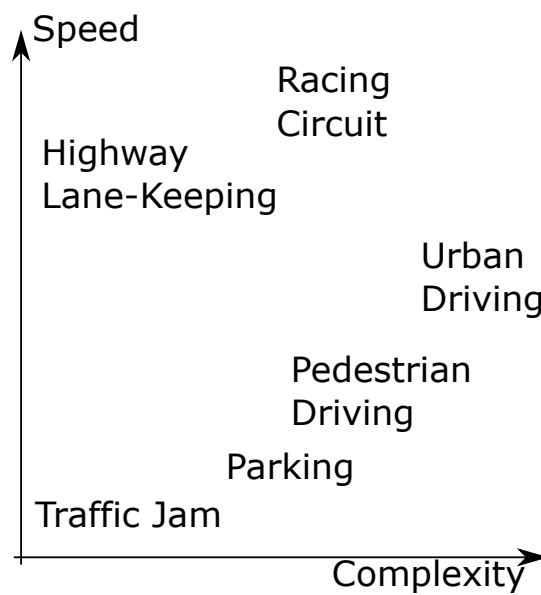


Figure 1. Complexity and operating velocity for various driving scenarios

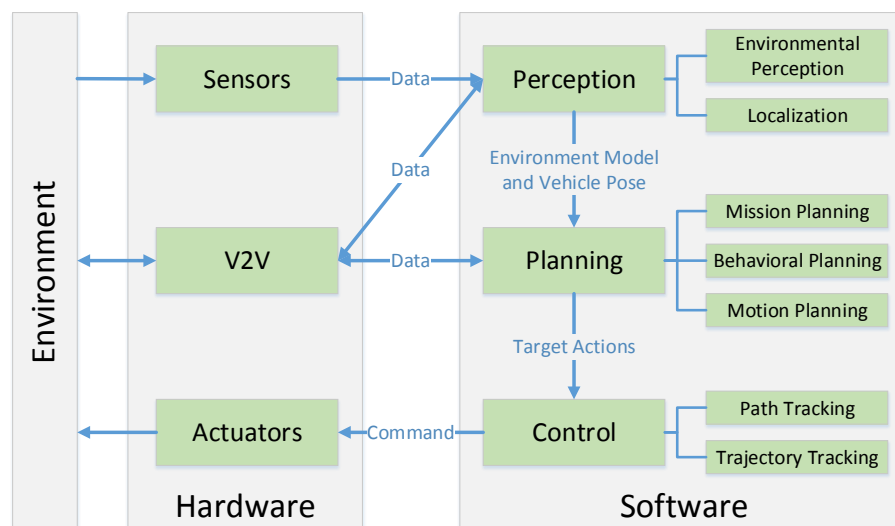


Figure 2. A typical autonomous vehicle system overview, highlighting core competencies

80 Planning refers to the process of making purposeful decisions in order to achieve the robot's
 81 higher order goals, typically to bring the vehicle from a start location to a goal location while avoiding
 82 obstacles and optimizing over designed heuristics.

83 Finally, the control competency, refers to the robot's ability to execute the planned actions that
 84 have been generated by the higher level processes.

85 The main objective of this paper is to provide a general overview of the recent developments
 86 in the realms of autonomous vehicle software system. However, as there has been a massive
 87 surge in research interest in the field of autonomous system in recent years, this paper is by no
 88 means a complete survey of the currently available hardware and software systems in the literature.
 89 The remainder of this paper is organized as follows: In Section 2, the topics of environmental
 90 perception and localization are discussed. Section 2.1 focuses on recent advances in LIDAR and
 91 camera based signal processing techniques in particular. Section 2.2 reviews the methods of localizing

92 the vehicle with respect to its environment, especially with map-based localization techniques.
93 Autonomous vehicle decision making processes are reviewed in Section 3, with greater emphasis in
94 the areas of behavioral and motion planning,. Section 4 discusses the theoretical design and practical
95 implementation of autonomous vehicle control systems. Recent advances in the field of multi-vehicle
96 cooperation will be reviewed in Section 5, and finally Section 6 concludes the paper.

97 2. Perception

98 2.1. Environmental Perception

99 Environment perception is a fundamental function to enable autonomous vehicles, which
100 provides the vehicle with crucial information on the driving environment, including the free drivable
101 areas and surrounding obstacles' locations, velocities, and even predictions of their future states.
102 Based on the sensors implemented, the environment perception task can be tackled by using LIDARs,
103 cameras, or a fusion between these two kinds of devices. Some other traditional approaches may also
104 involve the use of short/long-range radars and ultrasonic sensors, which will not be covered in this
105 paper. Regardless of the sensors being implemented, two critical elements of the perception task are
106 (i) road surface extraction and (ii) on-road object detection.

107 2.1.1. LIDAR

108 LIDAR refers to a light detection and ranging device, which sends millions of light pulses
109 per second in a well-designed pattern. With its rotating axis, it is able to create a dynamic,
110 three-dimensional map of the environment. LIDAR is the heart for object detection for most of the
111 existing autonomous vehicles. Fig.3 shows the ideal detection results from a 3D LIDAR, with all the
moving objects being identified.



Figure 3. The ideal detection result from a 3D LIDAR with all moving objects detected [22]

112 In a real scene, the points returned by the LIDAR are never perfect. The difficulties in handling
113 LIDAR points lie in scan point sparsity, missing points, and unorganized patterns. The surrounding
114 environment also adds more challenges to the perception as the surfaces may be arbitrary and erratic.
115 Sometimes it is even difficult for human beings to perceive useful information from a visualization of
116 the scan points.
117

118 2.1.1.1. Representation

119 The output from the LIDAR is the sparse 3D points reflected back from the objects, with
120 each point representing an object's surface location in 3D with respect to the LIDAR. Three main
121 representations of the points are commonly used, including point clouds, features, and grids [23].

122 Point cloud based approaches directly use the raw sensor data for further processing. This
123 approach provides a finer representation of the environment, but at the expense of increased
124 processing time and reduced memory efficiency. To mitigate this, usually a voxel-based filtering
125 mechanism is applied to the raw point cloud to reduce the number of points, e.g.[24] [25].

126 Feature based approaches first extract parametric features out of the point cloud and represent
127 the environment using the extracted features. The features that are commonly used include lines
128 [26] and surfaces [27]. This approach is the most memory-efficient, but it is often too abstract,
129 and its accuracy is subject to the nature of the point cloud, as not all environment features can be
130 approximated well by aforementioned set of feature types.

131 Grid based approaches discretize the space into small grids, each of which is filled with
132 information from the point cloud such that a point neighborhood is established [28]. As pointed
133 out in [23], this approach is memory-efficient and has no dependency on predefined features. But it is
134 not straightforward to determine the size of the discretization. In [29], an adaptive octree was created
135 to guide the segmentation from coarse grids to fine ones.

136 2.1.1.2. Segmentation algorithms

137 To perceive the 3D point cloud information, normally two steps are involved: segmentation
138 and classification. Some may include a third step, time integration, to improve the accuracy
139 and consistency. Segmentation of point cloud is the process of clustering points into multiple
140 homogeneous groups, while classification is to identify the class of the segmented clusters, e.g. bike,
141 car, pedestrian, road surface, etc.

142 As summarized in the survey paper [30], the algorithms for 3D point cloud segmentation can
143 be divided into five categories: edge based, region based, attributes based, model based, and graph
144 based. In this section, we will provide supplementary reviews to reveal the recent development in
145 this field. As a result, a new category is identified, which is based on deep learning algorithms.

146 Edge based methods are mainly used for particular tasks in which the object must have strong
147 artificial edge features, like road curb detection [31] [32]. But it is not a useful approach for nature
148 scene detection and is susceptible to noise. To improve the robustness, in [33], the elevation gradients
149 of principal points are computed, and a gradient filter is applied to filter out points with fluctuations.

150 Region based methods make use of region growing mechanisms to cluster neighborhood points
151 based on certain criteria, e.g. Euclidean distance [34][35] or surface normals [36]. In most cases,
152 the process starts with generating some seed points and then growing regions from those points
153 according to a predefined criteria. As compared against the edge based method, this approach
154 is more general and practical. It also avoids the local view problem as it takes neighborhood
155 information into account. In [37], a scan-line based algorithm was proposed to identify the local
156 lowest points, and those points were taken as the seeds to grow into ground segments based on
157 slope and elevation. A feature based on the normal vector and flatness of a point neighborhood was
158 developed in [38] to grow the regions in trees and non-planar areas. To make the growing process
159 more robust, a self-adaptive Euclidean clustering algorithm was proposed in [34]. In [39], a new
160 attribute "unevenness," which was derived based on the difference between the ranges of successive
161 scanning rings from each laser beam, was proposed as the growing criteria. As claimed in [40], [41],
162 and [42], it was more capable of detecting small obstacles and less sensitive to the presence of ground
163 slopes, vehicle pitch, and roll.

164 In the literature, some researchers also looked into how to effectively generate the seed points
165 by taking more heuristics into account so that they can lead to a more effective and robust region
166 growing process. In [43], Vieira *et al.* first removed points at sharp edges based on curvatures before

167 selecting the seed points, since good seed points are typically found in the interior of a region, rather
168 than at its boundaries. In [44], the normal of each point was first estimated, then the point with
169 the minimum residual was selected as the initial seed point, while in [45], the local plane, instead
170 of normal, at each point was extracted and a corresponding score was computed followed by the
171 selection of seed planes based on the score. A multi-stage seed generation process was proposed in
172 [28]. Non-empty voxels were grouped into segments based on proximity, and these segments served
173 as the seeds for the next segmentation process, which made use of the coherence and proximity of
174 the coplanar points. Finally the neighborhood coplanar point segments are merged based on plane
175 connection and intersection.

176 The region based segmentation methods have been implemented widely in the literature,
177 however as pointed out in [46] [47] [30] [29], the segmentation results depend too heavily on
178 the selection of the seed points. Poorly selected points may result in inadequate and inefficient
179 segmentations, and different choices of seed points usually lead to different segmentations [25].
180 Additionally, all of the region based methods require extensive computation resources, taxing both
181 time and memory [48] [29].

182 Model based methods, also known as parametric methods, first fit the points into predefined
183 models. These models, like plane, sphere, cone, and cylinder, normally can be expressed effectively
184 and compactly in a closed mathematic form. Those inliers to a particular model are clustered as one
185 segment. Most of the model based methods are designed to segment the ground plane. The two
186 most widely implemented model fitting algorithms in the literature are RANSAC (Random sample
187 consensus) and HT (Hough Transform). Therefore, the model based methods share the same pros
188 and cons as these two algorithms.

189 In [49], [50], [24], [32], and [27], the authors implemented the RANSAC algorithm to segment the
190 ground plane in the point cloud with the assumption of flat surface. However, as mentioned in [51]
191 and [23], for non-planar surfaces, such as undulated roads, uphill, downhill, and humps, this model
192 fitting method is not adequate.

193 To mitigate these defects, [52] fitted the plane into quadratic form instead of planar form based
194 on RANSAC. Then a region growing process was designed to refine the quadratic plane. Asvadi
195 *et al.* in [51] divided the space in front of the vehicle into several equal-distant (5m) strips and fit
196 one plane for each strip based on least square fitting. In [23], a piecewise ground surface estimation
197 was proposed, which consist of four steps: slicing, gating, plane fitting, and validation. The slicing
198 step slices the space in front of the vehicle into regions with approximately equal number of LIDAR
199 points, whereas the gating step rejects outliers in each region based on interquartile range method.
200 RANSAC plane fitting is then applied to each sliced region to find all the piecewise planes, and a final
201 validation step is carried out by examining the normal and height differences between consecutive
202 planes.

203 The HT model fitting methods can also be found in the literature to fit different models, e.g.
204 planes, cylinders, and spheres. In [53] and [54], the 3D HT was applied on point level and normal
205 vectors to identify planar structures in the point clouds, whereas in [55], the authors proposed a
206 sequential HT algorithm to detect cylinders in the point cloud. This sequential approach reduced the
207 time and space complexity as compared to the conventional approach which required 5-D Hough
208 space.

209 As elaborated above, the model based methods are well established in the literature for planar
210 surface extraction. Normally, these methods are used as a primary step in segmentation to remove
211 the ground plane, while other methods, e.g. region growing, are then applied to cluster the
212 remaining points. However, the major disadvantage of model based methods is that it does not
213 take neighborhood and context information into account, and thus it may force random points into
214 a particular model. Furthermore, the segmentation is sensitive to the point cloud density, position
215 accuracy, and noise [29].

216 Attribute methods normally take a two-step approach, where the first step is to compute the
217 attribute for each point, and the second step is to cluster the points based on the associated attributes.
218 As mentioned in [30], this set of methods allow for more cues to be incorporated into the formulation
219 on top spatial information. But the success of the segmentation also depends strongly on the derived
220 hidden attributes.

221 Besides those works reviewed in [30], the attribute based algorithm proposed in [56]
222 demonstrated that it was capable of segmenting pole-like objects, which was considered as
223 challenging due to its thin feature. In this algorithm, the optimal neighborhood size of each point
224 was first calculated. The geometric features, taking the neighboring information into account, were
225 derived based on PCA (Principle Component Analysis). Each point was then assigned with three
226 types of attributes (linear, planar, and spherical) using LIBSVM [57] by taking the geometric features
227 as input. Finally, segmentation rules were designed to cluster the points based on their associated
228 attributes.

229 The other group of methods that are widely used in the literature is graph based methods. These
230 methods cast the point cloud into a graph structures with each point as the vertex/node and the
231 connection between neighbor points as graph edges. The graph based method has demonstrated
232 its strength in image semantic segmentation as it is able to incorporate local and global cues,
233 neighborhood information, context, smoothness, and other customized features into its formulation
234 and optimize the segmentation globally across the entire image.

235 Following the graph cut methods in image segmentation, in the content of point cloud, they
236 always follow the form of CRF (Conditional Random Field [58]) or MRF (Markov Random Field),
237 and the optimization is normally through min-max flow cut algorithm or its variations.

238 In [59] and [60], the authors first created a k-nearest neighbors graph, assigned each node
239 according to a background penalty function, added hard foreground constraints, and solved the
240 foreground and background segmentation through min-cut. Moosmann *et al.* [25] used the graph
241 based method to segment ground and objects using a unified and generic criterion based on local
242 convexity measures.

243 As to be shown later, the graph based methods have also been implemented as the pipelines for
244 sensor fusion between LIDAR and vision. Compared to other methods, graph based ones are more
245 robust in dealing with complex scene due to their global features as aforementioned. The major issue
246 with these methods is that it normally takes more time to compute, especially for the optimization
247 part.

248 With the recent development in machine learning algorithms in computer vision, some
249 researchers also looked into how to apply machine learning architectures, which are normally applied
250 to 2D image, into the 3D point cloud for segmentation and detection. A commonly used dataset is
251 proposed in [61], which contains a colored 3D point cloud of several Haussmanian style facades.

252 In [62], the author implemented the Random Forest classifier to classify each point into one
253 semantic class. The classifier was trained based on the light-weight 3D features. Afterwards,
254 individual facades were separated by detecting differences in the semantic structure. To improve
255 the memory efficiency and segmentation accuracy, Riegler *et al.* [63] proposed an Octree Network
256 based on 3D convolution. It exploits the sparsity in the point cloud and focuses memory allocation
257 and computation in order to enable a deeper network without compromising resolution.

258 This set of algorithms is recently developed and thus has some crucial and practical issues which
259 makes it difficult to achieve real time operation. But they do provide new insights into the point cloud
260 segmentation problem. As to be shown in the detection algorithm, they can provide a unified pipeline
261 to combine the segmentation and detection processes.

262 2.1.1.3. Detection algorithm

263 After the segmentation, each cluster needs to be categorized into different objects. The
264 information embedded in each cluster is mainly from spatial relationship and the LIDAR intensity of

265 the points, which has very limited use in object recognition. Thus most of the algorithms will leverage
266 the detection problem on computer vision through some fusion mechanisms as to be shown later. But
267 there does exist some other research works exploring the possibility to perform object recognition
268 from point cloud data.

269 In [25], the authors proposed a primary classifier to recognize ground clusters. For each segment,
270 a histogram over all the surface normal vectors' height values was generated, and if the last bin
271 contained the most votes, that segment was classified as ground. This algorithm is not able to
272 differentiate the objects above the ground.

273 Zhang *et al.* [64] proposed an SVM (Support Vector Machine) based classifier to classify the
274 clusters into ground, vegetation, building, power line, and vehicle. In total 13 features were derived
275 as the input to the SVM classifier. But this classifier is still very coarse, which is not practical enough
276 for the autonomous vehicle applications.

277 The recently developed machine learning algorithms are more general and robust as compared
278 to the aforementioned ones as they are able to recognize more categories of objects. In [65], VoxNet
279 was proposed, which implemented a 3D convolutional neural network to classify the 3D point
280 cloud (in occupancy grid/volumetric representation). While in [66], the volumetric based 3D CNN
281 was improved by introducing auxiliary learning tasks on part of an object and combining data
282 augmentation with multi-orientation pooling. In [67], a 3D Convolutional Deep Belief Network
283 was proposed to learn the distribution of complex 3D shapes across different object categories and
284 arbitrary poses from raw CAD data.

285 However, as mentioned in [63], for 3D networks, the computational and memory requirements
286 increase cubically with the input size of the 3D point cloud. All the aforementioned methods can
287 only operate at the order of 30^3 voxels, which is able to fully exploit the rich and detailed geometry
288 of 3D objects. As reviewed in the segmentation part, the Octree Networks in [63] is a more efficient
289 architecture to handle the 3D point cloud. It has improved the input cluster resolution from the order
290 of 30^3 to 256^3 .

291 2.1.2. Vision

292 The vision system in autonomous vehicle environment perception normally involves road
293 detection and on-road object detection. The road detection also includes two categories: lane line
294 marking detection and road surface detection. In the following sections, we will review the works
295 under each of the categories. At the same time, the recently developed deep learning approaches
296 will be included. For more information on conventional hand-crafted feature/cue based approaches,
297 interested readers may refer to the following survey papers: [68] [69] for lane line marking detection,
298 [70] for road surface detection, [71] [72] for vehicle detection and [73] for pedestrian detection.

299 2.1.2.1. Lane line marking detection

300 Lane line marking detection is to identify the lane line markings on the road and estimate the
301 vehicle pose with respect to the detected lines. This piece of information can be served as the vehicle
302 position feedback to vehicle control systems. A vast amount of research work has been done in this
303 domain since a few decades ago [8]. However, it is yet to be completely solved and has remained as
304 a challenging problem due to the wide range of uncertainties in real traffic road conditions and road
305 singularities [74], which may include shadows from cars and trees, variation of lighting conditions,
306 worn-out lane markings, and other markings such as directional arrows, warning text, and zebra
307 crossings [75].

308 As summarized in the survey paper by Hillel *et al.* in [68], most of the lane line detection
309 algorithms share three common steps: 1) lane line feature extraction, by edge detection [76] [77]
310 and color [78] [79], by learning algorithms such as SVM [80], or by boost classification [81] [82],
311 2) fitting the pixels into different models, e.g. straight lines [83][84], parabolas [85][86], hyperbolas
312 [87][88][89], and even zigzag line [90], 3) estimating the vehicle pose based on the fitted model. A

313 fourth time integration step may exist before the vehicle pose estimation in order to impose temporal
314 continuity, where the detection result in the current frame is used to guide the next search through
315 filter mechanisms, such as Kalman filter [76] [91] and particle filter [80] [92] [90].

316 Lane line feature extraction is to identify the pixels that belong to lane line markings and
317 eliminate non-lane line marking pixels. Most approaches in the literature are based on the
318 observations that lane markings have large contrast compared to road pavement.

319 Some gradient based algorithms can be commonly found in the literature e.g. Sobel edge detector
320 with symmetrical local threshold [93], adaptive thresholding [91], and gradient-enhancing conversion
321 [94]. But these algorithms are sensitive to noise and can result in a large number of outliers from
322 clutter and shadows. Furthermore, they are limited to local view and ignore the shape feature of lane
323 line markings (long and thin bright structures).

324 Some other more advanced variants based on image gradient have been proposed in the
325 literature, which are less sensitive to noise. For example, the steerable filter ([69][85]) is based on
326 second order derivatives of 2D Gaussians, and ridge detector ([95][96]) is based on tensor field
327 construction of first order derivatives. Both methods are able to obtain the response of gradient
328 directions which facilitates to remove outliers if their directions deviate too much from the presumed
329 lane line direction.

330 Another set of algorithms attempts to detect lane line markings from a different perspective,
331 searching for low-high-low intensity pattern along image rows. The most common algorithm of this
332 type is the box filter (also known as the top-hat filter) or other forms of variants, e.g. [97], [98], [99],
333 and [100]. They are considered as more reliable than the aforementioned algorithms. In brief, they
334 convolute the image with a certain form of step filter and select the high response pixels as the lane
335 line candidates at each image row. Normally, they are capable of extracting the medial axis of lane
336 line markings instead of edges.

337 For this kind of algorithm to work properly, its scale or step width must be tuned accurately
338 according to the lane line marking width in the image, to prevent under/over filtering. Otherwise,
339 the original image has to be transformed through inverse-perspective mapping (IPM) to compensate
340 for the camera perspective effect (e.g. [101] [102]). But this also requires a good estimation of camera
341 pitch angle (or viewing angle). At the same time, interpolation is needed to make up for the missing
342 pixels in the IPM image. As the viewing distance becomes larger, the interpolation becomes more
343 and more inaccurate. To solve this problem, [90] provides an adaptive mechanism to update the step
344 width online based on the previous width measurements.

345 Another shortcoming that is common to the aforementioned lane line extraction algorithms is
346 that they cannot distinguish lane line markings from other on-road markings, such as warning letters,
347 humps and so on. These on-road markings may occasionally result in severe estimation errors.

348 The second step is model fitting. It is the process to extract a compact high-level representation
349 of the lane from the lane line detection results. Depending on the model used, the vehicle pose can
350 be derived from the fitted model as shown in [95] and [88]. The model can also be used to guide the
351 lane line detection in the next frame to improve continuity (e.g. [103] [104] [90]).

352 Various road models have been proposed in the literature. Those reviewed above are parametric
353 models. Another category is semi-parametric, which mainly consists of splines, such as B-Snake
354 [105], Cubic splines [80], active contours [106], etc. The advantage of these models is that they are
355 more flexible and can cover various road shapes. But they are more computationally demanding and
356 complex. They also require a good selection of control points. As concluded in [68], since there is no
357 single model that can cover all kinds of road shapes, online model selection should be considered.

358 The time integration step is to make use of previous information to guide the search in the current
359 image. It imposes smoothness and continuity between consecutive images. It can improve vehicle
360 pose estimation accuracy and prevent erroneous detection failures.

361 Most of the proposed approaches are stochastic. For example, the Kalman filter can be found in
362 [69], [97], and [107], and particle filter is applied in [80], [85], [92], and [104]. As pointed out in [68],

363 the particle filter is more reliable, especially under abrupt changes in between consecutive images
364 induced by vehicle vibrations or non-flat road surfaces.

365 In general, the particle filter can be implemented directly to the image (or pixels), lane line model,
366 and vehicle. For example, in [80], each particle contains the locations of control points in the image
367 for cubic spline fitting. In [92] and [102], each particle represents lane line model parameters. The
368 change of parameters is simply assumed to follow a Gaussian distribution. But they did not mention
369 how the covariance matrix was obtained. In [85], each particle represents the location of the vehicle
370 in real world coordinates, but again the motion of vehicle is simply assumed to be Gaussian. Since
371 the change between consecutive images is purely due to the vehicle motion, [90] provided a more
372 intuitive and straightforward approach which applied the particle filter to the moving vehicle and
373 took its explicit dynamic model into account.

374 The last step in the lane-level localization is to estimate the vehicle lateral position and moving
375 orientation based on the lane line model. To recover this information from 2D image to 3D real world,
376 depth is required. In most approaches, depth is derived from the camera viewing angle or pitch angle
377 by assuming constant camera height and flat road surface. One typical example is the IPM, but it
378 depends strongly on the pitch angle and it is sensitive to pitch angle estimation noise.

379 A more reliable and direct way to recover the depth is through stereo cameras, given that the
380 disparity image can be constructed effectively and accurately. However, as mentioned in [68], the
381 low texture of road surface poses a processing challenge to obtain the disparity image. This is
382 the main reason why stereo is not widely adopted in this research field. In [108], the author used
383 dense mapping to obtain disparity while in [109], Maximum A Posteriori - Markov Random Field
384 (MAP-MRF) approach was applied. But both methods are not very effective and subject to smoothing
385 noise. To mitigate these drawbacks, Du *et al.* [90] proposed a lane line model based correspondence
386 matching algorithm.

387 2.1.2.2. Road surface detection

388 Road surface detection informs the autonomous vehicle on the locations of free space where it
389 can drive without collision. It is the prerequisite for any online path planning and control operations.
390 Generally speaking, the approaches can be divided into three categories: feature/cue based detection,
391 feature/cue based learning, and deep learning.

392 The feature/cue based detection approaches first identify the feature points or patches in the
393 original image based on some predefined features (e.g. HOG). In the context of stereo images,
394 the feature may refer to the disparity. Based on the identified features, either model fitting or
395 segmentation kind of algorithms will be applied to identify the road surfaces.

396 In [110], a general B-spline model fitting algorithm was applied based on the stereo disparity
397 measurement to represent the road surface. This approach dropped the assumption of flat road
398 surface. And a Kalman filter was designed to further smooth the fitting results.

399 Instead of using model fitting, [111] cast the road surface detection problem into a CRF
400 optimization problem. The authors constructed the CRF energy function by taking both object class
401 labeling and dense stereo reconstruction into the formulation and jointly optimized these two tasks,
402 which improved the performance of each individual task.

403 The feature/cue learning based approaches also extract a set of features associated to pixels or
404 image patches and then train a classifier based on the features to assign a road or non-road label to
405 the pixels or patches.

406 In [112], the authors proposed a detection algorithm to learn the contextual information which
407 can facilitate the classification of the targeted image patch. For each image patch, besides itself, it is
408 also associated with another two types of auxiliary image patches: the contextual patches obtained
409 based on a predefined pattern surrounding the target image patch and road patches positioned at the
410 bottom part of the image. Three feature vectors are extracted from these three types of patches and
411 then concatenated into one single final vector. The vector is fed to a MLP (Multilayer Perceptron)

412 neural network to do classification. But this method is not able to take the global information into
413 account and the selection of the road patches is controversial, as it is based on the assumption that
414 the bottom part of the image is always road region.

415 Tobias *et al.* [113] proposed a two-hierarchy detection framework which incorporated the spatial
416 layout of the scene to handle a high variety of complex situations. The first layer consists of three base
417 classifiers for road boundary, road and lane markings. The three classifiers are trained separately to
418 generate three confidence maps. The spatial ray features that incorporate properties of the global
419 environment are generated based on the confidence maps. Finally, a GentleBoost classifier [114] was
420 trained based on the spatial ray features.

421 In both [115] and [116], the classifier, which used a joint boosting algorithm, incorporated the
422 feature maps based on textons (filter-bank, color, HoG and location) and disptons (U-disptons and
423 V-disptons).

424 However, all these aforementioned algorithms under feature detection or feature learning
425 categories are not robust enough under the erratic driving environments. The performances are still
426 subjected to all the noise factors as listed in the lane line marking detection section.

427 As shown in the well-know database KITTI [117], the top five performances for road detection
428 (excluding those non-published entries) all fall under the category of deep learning. As highlighted
429 in [70], the deep learning framework has gained popularity during the past few years, especially with
430 the development of suitable processors and implementations [118].

431 Both [119] and [120] took an image patch as the input to the Convolutional Neural Network
432 (CNN) which classified the center point of the image patch as to whether it was road or not. In [120],
433 the author also demonstrated how to incorporate the spatial information of the patch into the CNN
434 to enable the learning of spatial priors on top of appearances.

435 Different from these two approaches, Mohan [121] proposed a novel architecture that integrated
436 the CNN with deep de-convolutional neural networks. The architecture was also employed for
437 multi-patch training, which made it possible to effectively learn spatial priors from scenes. This
438 approach has yielded the state-of-the-art performance in the KITTI dataset.

439 Despite its excellent performance, the drawbacks of deep learning approaches are also very
440 obvious: huge computation and memory requirement, long process time, non-traceable, and tedious
441 ground truth annotation process. In [122], a new CNN structure was proposed with the aim to achieve
442 a good trade-off between segmentation quality and runtime. This also integrated a CNN with deep
443 de-convolution network, but a new mapping between classes and filters at the de-convolution side
444 was designed to reduce the runtime. It took the entire image at its original resolution, instead of
445 image patches, as network input and achieved a run time of about 50 ms.

446 To mitigate the difficulties in ground truth annotation, [123] proposed map-supervised deep
447 learning pipeline. In this approach, the ground truth annotation was done automatically based on
448 the vehicle position, heading direction, camera parameters, GPS, and OpenStreetMap data. The
449 annotation noise was further reduced by using pixel appearance features. A CNN was trained based
450 on these machine generated ground truth annotations.

451 2.1.2.3. On-road object detection

452 On-road object detection mainly concerns vehicle and pedestrian object classes. Due to the
453 various types, appearances, shapes, and sizes of the objects, those methods reviewed in [71] [72] and
454 [73] are not robust and not general enough for the application of autonomous vehicles. As listed in the
455 KITTI database, for car, pedestrian, and cyclist detections, all of the leading entries and state of the art
456 methods are based on deep learning schemes. Deep learning has shown its superior performance as
457 compared to conventional learning or feature based approaches in the domain of obstacle detection.
458 Therefore, in this section, we will only review the deep learning based approaches.

459 Normally, the general pipeline for deep learning approaches is that a set of proposal bounding
460 boxes needs to be generated around the input image, then each proposal box will be sent through the

461 CNN network to determine a classification (including background) and fine tune its bounding box
462 locations as well. The common methods for bounding box proposal are Selective Search [124] and
463 EdgeBoxes [125], which both rely on inexpensive hand-crafted features and economical inference
464 schemes.

465 In [126], an energy minimization approach was presented for bounding box proposal. These
466 proposals were generated by exhaustively placing 3D bounding boxes on the ground-plane,
467 projecting them to the image plane and scoring them via simple and efficiently computable image
468 features including semantic and object instance segmentation, context, shape features, and location
469 priors to score the boxes. Per-class weights were also learnt for these features using S-SVM, adapting
470 to each individual object class.

471 Faster-RCNN [127] was the first deep learning scheme that unify both the bounding box proposal
472 and detection under the same network and achieved an end-to-end training process. The network
473 consists of two major parts: proposal net and detection net, where these two nets share most of the
474 CNN layers. The output from the proposal net are the proposed bounding boxes, which is used as
475 the input to the detection net for recognition and bounding box fine tuning processes.

476 Although in the training process Faster-RCNN does not fix the proposal box sizes and thus is
477 supposed to be invariant to object scales, but when it comes to challenging scenarios where the scales
478 of the object vary dramatically, its performance on small object detection is not very satisfying. The
479 main reason is that for small objects in the original image, after several layers of convolution and
480 pooling, the remaining information in the last layer is too little for a good detection. This issue can
481 be addressed by enlarging the input image size or by using a set of images at different scale sizes as
482 input [128], but this will increase the computation time and memory requirement as well.

483 To address the scale issue, in [129], Yang *et al.* proposed a scale-dependent pooling (SDP)
484 network. Instead of pooling the feature vectors only from the last convolution layer in the network,
485 the feature vectors for smaller proposal bounding boxes were pooled in earlier convolution layers
486 according to box heights. The detection and bounding box fine tuning were carried out separately at
487 different layers accordingly. To improve the efficiency, the author also trained a classical cascaded
488 rejection classifiers (CRC) based on MLP to filter out some proposal boxes at every layer. This
489 approach is not unified and not able to be trained end-to-end. The bounding box proposal was based
490 on Edgebox.

491 In [130], the authors proposed a unified multi-scale deep learning network (MS-CNN), which
492 took the original image as the only input and output the bounding boxes and object categories for
493 the associated bounding boxes. Similar to Faster-RCNN, this network also combined a proposal
494 net and detection net. Similar to the SDP net, the proposal net in MS-CNN pooled features from
495 different layers to generate bounding box proposals. All these proposals were then passed to the
496 same detection net for object recognition and bounding box fine tuning.

497 All the aforementioned algorithms target to detect the object in the 2D image, with no output
498 information on the 3D world. In [131], by further dividing the object category into sub-categories
499 based on their 2D appearance, 3D pose and 3D shape, the authors were able to train the deep learning
500 network to recover both 2D and 3D information from the 2D image. The proposed network, named
501 as Sub-CNN, consisted of two CNN networks, subcategory-aware CNN and object detection CNN.
502 The subcategory-aware CNN generated proposal bounding boxes to the object detection network.
503 Unlike Faster-RCNN and MS-CNN, these two networks did not share any CNN layers. In the KITTI
504 benchmark, both MS-CNN and Sub-CNN achieved similar state-of-the-art performance in object
505 detection. Sub-CNN took longer run time (2s *vs.* 0.4s) since it had two separated CNN nets, but it
506 was able to reveal the 3D world information which is more useful for autonomous vehicles.

507 There also exists some other approaches in the literature to reduce the processing time so that
508 the deep learning approach can achieve (near) real time performance, e.g. YOLO (You Only Look
509 Once) [132], SSD (Single Shot Detection) [133]. They are able to process the images at more than 30
510 frames per second, varying with the size of the network. But the fast performance is achieved at the

511 expense of detection rate. As the technologies in both hardware and software develop further, a better
512 trade-off between the run time and detection rate can be achieved.

513 2.1.3. Fusion

514 Different sensors have different strengths and weaknesses. Sensor fusion techniques are required
515 to make full use of the advantages of each sensor. In the context of autonomous vehicle environment
516 perception, LIDAR is able to produce 3D measurements and is not affected by the illumination of
517 the environment, but it offers little information on objects' appearances; conversely, camera is able
518 to provide rich appearance data with much more details on the objects, but its performance is not
519 consistent across different illumination conditions; furthermore, camera does not implicitly provide
520 3D information.

521 Following [134], the techniques that have been applied to LIDAR and camera fusion can be
522 roughly divided into two main categories based on their fusion process locations, including fusion at
523 feature level (early stage, centralized fusion) and fusion at decision level (late stage, decentralized
524 fusion). Based on the fusion mechanisms, they can be divided into the following categories:
525 MRF/CRF based, probability based, and deep learning based.

526 In [135], each point in the point cloud has an associated pixel in the image, based on the transform
527 between the LIDAR device and camera. Thus the color intensity of the pixel can be assigned to the
528 point. An MRF was designed by converting the point cloud into a graph with all of the points being
529 graph nodes. The energy minimization function modelled the correlations between the changes in
530 intensity and depth of the points. This approach only made use of the intensity information from
531 image and ignored the rest of the image cues.

532 Xiao *et al.* also proposed a random field approach in [136] for sensor fusion but with different
533 energy formulation as compared to [135]. The energy function consists of three terms, out of which,
534 two were the same as normal MRF terms (value term and smoothness term). The third term was based
535 on the laser points. A classifier was pre-trained to classify the laser points as to whether they were
536 road or non-road points. These points were then projected to the image plane, and the corresponding
537 pixels were assigned with the same probability of the points. The third term was derived from these
538 probabilities.

539 In [137], instead of using sparse laser points directly, the author reconstructed the dense depth
540 map from the point cloud by upsampling the points. Two sets of HOG (histogram of gradient)
541 pyramids based on the original image and the dense depth map were extracted, and a multi scale
542 deformable part model [138] was learnt for pedestrian detection based on the HOG pyramids.

543 [139] provided a decentralized approach for sensor fusion. The camera data was used to train
544 an AdaBoost classifier while the LIDAR data was used to train a GMM (Gaussian Mixture Model)
545 classifier [140]. A sum decision rule, based on the posteriori probabilities calculated by each classifier
546 was then designed to ultimately classify an object.

547 The deep learning based sensor fusion scheme always requires a dense depth map or its variants,
548 indicating that the point cloud needs to be converted into depth map. For example, in [141], the image
549 and the depth map went through two separated CNN networks, and only the feature vectors from the
550 last layer were concatenated to jointly carry out the final detection task. In [142], the point cloud was
551 first converted into a three-channel HHA map (which contains Horizontal disparity, Height above
552 ground, and Angle). The HHA and RGB (Red-Green-Blue color channel) images went through two
553 different CNN networks as well but the author found that the fusion should be done at the early to
554 middle layers of the CNN instead of the last layer.

555 In conclusion, sensor fusion between LIDAR and camera is necessary in order to make the best
556 use of these devices and achieve a robust environment perception result for autonomous vehicles.
557 But the current fusion mechanisms are still in a preliminary stage and not able to fully make use of all
558 the information from both sensors. Furthermore, those newly developed deep learning algorithms
559 for object detection, as reviewed in Section 2.1.2, have not yet been extended to operate over fused

560 camera and LIDAR information, where such an extension could yield significant performance boosts
561 over individual sensor data processing.

562 2.2. Localization

563 Localization is the problem of determining the pose of the ego vehicle and measuring its own
564 motion. It is one of the fundamental capabilities that enables autonomous driving. However, it is
565 often difficult and impractical to determine the exact pose (position and orientation) of the vehicle,
566 and therefore the localization problem is often formulated as a pose estimation problem [143].

567 The problem of estimating the ego vehicle's pose can generally be divided into two
568 sub-problems, namely the pose fixing problem and the dead reckoning problem. In the pose fixing
569 problem, the measurement is related to the pose by an algebraic/transcendental equation. Pose fixing
570 requires the capacity to predict a measurement given a pose, e.g. a map. In the dead reckoning
571 problem, the state is related to the observation by a set of differential equations, and these equations
572 have to be integrated in order to navigate. In this case, sensor measurements may not necessarily be
573 inferable from a given pose. In this sense, pose fixing and dead reckoning complement each other.

574 One of the most popular ways of localizing a vehicle is the fusion of satellite-based navigation
575 systems and inertial navigation systems. Satellite navigation systems, such as GPS and GLONASS,
576 can provide a regular fix on the global position of the vehicle. Their accuracy can vary from a
577 few of tens of meters to a few millimetres depending on the signal strength, and the quality of
578 the equipment used. Inertial navigation systems, which use accelerometer, gyroscope, and signal
579 processing techniques to estimate the attitude of the vehicle, do not require external infrastructure.
580 However, without the addition of other sensors, the initiation of inertial navigation system can be
581 difficult, and the error grows in unbounded fashion over time.

582 The use of GPS in localization requires reliable service signals from external satellites. This
583 method is reliable only when the GPS signal and dead reckoning odometry of the vehicle is reliable,
584 and may require expensive, high-precision sensors. A few good examples of problematic areas are
585 in indoor environments, underground tunnels, and urban canyons, where tall buildings deny good
586 GPS signal readings to the vehicle. In [144,145], road matching algorithms which use a prior road
587 map to constrain the motion of the vehicle are used in conjunction with GPS and INS to update the
588 localization estimation of the vehicle. The inclusion of road matching improves the accuracy in global
589 localization. However, the method still couldn't fully achieve precise pose estimation of the vehicle
590 with respect to its environment to the level required for autonomous driving.

591 Map aided localization algorithms use local features to achieve highly precise localization, and
592 have seen tremendous development in recent years. In particular, Simultaneous Localization and
593 Mapping (SLAM) has received much attention. The goal of SLAM is to build a map and use it
594 concurrently as it is built. SLAM algorithms leverage old features that have been observed by
595 the robot's sensors to estimate its position in the map and locate new features. Although it is not
596 possible to determine the absolute position, SLAM uses statistical modelling that takes into account
597 the odometry of the vehicle to remove most of the inconsistency between where the features are
598 predicted to be and where it is based on the sensor readings. In general there are two approaches to
599 SLAM problem: Bayesian filtering and smoothing.

600 The goal of formulating SLAM as a Bayesian filtering problem is to estimate the joint posterior
601 probability $p(x_{1:t}, m | z_{1:t}, u_{1:t-1})$ about the map m and robot trajectory $x_{1:t} = x_1, \dots, x_t$, given its
602 sensor measurement $z_{1:t} = z_1, \dots, z_t$, and inputs to the system $u_{1:t-1} = u_1, \dots, u_{t-1}$. Popular
603 methods in this category are Extended Kalman Filter (EKF), Extended Information Filter (EIF), and
604 Particle Filter (PF) [146–149].

605 A variation of the Particle Filter, Rao-Blackwellized Particle Filters(RBPF), has also been
606 introduced as a solution to the SLAM problem in [150,151]. In RBPF, the vehicle's trajectory and
607 the associated map are represented by a particle, and factorizes the probabilities according to the
608 following equation:

$$p(x_{1:t}, m | z_{1:t}, u_{1:t-1}) = p(m | x_{1:t}, z_{1:t}) \cdot p(x_{1:t} | z_{1:t}, u_{1:t-1}) \quad (1)$$

609 This equation is referred to as Rao-Blackwellization, and allows the trajectory of the vehicle to
 610 be first computed before the map is constructed based on the computed trajectory. This approach
 611 provides efficient computation since the map is strongly correlated to the vehicle's trajectory.
 612 The posterior probability $p(x_{1:t} | z_{1:t}, u_{1:t-1})$ is computed with a particle filter, in which the prior
 613 distribution is obtained from the vehicle's odometry, and refined with observations/ sensor readings.

614 Pose graph mapping [152] is a popular example of smoothing based SLAM. The SLAM problem
 615 is formulated as an optimization problem to minimize the error, by exploiting the inherent sparsity of
 616 a map. A few recently proposed algorithms of this type are TreeMap[153], TORO [154], iSAM [155],
 617 iSAM2 [156], and g2o [157].

618 A key event in smoothing based SLAM is the loop closure, which happens when features that
 619 have not been seen for a while are observed again from the sensor readings. When a loop closure
 620 is detected, the error caused by imperfect odometry can then be removed, and a substantial portion
 621 of the map can be updated. The simplest way of doing loop closure is by performing pair wise
 622 matching for possible loop closure by considering all observations that are within a pre-determined
 623 radius from a node in the pose graph [158]. More elaborate ways of detecting loop closures are also
 624 available in the literature, such as by learning from range sensor data [159], or probabilistically from
 625 visual appearance [160].

626 Rejecting false loop closure constraints is still an open research problem. Robust automatic
 627 loop closure detection is still a very active research topic. Various extension to the current SLAM
 628 algorithm to make the loop closure detection more robust such as Switchable Constraint method [161],
 629 Max-Mixture Model [162], and Realizing, Reversing, Recovering techniques [163] have been proposed
 630 in recent literature.

631 Scan matching is another key event in pose graph construction. Popular algorithms include
 632 Iterative Closest Point (ICP) [164], where each reference scan is matched with a query scan by aligning
 633 them according to a distance metric [165], and feature histogram based scan matching algorithms,
 634 such as Normal Distribution Transform (NDT) [166] and Spin Images [167].

635 Embedding the map with additional information is another active research topic. The
 636 term semantic mapping is widely referred to in the literature as augmenting the traditional
 637 metric/topological map with a higher level semantic understanding of the environment. In general,
 638 approaches to semantic mapping can be categorized into three categories: object based, appearance
 639 based, and activity based.

640 Appearance based semantic mapping techniques interpret sensor readings to construct semantic
 641 information of the environment. A few examples, such as [168,169], use geometric features
 642 from planar LIDARS. Vision can also be fused with LIDAR data for further classification and
 643 understanding of the environment [170–172].

644 Object based semantic mapping uses the occurrence of key objects to build a semantic
 645 understanding of the environments [173,174], where object recognition and classification is often a
 646 very important event in object based semantic understanding of the environment.

647 The activity based approach to semantic mapping relies on information about the activities of
 648 the agents around the robot. This topic is relatively less mature compared to appearance and object
 649 based semantic mapping. A few examples of this technique are found in [174,175] where external
 650 agent activities are used to semantically understand and classify the context of the environment (e.g.
 651 sidewalk versus road, etc.).

652 The map-aided localization algorithms can then use these features to localize the robot to a
 653 pre-recorded map and based on its surrounding features. In [176], lane markers are extracted from
 654 the reflectivity values of LIDAR data and are used as local features. With this approach, instead of
 655 using a self learned map, prior knowledge from open source maps such as Open-Street Map can be
 656 used, eliminating the map building stage [177]. Virtual 2D ranging is then extracted from 3D point

657 clouds and matched with the map [178]; coupled with GPS and INS data, the position of the vehicle
658 can be estimated with Bayesian filtering methods.

659 Feature based localization is also another active research topic. The most popular method is
660 by using particle filter to localize the vehicle in real time with 3D LIDARs [179]. The algorithm
661 first analyses the laser range data by extracting points from the road surface. Then, the reflectivity
662 measurements of these points are correlated to a map containing ground reflectivity to update particle
663 weights. One underlying assumption in this algorithm is that the road surface remains relatively
664 constant, which may undermine the performance in some cases.

665 However, the cost of 3D LIDARs can be prohibitive to many applications. Synthetic methods can
666 be used to obtain 3D measurements from 2D sensors. For example, accumulated laser sweeps can be
667 used as local features. This type of algorithm first generates a swathe of laser data by accumulating 2D
668 laser scans from a tilted-down LIDAR [180], then the swathe is matched to a prior 3D data reference
669 by minimizing an objective function. This algorithm demonstrates its accuracy and robustness in
670 GPS-denied areas. Although an accurate 3D model of the environment is not required, an accurate
671 and consistent prior is always desired when the localization is integrated with other navigation
672 functions. Similarly in [181,182], a 3D point cloud of the environment is obtained by servoing a
673 2D LIDAR, and extracted 2D features are used to perform localization. This method has been shown
674 to work well in an indoor environment with well structured ceiling features.

675 3. Planning

676 3.1. Autonomous Vehicle Planning Systems

677 Early-stage self-driving vehicles (SDVs) were generally only semi-autonomous in nature, since
678 their designed functionality was typically limited to performing lane following, adaptive cruise
679 control, and some other basic functions [183]. Broader capabilities were notably demonstrated in the
680 2007 DARPA Urban Challenge (DUC) [184], where it was shown that a more comprehensive planning
681 framework could enable a SDV to handle a wide range of urban driving scenarios. Performance of
682 the SDVs was still far from matching the quality of human drivers and only six of the 35 competition
683 entrants were able to complete the final event, but nevertheless, this milestone demonstrated the
684 feasibility of self-driving in an urban environment [10,185–189] and revealed important research
685 challenges residing in autonomous driving [190].

686 Boss, the winning entry of the DUC, Junior, the second place entry, and Odin, the third place
687 entry, along with many others, employed similar three level hierarchical planning frameworks with
688 a mission planner, behavioral planner, and motion planner. While the fourth place entry Talos
689 reportedly used a two level planner with a *navigator* and a motion planner, the navigator essentially
690 performed the functions of both the mission planner and behavioral planner [191]. The *mission*
691 *planner* (or route planner) considers high level objectives, such as assignment of pickup/dropoff tasks
692 and which roads should be taken to achieve the tasks. The *behavioral planner* (or decision maker)
693 makes ad hoc decisions to properly interact with other agents and follow rules restrictions, and
694 thereby generates local objectives, e.g., change lanes, overtake, or proceed through an intersection.
695 The *motion planner* (or local planning) generates appropriate paths and/or sets of actions to achieve
696 local objectives, with the most typical objective being to reach a goal region while avoiding obstacle
697 collision. Many recent works since the DUC continue to inherit the same three level hierarchical
698 structure as described here, though the partitioning of the layers are somewhat blurred with
699 variations of the scheme occurring in literature.

700 3.2. Mission Planning

701 Mission planning generally is performed through graph search over a directed graph network
702 which reflects road/path network connectivity. In the DUC, a Route Network Definition File
703 (RNDF) was provided as prior information [192]. The RNDF represented traversable road segments

704 by a graph of nodes and edges, and further included information such as stop sign locations,
705 lane widths, and parking spot locations. The RNDF was generated manually by the competition
706 organizers, however ongoing research targets to generate richer network representations stored in a
707 Road Network Graph (RNG) through automated processes, via sensing the infrastructure (i.e. road
708 boundaries) directly [193], or even by inference from vehicle motions [194]. Regardless of whether the
709 RNG is generated through manual annotation or through an automated method, the route searching
710 problem is formulated by assigning edge weights corresponding to the cost of traversing a road
711 segment (commonly distance) and applying graph search algorithms. Classical algorithms such as
712 Dijkstra's [195] or A* [196] can be effective for smaller neighborhoods, however more advanced
713 methods exist to improve efficiency over large networks, which are detailed in a survey paper focused
714 more specifically on the topic of route planning [197].

715 3.3. Behavioral Planning

716 The behavioral planner is responsible for decision making to ensure the vehicle follows any
717 stipulated road rules and interacts with other agents in a conventional, safe manner while making
718 incremental progress along the mission planner's prescribed route. This may be realized through a
719 combination of local goal setting, virtual obstacle placement, adjustment of drivable region bounds,
720 and/or regional heuristic cost adjustment. Decisions were made onboard most DUC vehicles through
721 Finite State Machines (FSMs) of varying complexity to dictate actions in response to specific perceived
722 driving contexts [185,186,188,198]. The terms *precedence observer* and *clearance observer* were coined to
723 categorize functions which checked certain logical conditions required for state transitions, where
724 precedence observers were to check whether the rules pertaining to the vehicle's current location
725 would allow for it to progress, and clearance observers would check "time to collision" - the shortest
726 time by which a detected obstacle would enter a designated region of interest - to ensure safe clearance
727 to other traffic participants. For example, when approaching a stop sign, the SDV would have to both
728 ensure precedence by coming to a complete stop at the stop line and wait for any other stationary
729 vehicles at the intersection with priority to move off, and ensure clearance by measuring time to
730 collision along its intended path (where oncoming traffic may not have to stop at the intersection).

731 Finite state machines of this nature are limited in that they are manually designed for a set
732 number of specific situations. The vehicle may then perform unexpectedly in a situation that was not
733 explicitly accounted for in the FSM structure, perhaps finding itself in a livelock, or even a deadlock
734 state if there aren't sufficient deadlock protections. Recent research works have sought to improve
735 organization in large decision making structures to thus manage larger rules sets [199–201]. Other
736 works have sought provable assurances in the decision making structure to guarantee adherence to
737 rules sets [202]. In [203] and [204], road rules enforcement was checked using Linear-Temporal Logic
738 (LTL) considerations, with successful real-world overtaking experiments [204].

739 3.4. Motion Planning

740 Motion planning is a very broad field of research, applied to mobile robots and manipulating
741 arms for a wide variety of applications ranging from manufacturing, medical, emergency response,
742 security/surveillance, agriculture and transportation. In the context of mobile robotics, motion
743 planning refers to the process of deciding on a sequence of actions to reach a specified goal, typically
744 while avoiding collisions with obstacles. Motion planners are commonly compared and evaluated
745 based on their *computational efficiency* and *completeness*. *Computational efficiency* refers to the process
746 run time and how this scales based on the dimensionality of the configuration space. The algorithm
747 is considered *complete* if it terminates in finite time, always returns a solution when one exists, and
748 indicates that no solution exists otherwise [205].

749 The motion planning problem has been proven to exhibit great computational complexity,
750 especially in high dimensions. For example, the well known piano mover's planning problem has

751 been shown to be PSPACE-hard¹ [206]. Furthermore, to guarantee completeness may demand an
 752 exhaustive search of all possible paths, which leaves many approaches stuck with the “curse of
 753 dimensionality” in high dimensional configuration spaces; it is increasingly more difficult to represent
 754 all obstacle occupied spaces and check for obstacle free points as the dimension of the search space
 755 increases. A core idea behind motion planning is then to overcome this challenge by transforming
 756 the continuous space model into a discrete model [207]. Two general categories of approaches to
 757 this transformation exist: 1) *combinatorial planning*, which builds a discrete representation that *exactly*
 758 represents the original problem and 2) *sampling-based planning* which utilizes a collision checking
 759 module to conduct discrete searching over samples drawn from the configuration space [207].

760 3.4.1. Combinatorial Planning

761 Combinatorial planners aim to find a *complete* solution by building a discrete representation
 762 which *exactly* represents the original problem, but which is characterized by convenient properties
 763 for special case solvers. For example, geometric solutions may efficiently be generated in low
 764 dimensional spaces with discrete convex obstacle spaces by constructing visibility graphs (shortest
 765 path solution), Voronoi-diagrams (highest clearance solution), or decomposing the space into obstacle
 766 free “cells” using obstacle boundaries as cell borders [207]. However the computational burden
 767 of these methods increases with increased dimensionality of the configuration space and increased
 768 number of obstacles, and thus combinatorial methods are typically limited in application. This is the
 769 primary motivation for the development of sampling-based algorithms, which will be discussed in
 770 the following subsection [208–210].

771 While decomposing spaces directly from obstacle geometry may be difficult in practice, other
 772 decompositions became popular where checks would still need to be made against the presence
 773 of obstacles. A common simple approach is to apply a uniform discretization over either the
 774 configuration search space or set of robot actions such that a finite search may be applied to find
 775 solution paths. By working in discretized spaces, the complexity of an exhaustive search is greatly
 776 reduced. Although completeness can no longer be guaranteed by these means, these methods may
 777 be found to be *resolution-complete*. That is to say that if the space is discretized to a “fine enough”
 778 resolution, then completeness can be guaranteed. Fine resolutions may however still be hard to
 779 achieve in high dimensional spaces, leading to excessive computational burden, again from the curse
 780 of dimensionality.

781 Nevertheless, it is still common to employ discretized search methods for road navigation. In
 782 the DARPA Grand Challenges and the DUC, many teams implemented a simple motion planner by
 783 which a kinodynamic reachable trajectory set was discretized [10], and/or a trajectory search tree was
 784 generated based on road geometry [9,10,185]. Such methods are still being refined, with emphasis on
 785 optimization of smooth velocity profiles [211]. Cell decomposition over the configuration space has
 786 also been used with some success [186]. An optimal path would typically be found over the finite
 787 discretization by implementing graph search algorithms, such as A* [196].

788 Recent works have also made use of space discretization in order to apply more advanced
 789 decision making algorithms. For example, cell decomposition was used in [212] and [202] to then
 790 generate paths which would obey road rules specified via Linear Temporal Logic (LTL). [213] used
 791 similar LTL methods to further investigate situations where the robot was allowed to break some
 792 rules (such as always drive in your lane) in order to reach goals that were otherwise obstructed. Cell

¹ A problem is said to belong to PSPACE complexity class if it can be solved by a deterministic Turing machine using an amount of memory (space) that follows the asymptotic trend of $O(n^k)$, $k \geq 0$, for an input of length n as $n \rightarrow \infty$. A deterministic Turing machine is a hypothetical device which operates to change symbols/values on a tape, where each symbol may only be changed one at a time, and only one action is prescribed at a time for any given situation. A problem A is furthermore considered PSPACE-hard if every problem/language B in PSPACE is polynomial-time reducible to A , $B \leq_p A$, meaning any B can be translated into instances of A in polynomial time.

793 decomposition was also necessary to apply popular models for handling environment uncertainty,
794 such as Partially Observable Markov Decision Processes (POMDP) and Mixed Observability Markov
795 Decision Processes (MOMDP). In [214] and [215], other moving obstacles' intentions were inferred
796 in real-time while the robot's motion plan was executed concurrently. POMDPs assume uncertainty
797 in both the robot's motion and in observation and account for this uncertainty in solving for optimal
798 policies, where MOMDPs have extended this idea to situations in which some of the state variables
799 are partially observable and others are full observable [216]. It's worth noting that POMDPs have
800 been gaining popularity recently with the emergence of efficient point based value iteration solvers
801 like SARSOP [217]. Prior to the emergence of SARSOP and other popular approximation algorithms,
802 POMDPs were often avoided in robotics because solving POMDPs exactly is computationally
803 intractable and the framework scales poorly with increasing number of states and increasing planning
804 horizon [218]. Recent research has also targeted means to apply POMDP to continuous spaces [219].

805 3.4.2. Sampling-based Planning

806 Sampling-based methods rely on random sampling of continuous spaces, and the generation of
807 a feasible trajectory graph (also referred to as a tree or roadmap) where feasibility is verified through
808 collision checking of nodes and edges to connect these nodes. Roadmaps generated should ideally
809 provide good *coverage* and *connectivity* of all obstacle-free spaces. Paths over the roadmap are then
810 used to construct solutions to the original motion planning problem. Sampling-based algorithms
811 are popular for their guarantees of *probabilistic completeness*, that is to say that given sufficient time
812 to check an infinite number of samples, the probability that a solution will be found if it exists
813 converges to one. While sampling-based algorithms are generally applied over continuous spaces,
814 it should be noted that some discretization typically occurs in collision checking, especially along
815 edge connections in the roadmap.

816 Variants of sampling-based algorithms primarily differ in the method by which a search tree is
817 generated. Probabilistic RoadMaps (PRM) [210,220] and Rapidly-exploring Random Trees (RRT) [221,
818 222] are perhaps two of the most influential sampling-based algorithms, each of which have been
819 popular subjects of robotics research with many variants suggested. PRM is a multi-query method
820 which builds and maintains multiple graphs simultaneously, and has been shown particularly
821 effective in planning in high-dimension spaces [220]. RRT in contrast seeks to rapidly expand a single
822 graph, which is suitable for many mobile robotics applications where the map is not well known *a*
823 *priori* due to the presence of dynamic obstacles and limited sensor coverage concentrated around the
824 robot's current location.

825 In many applications, besides completeness guarantees and efficiency in finding a solution, the
826 quality of the returned solutions is also important. While an initial solution might be found quickly
827 in many cases, the algorithms are typically run for a longer period of time to allow for better solutions
828 to be found based on some heuristics. Some works have proposed to bias tree growth toward regions
829 that resulted in lower cost solutions [223]. Many sampling-based planners and variants of PRM
830 and RRT have since been proposed. A comprehensive evaluation of many popular planners was
831 presented in [208], where many popular planners were not only compared on a basis of computational
832 complexity and completeness, but also on *optimality*. The authors showed that the popular PRM
833 and RRT algorithms are actually asymptotically sub-optimal, and proposed asymptotically optimal
834 variants, PRM* and RRT*. Other asymptotically optimal planners have since been suggested, such
835 as Fast Marching Trees (FMT*) [224] and Stable Sparse Trees (SST*) [225], both of which claim speed
836 improvement over RRT*.

837 3.5. Planning in Dynamic Environments

838 Many operating environments are not static, and are therefore not known *a priori*. In an
839 urban environment, the traffic moves, road detours and closures occur for construction or accident
840 cleanup, and views are frequently obstructed. The robot must constantly perceive new changes

841 in the environment and be able to react while accounting for several uncertainties. Uncertainties
842 arise from perception sensor accuracy, localization accuracy, environment changes, and control policy
843 execution [226–233]. But in application, perhaps the largest source of uncertainty is the uncertainty in
844 surrounding obstacles' movements.

845 3.5.1. Decision Making Structures for Obstacle Avoidance

846 An approach taken by many DARPA Urban Challenge vehicles was to monitor regions along
847 the intended path for potential obstacle collisions, where these regions would be labeled as "critical
848 zones" [185], or merge zones at intersection, and checked against the trajectories of all nearby
849 vehicles to determine a "time to collision." Typically, if a collision was seen as imminent, the vehicle
850 would slow or stop accordingly, which was acceptable behavior for crossing and merging at many
851 intersections [191], though perhaps overly conservative in other situations. In [234], the lane ahead
852 was checked for presence of a vehicle traveling in the wrong direction on a collision path, where
853 if triggered, a "defensive driving" maneuver would be executed to pull off the lane to the right
854 side and stop. When defensive driving behavior was tested in other vehicles, the performance was
855 unsatisfactory in that the oncoming vehicle had to stop before the autonomous vehicle would move
856 to navigate around it [189]. The approaches had an advantage of computational simplicity in that
857 they planned in a low dimensional space neglecting the time dimension, but the resulting behaviors
858 were overly simplistic in that a deterministic set behavior was executed without heuristic weighting
859 of alternative actions or explicit consideration for environment evolution given the chosen course of
860 action. Nevertheless, recent works have still continued to use behavioral level decision making for
861 obstacle avoidance, especially to handle difficult maneuvers such as lane changing [199].

862 Other stochastic decision making structures, such as Partially Observable Markov Decision
863 Processes (POMDP), can explicitly model uncertainties in vehicle controls and obstacle movements
864 and have been applied with success in some complex scenarios [214], but these methods can be
865 difficult to generalize and required discretization of the state space and vehicle controls.

866 3.5.2. Planning in Space-Time

867 To better account for obstacle movement, it is necessary to include time as a dimension in the
868 configuration space, which increases the problem complexity. Furthermore, while instantaneous
869 position and velocity of obstacles may be perceived, it is yet difficult to ascertain future obstacle
870 trajectories. Prior approaches have aimed to use simple assumptions, such as constant velocity
871 trajectory, in predicting obstacle movement, with errors accounted for by rapid iterative re-planning.
872 Other more conservative approaches have aimed to account for variations in obstacle trajectory by
873 bounding larger obstacle-occupied sub-spaces within the configuration space, within which samples
874 are rejected by the planner [235,236].

875 Given a situation in which the instantaneous position and velocity of obstacles can be observed,
876 it logically follows that future obstacle trajectories can be predicted. The common assumption of
877 deterministic constant velocity requires frequent verification or correction with each new observation.
878 Another method is to assume a bounded velocity on obstacles and represent them as conical
879 volumes in space-time, thus reducing the need for observation updating and re-planning [235].
880 Other assumptions can be applied to obstacles as well, such as static assumption, constant velocity
881 assumption, bounded velocity, and bounded acceleration, each of which yields a bounded volume of
882 a different shape in space-time [236]. A visualization of \mathcal{R}^2 configuration-space obstacle trajectory
883 predictions over space-time is shown in Figure 4. A naive assumption would be to ignore the
884 uncertainty in the prediction of an obstacle's trajectory, in which case the obstacle bounded space
885 does not grow over time (left two cases in Figure 4). A more conservative approach would be to
886 assume a larger bounded area of possible obstacle occupancy, where the obstacle space bounds grow
887 over time according to assumed limitations on the obstacle's velocity and or acceleration (right two
888 cases in Figure 4).

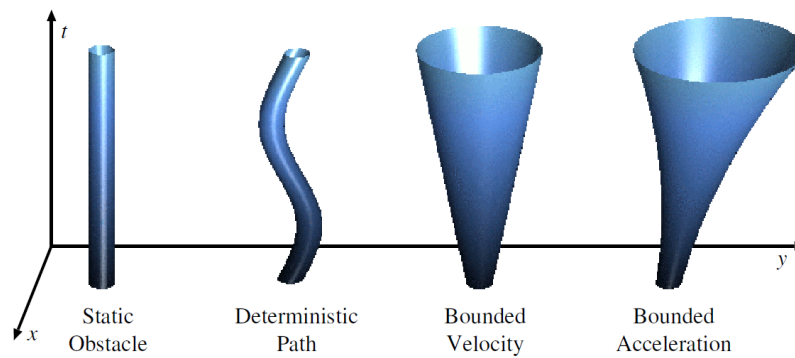


Figure 4. Obstacles as space-time volumes in $\mathbb{R}^2 \times \text{Time}$ space [236]. Time is shown in vertical axis. When accounting for uncertainty, obstacle size grows with respect to time.

889 3.5.3. Control Space Obstacle Representations

890 Rather than check for collisions directly in the robot's configuration space, another popular
 891 approach is to directly plan in the control space by prohibiting certain control actions which are
 892 predicted to lead to collision. For example, the velocity obstacles method assumes that obstacles
 893 will maintain their observed trajectories and forbids a robot from choosing relative velocities that
 894 would lead to collision with the obstacle's current trajectory [237]. This was generally applied
 895 to circular, holonomic robots, but due to the ease of computation it has gained popularity in
 896 multi-robot planning, with proposed Reciprocal Velocity Obstacles [238]. Recent extensions to the
 897 velocity obstacles method have further incorporated acceleration constraints [239], and adjustments
 898 for nonholonomic robots [240].

899 3.6. Planning Subject to Differential Constraints

900 Motion planning is ultimately a high-level control problem. In practice, control limitations
 901 may be ignored to various degrees in the motion planner in the name of simplicity or reduction
 902 of computational burden, however poor accounting for constraints on the robot motion during the
 903 planning phase can lead to high control errors and result in trajectory inefficiencies and/or hazardous
 904 operations. Trajectories with longer path length which can be followed closely might have shorter
 905 execution times than shorter paths which are more difficult to follow in reality. Discrepancies between
 906 the planned trajectory and the executed trajectory present a danger since this lessens the validity
 907 of collision checking during the planning phase. Paths can be generated from directly sampling
 908 admissible controls [241], however these methods do not optimize paths through tree rewiring, and
 909 popular asymptotically optimal planners, such as RRT* [208] require sampling from the configuration
 910 space. Incorporating differential constraints into state-sampling planners is still a challenging matter,
 911 and requires a steering function to draw an optimal path between two given states which obeys
 912 control constraints (if such a path exists), as well as efficient querying methods to tell whether a
 913 sampled state is reachable from a potential parent state.

914 One of the most fundamental differential constraints in a system is the evolution of time, where
 915 time t must increase at a constant rate $\dot{t} = 1$. Whether or not time is explicitly included as a state
 916 parameter, other state parameters will typically have differential constraints with respect to time,
 917 such as velocity and/or acceleration limits. Robot differential constraints are applied to generate
 918 velocity profiles, which may be solved for in a decoupled manner only over the chosen geometric path
 919 [242,243], or in a direct integrated manner simultaneously with geometric path solving over every
 920 connection in the tree as it is built [209,241,244–246]. Turning radius limitations are also common,
 921 where paths for car-like models are often solved through Dubins curves [247] or Reeds-Shepp curves
 922 [248], which are proven to have shortest distance given a minimum turning radius, though more

923 sophisticated methods exist which also consider a weighted control effort heuristic [245]. Decoupled
924 differential constraint handling can result in very inefficient trajectories or failure to find a trajectory
925 due to the decoupling. Conversely, direct integrated differential constraint handling can overcome
926 these shortcomings but is more computationally complex.

927 State sampling can be made more efficient by limiting the states that are sampled to only
928 those from within a set of states known to be reachable from the initial condition given the robot's
929 kinodynamic constraints applied to an obstacle free environment. Likewise it is only beneficial to
930 check for connectivity between neighboring states when they fall within each other's reachable sets;
931 checking any states that are nearby by Euclidean distance metric but not reachable within a short
932 period of time given kinodynamic constraints is a waste of computational effort. Adding Reachability
933 Guidance (RG) to state sampling and Nearest Neighbor (NN) searching can provide significant
934 efficiency boosts to planning speed, especially for systems where motion is highly constrained or
935 the motion checking cost is high, and the standard naive approaches of uniform sampling over
936 a hyperrectangle and NN searching by Euclidean distance metric would otherwise result in slow
937 planner performance.

938 Several recent works have presented analytical approaches to incorporate RG into motion
939 planning. The asymptotic optimality of RRT* was shown to extend to a reachability guided variant
940 where the reachable subspace was represented as a hyperrectangle derived from the linearized
941 dynamics approximation of a system through the Ball Box Theorem presented in [244], where
942 the "box" was an under-approximation of the true reachable subspace. A similar approach was
943 taken in [246] to prove asymptotic optimality in differential constraint handling variants of PRM
944 (Probabilistic RoadMaps) and FMT (Fast Marching Tree). Another asymptotically optimal sampling
945 based algorithm to handle differential constraints, Goal-Rooted Feedback Motion Tree (GR-FMT)
946 was presented in [249], limited in application to controllable linear systems with linear constraints.
947 An analytical method for solving a two point boundary value problem subject to kinodynamic
948 constraints was presented in [245], which could be used for finding optimal state-to-state connections
949 and NN searching but was limited to systems with linear dynamics.

950 A machine learning approach was taken in [250] to query for whether a state was reachable from
951 a given base state, though this method required applying a Support Vector Machine (SVM) classifier
952 over a feature set of 36 features for the Dubins car model, where online solving for 36 features could
953 be relatively computationally expensive.

954 The Reachability Guided RRT planner presented in [251] relied on construction of Voronoi
955 diagrams to build approximations of reachable sets rooted from each graph node for sampling
956 biasing, where Euclidean distance metric was still used for NN searching. This method may not easily
957 be extended to higher dimensional spaces, as Voronoi diagrams are then no longer easily constructed.

958 There are also relatively few planning methods that have been demonstrated to be effective for
959 solving over a configuration space with an appended time dimension. Early works explored control
960 sampling approaches [241], and recent state sampling works have made model simplifications to
961 handle the differential constraints in an online manner, such as keeping to a constant ego robot
962 speed [252]. Others have performed planning by graph search over a discrete, time-bounded lattice
963 structure built from motion primitives [253], or a grid cell decomposition of the state space [254],
964 though these methods lose the benefits of sampling based approaches (which are less limited in
965 resolution, and have potential for rewiring and optimization).

966 3.7. Incremental Planning and Replanning

967 Limited perception range and the dynamic nature of operating environments are common
968 challenges for autonomous vehicle planning. The sensing range of the mobile robot is typically
969 limited not only by sensor specifications, but also reduced by view obstruction in the presence
970 of obstacles. It is often the case that the robot will not be able to perceive the entire route from
971 a start location to goal location at any one specific instant of time. Thus the robot will need to

972 generate incremental plans to follow trajectories which lead to forward progress towards the robot's
973 ultimate goal location. Furthermore, as the robot progressively executes its planned trajectory, other
974 moving agents will have their own goals in mind and may move unexpectedly. Given a substantial
975 environment change, robot trajectories that were believed to be safe at a prior time instance may not
976 longer be safe at a subsequent time instance. Replanning is then necessary to adjust for dynamic
977 changes to the environment.

978 Incremental planning requires a means of incrementally generating sub-goals, or otherwise
979 choosing the best trajectory from amongst a set of possible trajectories based on some heuristics.
980 A new plan must be generated at least as often as a new sub-goal is defined. In [243], a finite
981 state machine generates new sub-goals for a sampling based replanner only when the robot was
982 forced to come to a stop due to path blockage, where each subgoal was set at a predefined distance
983 ahead along the predefined path. In [255], no sub-goals were defined, nor was there a predefined
984 path to utilize, but rather the best choice trajectories were decided based on a combined weighted
985 heuristic of trajectory execution time and distance to goal from the end trajectory state. [255] applied
986 a constant rate replanning timer, where each current solution plan was executed concurrently while
987 the subsequent plan was being generated, and each newly planned trajectory would be rooted from
988 an anticipated committed pose given the previous committed solution trajectory. Note that in a
989 Mobility-on-Demand (MoD)² context, a mission planner should be able to provide a predefined path
990 which leads from a starting point to an end destination based on a passenger service request, and the
991 presence of a predefined path can help to overcome dangers of getting stuck due to local minima.

992 Iteratively replanning to generate new solution trajectories presents a potential opportunity to
993 carry over knowledge from previous planning iterations to subsequent planning iterations. While of
994 course each new plan could start from scratch, better solutions may be found faster if prior planning
995 information is well utilized. For example, sampling could be biased to sample near waypoints
996 along the previously chosen solution path, as with Extended RRT (ERRT) [256]. Other works have
997 suggested redoing collision-checks over the entire planning tree, as in Dynamic RRT (DRRT) [257],
998 where the tree structure was utilized to trim child "branches" once a parent state was found to be
999 no longer valid, and sampling is biased towards trimmed regions. Recently, a replanning variant
1000 of RRT* was presented, RRT^X [258], which trims the previous planning iteration's planning tree in
1001 similar fashion to DRRT, but furthermore efficiently reconnects disconnected branches to other parts
1002 of the tree and maintains the rewiring principal of RRT* responsible for asymptotic optimality.

1003 Safety mechanisms should also be carefully designed considering that each planning cycle
1004 requires a finite time for computation and the environment may change during that time (e.g.
1005 obstacles may change trajectories). Several works have prescribed passive safety mechanisms to
1006 reduce speed in response to obstacle presence, where passive safety refers to the ability to avoid
1007 collision while the robot is in motion (escaping from a hostile agent is a more advanced planning
1008 topic). In [259], spatial path planning was decoupled from velocity planning, and a "Dynamic
1009 Virtual Bumper" approach would prescribe reduced speed based on the proximity of the nearest
1010 obstacle as measured by a weighted longitudinal and lateral offset from the desired path. Moving
1011 obstacles were treated as enlarged static obstacles in [259], where the obstacles were assumed to
1012 occupy the area traced by their current constant velocity trajectory over a short time frame in addition
1013 to their current spatial location. While decoupled approaches are generally simpler to implement,
1014 they may give rise to inefficiencies, or even failure to find a solution when one exists by integrated
1015 planning problem formulation. Several other trajectory planning methods which consider spatial
1016 paths and velocity in an integrated manner were benchmarked for safety evaluation in [260], where

² Mobility-on-Demand (MoD) refers to vehicle sharing schemes whereby passenger services are provided to customers throughout a city with instant booking of vehicles available. A distributed MoD fleet is meant to provide responsive "first and last mile" transportation (short connections to rapid transit systems from unserved areas), or other short distance trips, thereby reducing the need for private vehicle ownership by increasing public transportation accessibility.

1017 Inevitable Collision State Avoidance (ICS-AVOID) [261], was deemed to outperform Non-Linear
 1018 Velocity Obstacles (NLVO) [262] and Time-Varying Dynamic Window [263]. ICS-AVOID maintained
 1019 a finite control set kernel to test over each trajectory's end state to ensure that no executed trajectory
 1020 would end in an ICS [261].

1021 4. Control

1022 The execution competency of an autonomous system, also often referred to as motion control,
 1023 is the process of converting intentions into actions; its main purpose is to execute the planned
 1024 intentions by providing necessary inputs to the hardware level that will generate the desired motions.
 1025 Controllers map the interaction in the real world in terms of forces, and energy, while the cognitive
 1026 navigation and planning algorithms in an autonomous system are usually concerned with the
 1027 velocity and position of the vehicle with respect to its environment. Measurements inside the control
 1028 system can be used to determine how well the system is behaving, and therefore the controller can
 1029 react to reject disturbances and alter the dynamics of the system to the desired state. Models of the
 1030 system can be used to describe the desired motion in greater detail, which is essential for satisfactory
 1031 motion execution.

1032 4.1. Classical Control

1033 Feedback control is the most common controller structure found in many applications. Feedback
 1034 control uses the measured system response and actively compensates for any deviations from the
 1035 desired behavior. Feedback control can reduce the negative effects of parameter changes, modelling
 1036 errors, as well as unwanted disturbances. Feedback control can also modify the transient behavior of
 1037 a system, as well as the effects of measurement noise.

1038 The most common form of classical feedback control is the Proportional-Integral-Derivative
 1039 (PID) controller. The PID controller is the most widely used controller in the process control industry.
 1040 The concept of PID control is relatively simple. It requires no system model, and the control law is
 1041 based on the error signal as:

$$u(t) = k_d \dot{e} + k_p e + k_i \int e(t) dt \quad (2)$$

1042 where e is the error signal, k_p , k_i , and k_d are the proportional, integral, and derivative gains of the
 1043 controller, respectively.

1044 However, the use of only feedback terms in a controller may suffer from several limitations. The
 1045 first significant limitation of a feedback only controller is that it has delayed response to errors, as
 1046 it only responds to errors as they occur. Purely feedback controllers also suffer from the problem of
 1047 coupled response, as the response to disturbances, modelling error, and measurement noise are all
 1048 computed by the same mechanism. It is more logical then to manipulate the response to a reference
 1049 independently from the response to errors.

1050 Another degree of freedom can be added to the controller by including a feedforward term to the
 1051 controller, where this controller architecture is shown in Fig. 5. The addition of a feedforward term
 1052 in the controller can help to overcome the limitations of feedback control. The feedforward term is
 1053 added to the control signal without considering any measurement of the controlled system. However,
 1054 the feedforward term may involve the measurement of disturbances, etc. Designing a feedforward
 1055 control requires a more complete understanding of the physical system, and therefore, oftentimes, a
 1056 model reference is used for the feedforward controller. The method of combining a feedforward and
 1057 a feedback term in the controller is also known as two degree of freedom controller.

1058 Table 1 summarizes the roles of feedforward and feedback control [143].

1059 State space control, often referred to as modern control, is a technique that tries to control the
 1060 entire vector of the system as a unit by examining the states of the system. The field of state space

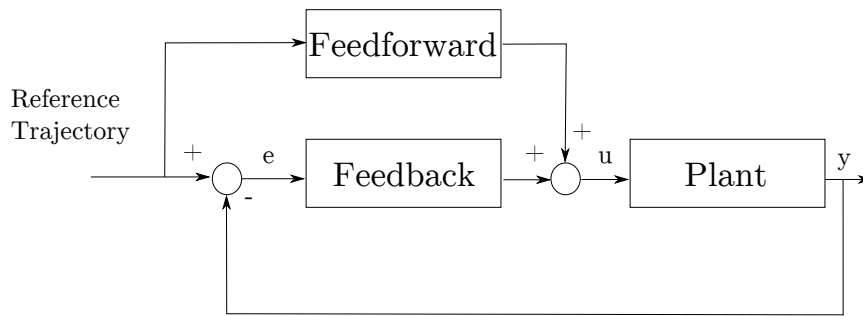


Figure 5. Two Degree of Freedom Controller

Table 1. Feedforward vs Feedback Control

	Feedback	Feedforward
Removes Unpredictable Errors and Disturbances	(+) yes	(-) no
Removes Predictable Errors and Disturbances	(-) no	(+) yes
Removes Errors and Disturbances Before They Happen	(-) no	(+) yes
Requires Model of a System	(+) no	(-) yes
Affects Stability of the System	(-) yes	(+) no

1061 control is a very large field and there is still much active ongoing research in this area. A linear state
1062 space model can be written as:

$$\dot{x}(t) = A(t)x(t) + B(t)u(t) \quad y(t) = C(t)x(t) + D(t)u(t) \quad (3)$$

1063 where $x(t)$ is the system state vector, $u(t)$ is the control input vector, and $y(t)$ is the output of the
1064 system.

1065 The observations in an autonomous system are mostly nonlinear, and therefore a linear model
1066 of the nonlinear system may have to be produced by first linearizing the state space equation of the
1067 system.

$$\dot{x}(t) = f(x(t), u(t)) \quad y(t) = h(x(t), u(t)) \quad (4)$$

1068 The two degree of freedom controller can also be applied to nonlinear systems. Feedforward is
1069 used to generate a reference trajectory, while the feedback is used to compensate for disturbances and
1070 errors.

1071 The nonlinear system can be linearized about a reference trajectory $x_r(t)$ to produce linearized
1072 error dynamics.

$$\delta \dot{x}(t) = A(t)\delta x(t) + B(t)\delta u(t) \quad \delta y(t) = C(t)\delta x(t) + D(t)\delta u(t) \quad (5)$$

1073 where $A, B, C,$ and D are the appropriate Jacobians. If there exists a trajectory generation process
1074 that can be designed to produce a reference input $u_r(t)$, such that $u_r(t)$ generates a feasible trajectory
1075 which satisfies the nonlinear system dynamics of the system, state space controllers can be configured
1076 to perform feedback compensation for the linearized error dynamics.

1077 4.2. Model Predictive Control

1078 Autonomous systems need motion models for planning and prediction purposes. Models can
1079 also be used in control execution. A control approach which uses system modelling to optimize

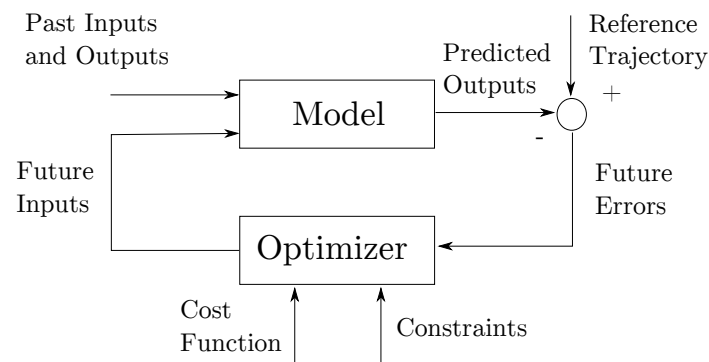


Figure 6. Basic Structure of Model Predictive Control

1080 over a forward time horizon is commonly referred to in the literature as Model Predictive Control
 1081 (MPC). The basic structure of MPC is shown in Fig.6. Model predictive control has been developed
 1082 to integrate the performance of optimal control and the robustness of robust control. Typically the
 1083 prediction is performed for a short time horizon called the prediction horizon, where the goal of
 1084 the model predictive controller is to compute the optimal solution over this prediction horizon. The
 1085 model, and thus the controller can be changed online to adapt to different conditions.

1086 Model predictive control has seen tremendous success in the industrial process control
 1087 applications, due mainly to its simple concept and its ability to handle complicated process models
 1088 with input constraints and nonlinearities [264].

1089 Model predictive control has several other attractive features, such as the simplicity of designing
 1090 a multi variable feedback controller. It also allows for easy specification of system inputs, states,
 1091 and outputs that must be enforced by the controller. MPC furthermore permits specification of an
 1092 objective function to optimize the control effort. MPC can also address time delay, rejecting measured
 1093 and unmeasured disturbances and taking advantage of previously stored information of expected
 1094 future information. This feature can be very useful for repeated tasks, such as following a fixed path.
 1095 MPC embodies both optimization and feedback adjustment, thus mimicking natural processes.

1096 Model predictive control has also been widely adapted to automotive applications [265]. The
 1097 operations of the overall vehicle system must be optimal throughout the operating range in order
 1098 to increase the fuel economy, emission, and safety performance. However, applying a model
 1099 predictive controller in an automotive system meets different challenges than those faced in the
 1100 process control industry. In the process control industry, the sampling time is relatively longer, and
 1101 the computing resources available are ample. The sampling period for processes in an automobile
 1102 is a few milliseconds, and the amount of computing resources available is limited due to space
 1103 constraints. Advances in processor speed and memory, as well as development of new algorithms
 1104 is therefore important in pushing the adoption of MPC into greater prevalence in the automotive
 1105 industry.

1106 MPC has already been applied in several automotive control applications, including traction
 1107 control [266], braking and steering [267,268], lane keeping [269] etc. Model predictive techniques
 1108 have also been applied to the trajectory tracking problem in various works [270–276].

The general model predictive control problem is formulated as

$$\underset{U(t)}{\text{minimize}} \quad F(x(N|t)) + \sum_{k=0}^{N-1} L(x(k|t), y(k|t), u(k|t)) \quad (6a)$$

$$\text{subject to} \quad x(k+1|t) = f(x(k|t), u(k|t)) \quad (6b)$$

$$y(k|t) = h(x(k|t), u(k|t)) \quad (6c)$$

$$x_{min} \leq x(k|t) \leq x_{max}, \quad k = 1, \dots, N_c \quad (6d)$$

$$y_{min} \leq y(k|t) \leq y_{max}, \quad k = 1, \dots, N_c \quad (6e)$$

$$u_{min} \leq u(k|t) \leq u_{max}, \quad k = 1, \dots, N_{cu} \quad (6f)$$

$$x(0|t) = x(t) \quad (6g)$$

$$u(k|t) = \kappa(x(k|t)) \quad k = N_u, \dots, N-1 \quad (6h)$$

1109 where t is the discrete time index. The notation for a vector $v(h|t)$ denotes the value for v predicted
 1110 at h time steps as referenced from time t , based on information up to t . Equations 6b and 6c are the
 1111 discrete time model of the system dynamics with sampling period T_s where $x \in \mathbb{R}^n$ is the system's
 1112 state, $u \in \mathbb{R}^m$ is the control input, and $y \in \mathbb{R}^p$ is the system output. The optimizer is the control
 1113 input sequence $U(t) = (u(0|t), \dots, u(N-1|t))$, where N is the prediction horizon. Similar to the
 1114 optimal control formulation, the cost function represents the performance objective that consists of
 1115 the stage cost L and the terminal cost F . The constraints on the states and outputs are enforced along
 1116 the horizons N_c and N_{cu} , respectively. The control horizon N_u is given as the number of optimized
 1117 steps before the terminal control law is applied.

1118 At any control cycle t , the model predictive control strategy for the general problem operates as
 1119 follows: system outputs are measured and the state $x(t)$ is estimated. This state estimation is acquired
 1120 to initialize Equation 6a and impose the limit in 6g. Once the MPC optimization problem is solved
 1121 and the optimal input sequence $U^*(t)$ is obtained, the first element of the optimal input sequence is
 1122 then applied to the system $u(t) = u^*(0|t)$. At the following cycle, the process is repeated using the
 1123 newly acquired state estimate, thus applying the feedback.

1124 4.3. Trajectory Generation and Tracking

1125 There are two general approaches to trajectory generation with known path information. The
 1126 first approach uses the optimization method to both generate a trajectory and track it simultaneously,
 1127 while another approach is to decouple trajectory generation and tracking.

1128 4.3.1. Combined Trajectory Generation and Tracking

1129 The combined approach integrates both the generation and execution/tracking tasks into one
 1130 optimization problem. This approach is often applied for optimal time application such as in [277].
 1131 Running the optimization problem in real time is a challenge due to limited processing power, and it
 1132 may not be advantageous for planning in a complex environment.

1133 4.3.2. Separate Trajectory Generation and Tracking

1134 4.3.2.1. Trajectory Generation

1135 The problem of trajectory generation is to find an entire control input $u(t)$, which corresponds to
 1136 some desired state trajectory $x(t)$.

1137 The trajectory generation problem can be posed as a two point boundary value problem. The
 1138 boundary conditions are typically the constraints that include a starting state $x(t_0) = x_0$ and the final
 1139 goal state $x(t_f) = x_f$, with the system dynamics $\dot{x} = f(x, u)$ as an added constraint. A trajectory is

1140 defined as infeasible if there is no control input $u(t)$ for a given state trajectory $x(t)$ which satisfies
1141 the boundary conditions.

1142 A trajectory is a representation of a motion confined to some time interval. This could be a
1143 specification of the state vector over an interval $\{x(t)|(t_0, t < t_f)\}$, or a specification of the input
1144 over an interval $\{u(t)|(t_0, t < t_f)\}$.

1145 The problem of trajectory generation for an autonomous vehicle can be solved with multiple
1146 techniques. However, the literature for trajectory generation can generally be classified into two
1147 approaches: (i) sensor based and (ii) dynamics based. The first approach is more oriented towards
1148 the field of robotics. Robotics researchers have been tackling the problem of trajectory generation
1149 for decades, where it has been applied in both industrial robots and autonomous mobile robots.
1150 The sensor based approach generally concentrates on integrating the perception of the environment,
1151 without taking much of the vehicle dynamics into account.

1152 Another approach to trajectory generation for an autonomous vehicle is based more on vehicle
1153 dynamics. Various optimization methods for finding an optimal trajectory have been proposed in
1154 the literature, such as the application of genetic algorithms, and gradient descent method. A deep
1155 understanding in vehicle dynamics and control can push the limits of the autonomous vehicle, as
1156 demonstrated in [278]. Research in trajectory generation and tracking is also pursued for application
1157 in semi-autonomous vehicles, for more advanced driver's assistance systems, such as advanced
1158 collision avoidance with stability control [279–281].

1159 A good balance between the sensor based trajectory planning and the vehicle dynamics control
1160 methods should be considered to fully realize the goal of autonomous vehicle control systems: to
1161 ensure that the vehicle can track the desired trajectory well, and operate safely, comfortably, and
1162 efficiently for all potential operating complexities and velocities.

1163 4.3.2.2. Trajectory Tracking

1164 In this section, an overview of the available path and trajectory tracking methods will be
1165 discussed. We consider a path to be a geometric representation of a plan to move from a start pose to a
1166 goal pose, whereas a trajectory additionally includes the velocity information of the motion. Various
1167 methods have been presented in the literature. Two of the most popular types are (i) geometric
1168 methods and (ii) model based methods [282]. Controllers derived from model based path tracking
1169 methods use a kinematic and/or dynamic model of the vehicle. Kinematic model based controllers
1170 perform well at low speed applications, but the error increases as the vehicle speed and curvature
1171 rate of the path increases. On the other hand, the dynamic model based controllers tend to perform
1172 well for higher speed driving applications such as autonomous highway driving, but also tend to
1173 cut corners as the vehicle rapidly accelerates and decelerates and pursues paths with large curvature.
1174 Model based methods require the path to be continuous, and are not robust to disturbances and large
1175 lateral offsets.

1176 4.3.2.3. Geometric Path Tracking

1177 Geometric path tracking algorithms use simple geometric relations to derive steering control
1178 laws. These techniques utilize look ahead distance to measure error ahead of the vehicle and
1179 their complexity range from simple circular arc calculations to much more sophisticated geometric
1180 theorems, such as the vector pursuit method[283].

1181 One of the most popular geometric path tracking algorithms is the pure pursuit path tracking
1182 algorithm. The pure pursuit algorithm pursues a point along the path that is located at a certain
1183 lookahead distance away from the vehicle's current position. The algorithm is relatively simple and
1184 easy to implement, and is robust to disturbances and large lateral error. The input to the algorithm
1185 is also waypoints, rather than smooth curves, and is therefore less susceptible to discretization
1186 related issues. This algorithm still suffers from corner cutting and steady state error problems if

1187 the lookahead distance selected is not appropriate, especially at higher speed, when the lookahead
 1188 distance increases (lookahead distance is generally set as an increasing function with respect to
 1189 speed).

1190 In order to avoid constricting the way that the paths are generated, the paths shall be represented
 1191 in a piece wise linear way [284]. By this principle, a smooth trajectory having continuous first and
 1192 second order derivatives, e.g. a Bezier curve should be represented as a sequence of dense points,
 1193 enabling a wider range of potential tracking algorithms to be applied. A point is joined to the
 1194 following point in the path by linear path segments. In order to closely approximate the continuous
 1195 path, a denser discretization of the path has to be implemented. The discrete nodes are contained in
 1196 an ordered list, and the waypoints are tracked sequentially (waypoint i is tracked before waypoint
 1197 $i + 1$).

1198 The pure pursuit algorithm has a single tunable parameter, the lookahead distance L_{fw} . Using
 1199 Ackermann steering geometry, the algorithm defines a virtual circular arc that connects the anchor
 1200 point (the rear axle) to the tracked point found along the path that is located L_{fw} away from the
 1201 anchor point. A variation of this algorithm has been introduced by [285], where the anchor point is
 1202 not necessarily selected as the rear axle, but can be located at a distance ϵ away from the rear axle
 1203 along x_b . However, hereafter, the anchor point will be assumed to be the rear axle. The stability limits
 1204 of the algorithm has also been studied in [286], and it has been shown that the pure pursuit algorithm
 1205 is stable for a correct combination of minimum lookahead distance and process delay involved in the
 1206 system.

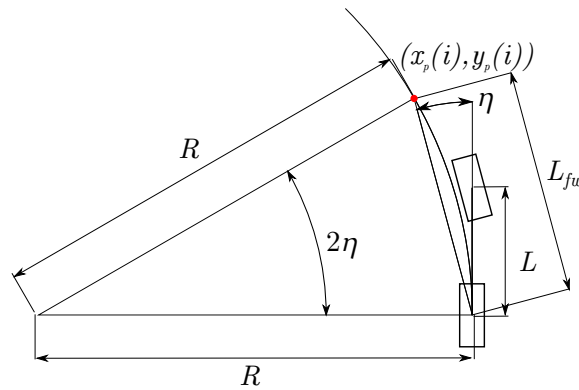


Figure 7. Pure pursuit steering geometry

1207 The virtual arc is constrained to be tangential to the velocity vector at the origin of the body fixed
 1208 frame and to pass through the tracked point found along the path. Referring to Fig. 7 and using the
 1209 law of sines, the arc's radius of curvature R can be geometrically computed as:

$$\frac{L_{fw}}{\sin(2\eta)} = \frac{R}{\sin(\frac{\pi}{2} - \eta)}$$

$$\frac{L_{fw}}{2\sin(\eta)\cos(\eta)} = \frac{R}{\cos(\eta)}$$

$$\frac{L_{fw}}{\sin(\eta)} = 2R$$

1210 where R is the turning radius, and η is the lookahead heading. The curvature κ of the arc is defined
 1211 as:

$$\kappa = \frac{2\sin(\eta)}{L_{fw}} \quad (7)$$

And therefore the vehicle's steering angle δ can be computed by applying the kinematic bicycle model:

$$\delta = \tan^{-1}(\kappa L)$$

$$\delta(t) = \tan^{-1}\left(\frac{2L\sin(\eta(t))}{L_{fw}}\right) \quad (8)$$

1212 The lookahead distance is commonly formulated as a function of longitudinal velocity, and
1213 saturated at a certain maximum and minimum value, and thus equation (8) can be rewritten as

$$\delta(t) = \tan^{-1}\left(\frac{2L\sin(\eta(t))}{kv(t)}\right) \quad (9)$$

1214 At lower speed, when the lookahead distance is smaller, the vehicle is expected to track the path
1215 closely, and oscillatory behavior is also expected; meanwhile at higher velocity, when the lookahead
1216 distance is larger, the vehicle is expected to track the path smoothly, however this will result in the
1217 cutting corner problem.

1218 Since the lookahead distance is a function of the gain k , selecting the appropriate value for the
1219 gain will result in significant trade-offs in the tracking performance. On one hand, if the gain k is
1220 set to be too low, the algorithm will track a point that is very close to the vehicle's current pose. As
1221 the vehicle's control may not be perfect, a vehicle tracking a constant curvature path may oscillate
1222 between being inside and outside of the curve; this can result in steering control towards the opposite
1223 direction, and therefore instability may occur. On the other hand, if the gain k is set to be too large,
1224 the opposite effect is expected. The autonomous vehicle is expected to stay inside/outside of the
1225 curve for a very long time rather than moving closer and closer to the curvature, and therefore poor
1226 tracking performance is expected.

1227 Tuning the pure pursuit controller to achieve a good path tracking result which minimizes the
1228 corner cutting and overshoot problems can be a tedious and course dependent challenge. One of
1229 the main reasons is that the pure pursuit path tracking algorithm does not consider the target path
1230 curvature, and the heading of the tracked point along the path. The pure pursuit algorithm simply
1231 calculates a circular arc based on the geometry of the vehicle model. Ignoring the vehicle's lateral
1232 dynamics that are more and more influential as the speed increases, which results in discrepancies
1233 between the predicted circular arc and the actual travelled circular arc. This dynamic effect can be
1234 compensated by increasing the gain k until the circular arc that is computed is of smaller radius than
1235 the circular arc of the path at a proportion that would cancel out the dynamic side slip of the vehicle.

1236 The Stanley method is another popular geometric steering controller that was first introduced
1237 with Stanford University's entry in the DARPA Urban Challenge[287].

1238 Referring to Fig. 8, the Stanley method computes the steering command based on a nonlinear
1239 control law which considers the cross track error e_{fa} measured from the center of the front axle of the
1240 vehicle to the path at (x_p, y_p) , as measured from the front axle of the vehicle, as well as the heading
1241 error θ_e of the vehicle with respect to the path:

$$\theta_e = \theta - \theta_p \quad (10)$$

1242 where θ is the heading of the vehicle, and θ_p is the heading of the path. The resulting control law for
1243 the steering angle δ can be written as:

$$\delta(t) = \theta_e(t) + \tan^{-1}\left(\frac{ke_{fa}(t)}{v_x(t)}\right) \quad (11)$$

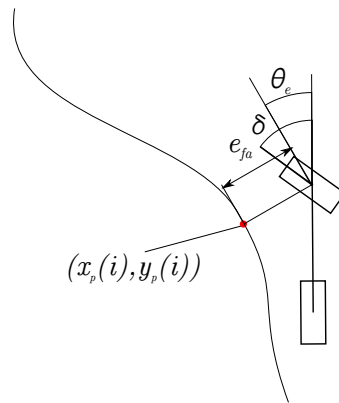


Figure 8. Stanley method steering geometry

1244 The second term in equation 11 adjusts the steering angle such that the intended trajectory intersects
 1245 the path at $\frac{v_x(t)}{k}$ distance away from the path tangent to (x_p, y_p) , where k is the gain parameter and
 1246 $v_x(t)$ is the instantaneous longitudinal velocity of the vehicle.

1247 The algorithm has been proven to exponentially converge to zero cross track error. Compared to
 1248 the pure pursuit method, the Stanley method, has better tracking results and does not cut corners as
 1249 it uses cross track error and yaw heading error information of the vehicle with respect to the path as
 1250 measured from the front axle rather than pursuing a point that is located at a certain distance ahead
 1251 of the vehicle. It also performs better at high speed driving as compared against the pure pursuit
 1252 method.

1253 However, the Stanley method is not as robust to disturbances, and has higher tendency for
 1254 oscillation as compared to the pure pursuit method, as it only considers the current cross track error
 1255 rather than considering the path ahead. In instances where the controller is not ideal, tracking a
 1256 constant curvature path with the Stanley method may result in similar symptoms as tracking the path
 1257 with a pure pursuit controller with small lookahead distance. The vehicle's position may oscillate
 1258 between the inside and the outside of the curvature, and the computed steering angle may oscillate
 1259 between positive and negative values (left or right). The Stanley method also requires continuous
 1260 curvature path rather than discrete waypoints, as it considers the cross track error in a continuous
 1261 manner, which makes it susceptible to discretization related problems [288].

1262 4.3.2.4. Trajectory Tracking with a Model

1263 For a given path/trajectory there are several model based tracking methods to choose from. At
 1264 slower speeds, vehicle kinematics models or linearized dynamics are often used. When attempting
 1265 stability in control at higher velocity, a more complex model is usually required.

1266 De Luca, Oriolo, and Samson [289] have proposed a kinematic car controller based on the
 1267 kinematic bicycle model. This method can apply not only to car like robots, but also to many other
 1268 kinematic models for various mobile robots.

Referring to Fig. 9, De Luca et al. defined the path according to a function of its length s . Let $\theta_p(s)$ represent the angle between the path tangent at (x_p, y_p) and the global x axis. Orientation error θ_e of the vehicle with respect to the path is then defined as

$$\theta_e = \theta - \theta_p(s)$$

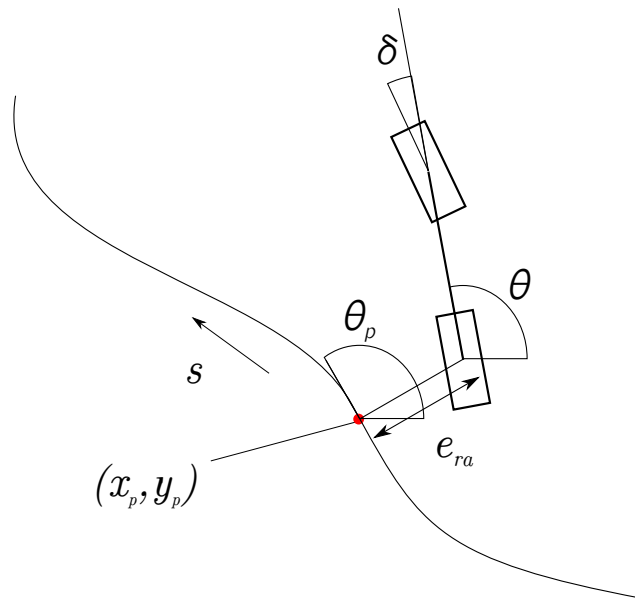


Figure 9. Path representation for kinematic car model as proposed in [289]

and the curvature along the path is defined as

$$\kappa(s) = \frac{e_{ra} \theta_p(s)}{ds}$$

1269 multiplying both sides by \dot{s}

$$\dot{\theta}_p(s) = \kappa(s) \dot{s}$$

Given that cross track error e_{ra} is the orthogonal distance from the anchor point (midpoint of the rear axle) to the path, the quantities \dot{s} and \dot{e}_{ra} can be expressed as

$$\begin{aligned} \dot{s} &= v \cos(\theta_e) + \dot{\theta}_p e_{ra} \\ \dot{e}_{ra} &= v \sin(\theta_e) \end{aligned}$$

The kinematic model in path coordinates can now be written as

$$\begin{bmatrix} \dot{s} \\ \dot{e}_{ra} \\ \dot{\theta}_e \\ \dot{\delta} \end{bmatrix} = \begin{bmatrix} \frac{\cos(\theta_e)}{1 - \dot{e}_{ra} \kappa(s)} \\ \sin(\theta_e) \\ \left(\frac{\tan \delta}{L}\right) - \frac{\kappa(s) \cos(\theta_e)}{1 - \dot{e}_{ra} \kappa(s)} \\ 0 \end{bmatrix} v \begin{bmatrix} 0 \\ 0 \\ 0 \\ 1 \end{bmatrix} \delta \quad (12)$$

1270 Canonical forms for kinematic models of nonholonomic systems are commonly used in
 1271 controller design. One particular canonical structure that is used in deriving the controller is the
 1272 chained form, intended for general two input systems such as the driftless kinematic car model. The
 1273 chained form can be written as:

$$\dot{x}_1 = u_1 \quad (13)$$

$$\dot{x}_2 = u_2 \quad (14)$$

$$\dot{x}_3 = x_2 u_1 \quad (15)$$

$$\vdots \quad (16)$$

$$\dot{x}_n = x_{n-1} u_1 \quad (17)$$

1274 where x represents state variable, and u represents input to the system. The problem can be further
 1275 simplified as a single input system by assigning the first control input u_1 to be a function of time.
 1276 Murray in [290] has proposed a way of converting the kinematic car model into the chained form, by
 1277 a change of coordinates $x = \phi(q)$ and invertible transformation $v = \beta(q)u$. The kinematic car model
 1278 can then be put into chained form by using the following coordinate change:

$$\begin{aligned} x_1 &= s \\ x_2 &= \kappa'(s)e_{ra}\tan(\theta_e) - \kappa(s)(1 - e_{ra}\kappa(s))\frac{1 + \sin^2(\theta_e)}{\cos^2(\theta_e)} + \frac{(1 - e_{ra}\kappa(s))\tan(\delta)}{L\cos^3(\theta_e)} \\ x_3 &= (1 - e_{ra}\kappa(s))\tan(\theta_e) \\ x_4 &= e_{ra} \end{aligned}$$

and the input transformation

$$\begin{aligned} v &= \frac{1 - e_{ra}\kappa(s)}{\cos(\theta_e)} u_1 \\ \dot{\delta} &= \alpha_2(u_2 - \alpha_1 u_1) \end{aligned}$$

where α_1 and α_2 are defined as

$$\begin{aligned} \alpha_1 &= \frac{\partial x_2}{\partial s} + \frac{\partial x_2}{\partial e_{ra}}(1 - e_{ra}\kappa(s))\tan(\theta_e) + \frac{\partial x_2}{\partial \theta_e} \left(\frac{\tan(\delta)(1 - e_{ra}\kappa(s))}{L\cos(\theta_e)} - \kappa(s) \right) \\ \alpha_2 &= \frac{L\cos^3(\theta_e)\cos^2(\delta)}{(1 - e_{ra}\kappa(s))^2} \end{aligned}$$

1279 De Luca et al then proposed the following smooth feedback stabilization method. Their method
 1280 takes advantage of the internal structure of the chained form and breaks the design solution into two
 1281 phases. The first phase assumes that one control input is given, while the additional control input is
 1282 used to stabilize the remaining sub-vector of the system state. The second phase consists of specifying
 1283 the first control input to guarantee convergence and stability.

1284 The variables of the chained form are reordered for simplicity as

$$\chi = (\chi_1, \chi_2, \chi_3, \chi_4) = (x_1, x_2, x_3, x_4)$$

so the the chained form system can be written as

$$\dot{\chi}_1 = u_1 \quad (18)$$

$$\dot{\chi}_2 = \chi_3 u_1 \quad (19)$$

$$\dot{\chi}_3 = \chi_4 u_1 \quad (20)$$

$$\dot{\chi}_4 = u_2 \quad (21)$$

1285 The ordering of x_2 and x_4 is made such that the position of the rear axle is (χ_1, χ_2) . Let $\chi =$
 1286 (χ_1, χ_2) , where $\chi_2 = (\chi_2, \chi_3, \chi_4)$, and the goal is to stabilize χ_2 to zero. χ_1 represents the arc length
 1287 s along the path, while χ_2 represents the cross track error e_{ra} , and χ_3, χ_4 are related to the steering
 1288 angle and orientation error of the tracked path respectively.

1289 If u_1 is assigned as a function of time, the chained system can be written as

$$\dot{\chi}_2 = 0$$

$$\dot{\chi}_2 = \begin{bmatrix} 0 & u_1(t) & 0 \\ 0 & 0 & u_1(t) \\ 0 & 0 & 0 \end{bmatrix} \chi_2 + \begin{bmatrix} 0 \\ 0 \\ 1 \end{bmatrix} u_2$$

with

$$\tilde{\chi}_1 = \chi_1 - \int_0^t u_1(t) dt$$

When u_1 is assigned *a priori*, $\tilde{\chi}_1$ is not controllable. However, the structure of the differential equation for χ_2 is similar to the controllable canonical form that is widely studied in state space control. The system also becomes time invariant as u_1 is set at a constant non-zero value. If u_1 is a piecewise continuous, bounded, and strictly positive/negative function, then χ_2 is controllable. Under this assumption

$$\frac{d}{dt} \chi_1 = \frac{d}{d\chi_1} \dot{\chi}_1 = \frac{d}{d\chi_1} u_1$$

$$\text{sign}(u_1) \frac{d}{d\chi_1} \dot{\chi}_1 = \frac{1}{|u_1|} \cdot \frac{d}{dt}$$

and thus the state space equation can be rewritten as

$$\chi_2^{[1]} = \text{sign}(u_1) \chi_3 \quad (22)$$

$$\chi_3^{[1]} = \text{sign}(u_1) \chi_4 \quad (23)$$

$$\chi_4^{[1]} = \text{sign}(u_1) u_2' \quad (24)$$

By applying the definition

$$\chi_i^{[j]} = \text{sign}(u_1) \frac{d^j \chi_i}{d\chi_1^j}$$

$$u_2' = \frac{u_2}{u_1}$$

the system has an equivalent input-output representation of

$$\chi_2^{[n-1]} = \text{sign}(u_1)^{n-1} u_2'$$

and the system is controllable, admitting an exponentially stable linear feedback in the form of

$$u_2'(\chi_2) = -\text{sign}(u_1)^{n-1} \sum_{i=1}^{n-1} k_i \chi_2^{[i-1]}$$

where the gain $k_1 > 0$ for stability, and the time varying control

$$u_2(\chi_2, t) = u_1(t) u_2'(\chi_2)$$

1290 is globally asymptotically stable at the origin $\chi_2 = 0$.

1291 The goal of the path tracking problem is to bring $\chi_2, \chi_3, \text{ and } \chi_4$ down to zero, the solution to the
1292 path tracking problem for an Ackermann steered vehicle for any piecewise continuous, bounded and
1293 strictly positive/negative u_1 can be written as:

$$u_2'(\chi_2, \chi_3, \chi_4) = -\text{sign}(u_1) [k_1\chi_2 + k_2\text{sign}(u_1)\chi_3 + k_3\chi_4]$$

and the final path tracking feedback control law can be obtained as

$$u_2(\chi_2, \chi_3, \chi_4, t) = -k_1|u_1(t)|\chi_2 - k_2u_1(t)\chi_3 - k_3|u_1(t)|\chi_4$$

1294 Model predictive techniques have also been applied to trajectory tracking problem. The main
1295 challenge with model predictive approaches in trajectory tracking and control is that the nonlinear
1296 optimization problem has to be solved several times per second. With recent advances in available
1297 computational power, solving nonlinear optimization in real time is now feasible. A few variations
1298 of the MPC problem for trajectory tracking that can be found in the literature are as follows:

- 1299 • Path Tracking Model Predictive Controller : with a center of mass based linear model, Kim et
1300 al. [291] formulated an MPC problem for a path tracking and steering controller. The resulting
1301 integrated model is simulated with a detailed automatic steering model and a vehicle model in
1302 CarSim.
- 1303 • Unconstrained MPC with Kinematic Model: by implementing CARIMA models without
1304 considering any input and state constraints, the computational burden can be minimized. The
1305 time-varying linear quadratic programming approach with no input or state constraints, using
1306 a linearized kinematic model, can be used to solve this sub class of problems, as demonstrated
1307 in [272].
- 1308 • MPC Trajectory Controller with Dynamic Car Model : A wide array of methods are available
1309 in the literature. An approach with nonlinear tire behavior for tracking trajectory on various
1310 road conditions is explored in [268], and the simulation results suggest that the vehicle can
1311 be stabilized on challenging icy surfaces at a 20 Hz control frequency. The complexity of the
1312 model and inadequacy in available computing power at the time of publishing resulted in
1313 computational time that was more than the sample time of the system, hence only simulation
1314 results are available. The authors explored the linearization of the state of the vehicle about
1315 the state at the current time step in [292]. By reducing the complexity of the quadratic
1316 programming problem, a more reasonable computing time can be achieved, and the controller
1317 has been experimentally validated on challenging icy surfaces for up to 21 m/s driving speed.
1318 A linearization based approach was also investigated in [292] based on a single linearization
1319 about the state of the vehicle at the current time step. The reduced complexity of solving the
1320 quadratic program resulted in acceptable computation time, and successful experimental results
1321 are reported for driving in icy conditions at speeds up to 21 m/s.

1322 5. Vehicle Cooperation

1323 Cooperation between multiple autonomous vehicles (AVs) is possible with the development of
1324 vehicular communication. In particular, state estimation can be improved with multiple sources
1325 of information gathered from different vehicles. Cooperative state estimation can also improve
1326 robustness against communication failure. With future trajectories shared among nearby vehicles,
1327 the motion can be coordinated to make navigation safer and smoother for AVs.

1328 5.1. Vehicular Communication

1329 Vehicular communication technology has been progressing rapidly, enabling connection
1330 between vehicles via wireless networks [293]. The bandwidth and range of wireless communication
1331 are increasing rapidly while the latency is being significantly reduced. For example, the
1332 communication range of Dedicated Short Range Communications (DSRC) can be up to 1000 meters,
1333 allowing a vehicle to connect to nearby vehicles even beyond line-of-sight and field-of-view.
1334 Furthermore, the information can be relayed and multi-hop connections are possible, which can
1335 significantly increase the connectivity. For vehicular communication, the IEEE 802.11p standard
1336 has been designed to allow information exchange between high speed cars, and between vehicles
1337 and roadside infrastructure. Many companies, such as Autotalks, Commsignia, Cohda Wireless, and
1338 Denso, are already selling their V2V communication devices at affordable prices to the mass market.
1339 Other wireless communication technologies, such as 3G, 4G and WiFi, are also suggested in [294–296].

1340 The various communication technologies allow AVs to share their sensing information, such
1341 as GPS location, turning angle, driving speed, and the states of detected vehicles or pedestrians.
1342 This allows AVs to “see” beyond their own line-of-sight and field-of-view [294]. Multiple sources of
1343 information from remote vehicles can substantially improve the observability of the nearby vehicles’
1344 states since their view points can be very different, and thereby improve environmental awareness.
1345 The augmented sensing range will significantly improve driving safety. Meanwhile, planned future
1346 trajectories can also be shared so that the prediction of cooperating vehicles’ future positions can
1347 be better facilitated. Potential motion conflicts can then be identified and mitigated with motion
1348 coordination algorithms, which can guarantee that decisions are jointly feasible.

1349 The same communication protocols could also be used for Vehicle to Infrastructure (V2I)
1350 communications, where the IEEE 802.11p standard has also seen adoption into DRSC devices
1351 intended for intersection handling (broadcasting traffic light information). Besides enabling more
1352 robust traditional traffic control for autonomous cars, new V2I devices could be leveraged as
1353 suggested in [297] to enable centralized vehicle coordination algorithms to prescribe continuous flow
1354 intersection behavior (traffic does not stop, only slows to avoid collision with cross traffic), which
1355 would increase the overall traffic throughput rate.

1356 5.2. Cooperative Localization

1357 It has been found that simply adding the information together from multiple source vehicles
1358 is not sufficient, and inconsistent perception results can lead to dangerous driving behaviors [294].
1359 Since the vehicles are mobile and their locations are uncertain, their perception results may be
1360 “unaligned” or inconsistent. Map merging is proposed to align multiple local sensing maps so that
1361 the observations are consistent [295]. Nonetheless, transmitting a local sensing map uses substantial
1362 communication resources. A more efficient way is to localize them well on a global map so that
1363 sensing information can be accurately projected onto a global map. In this way, perception results
1364 would consequently be aligned. The well-aligned observations or perception results allow AVs to
1365 have a larger area of environmental understanding, and thereby significantly improve environmental
1366 awareness. Also, fusing sensing information can potentially reduce perception uncertainty, increase
1367 localization accuracy, and improve state observability. More importantly, the merged information
1368 would allow the early detection of possible hazards and thereby allow AVs to have a faster response
1369 to avoid dangerous accidents.

1370 5.2.1. Vehicle Shape Information Utilization

1371 Cooperative localization essentially exploits the correlations, i.e., the joint and relative
1372 observations, to further improve localization accuracy cooperatively. The relative observation is often
1373 utilized for cooperative localization [298–306]. For example, relative range is measured by via the
1374 one-way-travel-time (OWTT) and utilized in cooperative localization [304–306]. The relative bearing

1375 is also measured with a range sensor in [301,303] so that the relative position can be determined. The
1376 relative orientation is not considered in cooperative localization, partially because the shapes of the
1377 robots are arbitrary and it is difficult to measure relative heading. However, the relative orientation
1378 is of great importance for autonomous driving and it would be appealing to have the uncertainty
1379 of relative orientation further reduced. An indirect relative pose estimation method is proposed
1380 in [307]. Nonetheless, that method requires merging two local maps, which would use substantial
1381 computational and communicational resources. For vehicles, their shapes are usually rectangular
1382 when projected onto a plane parallel to the ground. When detected by a range sensor, such as a 2D
1383 LIDAR sensor, the shape of vehicle is expected to resemble the letter "L". In [308], an efficient L-shape
1384 fitting algorithm is proposed to obtain accurate relative poses for cooperative localization.

1385 5.2.2. Minimal Sensor Configuration

1386 Multi-vehicle cooperative localization has been studied extensively [298–303], where the cited
1387 works mainly consider a full sensor configuration for each vehicle. With a full sensor configuration,
1388 each vehicle is able to localize independently without any cooperation. However, the number of
1389 required sensors could be reduced for a fleet of vehicles that share sensing information. The minimal
1390 number of sensors for a fleet of vehicles to simultaneously and continually localize themselves
1391 remains to be an open question.

1392 Many cooperative localization experiments [298,299,301–303] have been performed indoors or
1393 in simulations where features are distinct, sensing error is minor and perception range is small.
1394 Madhavan *et al.* has furthermore conducted outdoor multi-robot localization experiments [300],
1395 but the moving speeds of the robots are quite low. Even though promising experimental results
1396 have been achieved, they may not extend to outdoor fast moving vehicles. The scalability of
1397 cooperative localization using the minimal sensor configuration is proved in [309]. The proposed
1398 sensor configuration can be used by autonomous truck convoy systems [310], which can greatly
1399 reduce the cost of such convoys.

1400 5.2.3. General Framework

1401 One of the challenges for cooperative localization is optimal estimation. Transmitting the state
1402 estimates for decentralized data fusion will lead to circular inference if special measures are not
1403 taken [311]. Circular inference would essentially count the same information multiple times, and
1404 thus the resulting estimate is usually biased and overconfident. Covariance Intersection (CI) is
1405 a common suboptimal technique used to avoid overconfident estimation [312,313]. An optimal
1406 estimation scheme transmits measurements instead of state estimates and builds a pose graph
1407 for multi-vehicle cooperative localization [304–306], but is susceptible to communication failure.
1408 Communication loss can result in missing some links of the graph, and the pose graph can then break
1409 into multiple disconnected subgraphs, which leads to non-uniqueness of the optimal solution. Walls
1410 *et al.* proposed a factor decomposition scheme to recover the odometry factor when packets are lost
1411 during transmission [304]. The proposed framework is also able to handle delayed or out-of-sequence
1412 packets. The data association is determined by the differences in the transmission signals among the
1413 servers, which is usually not applicable to V2V communication. Only relative distance is utilized as
1414 the correlation in that framework and each vehicle only receives a subset of all the measurements
1415 because of the server-client scheme. In [314], a more general cooperative localization framework is
1416 proposed to handle data associations and ambiguities in the relative observations. Besides, relative
1417 pose is used as the correlation between vehicles to maximize the usage of the vehicle detection
1418 information. The proposed framework is also robust against communication loss, communication
1419 delays or out-of-sequence measurements.

1420 5.3. Motion Coordination

1421 Sharing future trajectories among AVs can help them to predict dynamic changes in the
1422 surrounding environments. Conflicts between future trajectories can be detected in advance and
1423 should be resolved in time. Centralized multi-vehicle motion planning is a way to avoid potential
1424 collisions in the composite configuration space, which is formed by the Cartesian product of the
1425 configuration spaces of individual vehicles [315]. The inherent high complexity hinders these
1426 methods from being applicable in real-time multi-vehicle motion planning. *Decoupled* planning is
1427 more efficient, which can be further divided into *prioritized* planning [316–318] and *path-velocity*
1428 planning [319,320]. Since the path of the vehicle typically follows the lane, the centralized
1429 multi-vehicle motion planning to explore all the possible paths may be over-kill. It would be more
1430 efficient and applicable to just coordinate the vehicles' velocities while the vehicles follow fixed paths.
1431 A D* search in the coordination diagram was proposed in [320], however, the Euclidean distance
1432 metric, being part of the cost formulation, may not have a physical meaning in the coordination
1433 diagram. The vehicles' waiting time would be a more suitable metric of the quality of the solution. In
1434 [321], an efficient motion coordination algorithm is presented to resolve conflicts in future trajectories
1435 and minimize the total waiting time, where V2V communication is adopted.

1436 6. Conclusion

1437 Aided by the increase in availability and reduction in cost of both computing power and sensing
1438 equipments, autonomous driving technologies have seen rapid progress and maturation in the past
1439 couple of decades. This paper has provided a glimpse of the various components that make up
1440 an autonomous vehicle software system, and capture some of the currently available state of the
1441 art techniques. This paper is by no means a comprehensive survey, as the amount of research and
1442 literature in autonomous vehicles has increased significantly in the last decade. However, there are
1443 still difficult challenges that have to be solved to not only increase the autonomous driving capabilities
1444 of the vehicles, but also to ensure the safety, reliability, and social and legal acceptability aspects of
1445 autonomous driving.

1446 Environmental perception systems can be made more robust through sensor fusion, where we
1447 expect further development in this area to more fully make use of all information provided by the
1448 sensors. Also, while newly developed deep learning algorithms for object detection have achieved
1449 great performance boosts, they have yet to be extended to operate over fused sensor data from
1450 multiple sensor source types.

1451 Recent advancements in the field of SLAM has contributed significantly to the localization
1452 capabilities of autonomous vehicles. However, the problem of robust automated loop closure is still
1453 an active research topic with a lot of open challenges. Another active research topic in the field of
1454 vehicle mapping is long-term mapping. Updating the maps with static, topometric, activity and
1455 semantic data over time is important in order to ensure that the vehicle can localize itself precisely
1456 and consistently with respect to its environment.

1457 While impressive capabilities have also been demonstrated in the realm of planning algorithms,
1458 we anticipate further advancement to improve real-time planning in dynamic environments. Recent
1459 related research is progressing toward better inclusion of robot differential motion constraints and
1460 efficient strategies for knowledge retention between subsequent iterations of replanning.

1461 There has been significant theoretical progress in the field of autonomous vehicle control in
1462 recent years. However, many of the breakthrough results have only been tested in simulation.
1463 Ensuring that the autonomous system robustly follows the intention of higher level decision making
1464 processes is crucial. Model Predictive Control (MPC) based techniques have been an active research
1465 topic in this area, due to its flexibility and performance. Computational time is essential in real
1466 time applications, and therefore model selection and MPC problem formulation varies from one
1467 application to another.

1468 It has been shown that vehicle cooperation can enable better performance in perception and
 1469 planning modules, however there is much room for advancement to improve the scalability of
 1470 multi-vehicle cooperative algorithms. Furthermore, although hardware is being standardized for
 1471 V2V communications, no standard yet exist for what information content should be passed between
 1472 vehicles.

1473 Autonomous vehicles are complex systems. It is therefore more pragmatic for researchers to
 1474 compartmentalize the AV software structure and focus on advancement of individual subsystems as
 1475 part of the whole, realizing new capabilities through improvements to these separate subsystems.
 1476 A critical but sometimes overlooked challenge in autonomous system research is the seamless
 1477 integration of all these components, ensuring that the interaction between different software
 1478 components are meaningful and valid. Due to overall system complexity, it can also be difficult
 1479 to guarantee that the sum of local process intentions results in the desired final output of the system.
 1480 Balancing computational resource allotments amongst the various individual processes in the system
 1481 is also a key challenge.

1482 Recognizing the fast pace of research advancement in AVs, we eagerly anticipate the near future
 1483 developments which will overcome the cited challenges and bring AVs to greater prevalence in urban
 1484 transportation systems.

1485 Acknowledgement

1486 This research was supported by the National Research Foundation, Prime Minister's Office,
 1487 Singapore, under its CREATE programme, Singapore-MIT Alliance for Research and Technology
 1488 (SMART) Future Urban Mobility (FM) IRG. We are grateful for their support.

1489 Bibliography

- 1490 1. Sousanis, J. World vehicle population tops 1 billion units. [http://wardsauto.com/ar/world_vehicle_](http://wardsauto.com/ar/world_vehicle_population_110815)
 1491 [population_110815](http://wardsauto.com/ar/world_vehicle_population_110815). Accessed: 2015-02-25.
- 1492 2. of the Department of Economic, P.D.; of the United Nations Secretariat, S.A. World population prospects:
 1493 The 2012 revision. <http://esa.un.org/unpd/wpp/index.htm>. Accessed: 2015-02-25.
- 1494 3. Systematics, C. Crashes vs. Congestion—What's the Cost to Society? Prepared for the American
 1495 Automobile Association, 2011.
- 1496 4. Schrank, D.; Eisele, B.; Lomax, T.; Bak, J. Urban mobility scorecard. *College Station: Texas A&M*
 1497 *Transportation Institute and INRIX 2015*.
- 1498 5. Levy, J.I.; Buonocore, J.J.; Von Stackelberg, K. Evaluation of the public health impacts of traffic congestion:
 1499 a health risk assessment. *Environmental health 2010*, 9, 1.
- 1500 6. Stenquist, P. The Motor Car of the Future. *the Oakland Tribune 1918*.
- 1501 7. Clemmons, L.; Jones, C.; Dunn, J.W.; Kimball, W. Magic Highway U.S.A. [https://www.youtube.com/](https://www.youtube.com/watch?v=L3funFSRAbU)
 1502 [watch?v=L3funFSRAbU](https://www.youtube.com/watch?v=L3funFSRAbU). Accessed: 2016-12-30.
- 1503 8. Thorpe, C.; Hebert, M.H.; Kanade, T.; Shafer, S.A. Vision and navigation for the Carnegie-Mellon Navlab.
 1504 *IEEE Transactions on Pattern Analysis and Machine Intelligence 1988*, 10, 362–373.
- 1505 9. Thrun, S.; Montemerlo, M.; Dahlkamp, H.; Stavens, D.; Aron, A.; Diebel, J.; Fong, P.; Gale, J.; Halpenny,
 1506 M.; Hoffmann, G.; others. Stanley: The robot that won the DARPA Grand Challenge. *Journal of field*
 1507 *Robotics 2006*, 23, 661–692.
- 1508 10. Urmson, C.; Anhalt, J.; Bagnell, D.; Baker, C.; Bittner, R.; Clark, M.N.; Dolan, J.; Duggins, D.; Galatali,
 1509 T.; Geyer, C.; Gittleman, M.; Harbaugh, S.; Hebert, M.; Howard, T.M.; Kolski, S.; Kelly, A.; Likhachev,
 1510 M.; McNaughton, M.; Miller, N.; Peterson, D. Autonomous driving in urban environments: Boss and the
 1511 Urban Challenge. *J. Field Robotics 2008*, 25, 425–466.
- 1512 11. Zhang, R.; Spieser, K.; Frazzoli, E.; Pavone, M. Models , Algorithms , and Evaluation for Autonomous
 1513 Mobility-On-Demand Systems. *American Control Conference 2015*, pp. 2573–2587.
- 1514 12. Google Self-Driving Car Project. <https://www.google.com/selfdrivingcar/>. Accessed: 2017-02-02.
- 1515 13. Tesla Motors: Model S Press Kit. <https://www.tesla.com/presskit/autopilot>. Accessed: 2016-12-30.
- 1516 14. Newton, C. Uber will eventually replace all its drivers with self-driving cars. *The Verge 2014*, 5, 2014.

- 1517 15. Pittsburgh, your Self-Driving Uber is arriving now. [https://newsroom.uber.com/
1518 pittsburgh-self-driving-uber/](https://newsroom.uber.com/pittsburgh-self-driving-uber/). Accessed: 2016-12-30.
- 1519 16. de Graaf, M. PRT Vehicle Architecture and Control in Masdar City. Proceedings of the 13th Int.
1520 Conference on Automated People Movers and Transit Systems, 2011, pp. 339–348.
- 1521 17. Alessandrini, A.; Cattivera, A.; Holguin, C.; Stam, D. CityMobil2: Challenges and Opportunities of Fully
1522 Automated Mobility. In *Road Vehicle Automation*; Springer, 2014; pp. 169–184.
- 1523 18. Eggers, A.; Schwedhelm, H.; Zander, O.; Izquierdo, R.C.; Polanco, J.A.G.; Paralikas, J.; Georgoulas, K.;
1524 Chryssolouris, G.; Seibert, D.; Jacob, C. Virtual testing based type approval procedures for the assessment
1525 of pedestrian protection developed within the EU-Project IMVITER. Proceedings of 23rd Enhanced Safety
1526 of Vehicles (ESV) conference, 2013.
- 1527 19. Makris, S.; Michalos, G.; Efthymiou, K.; Georgoulas, K.; Alexopoulos, K.; Papakostas, N.; Eytan, A.;
1528 Lai, M.; Chryssolouris, G. Flexible assembly technology for highly customisable vehicles. (AMPS 10),
1529 International Conference on Competitive and Sustainable Manufacturing, Products and Services, 2010.
- 1530 20. Buehler, Martin; Iagnemma, Karl; Singh, S., Ed. *The Darpa Urban Challenge Autonomous Vehicle in City
1531 Traffic*; Springer: Berlin, 2009; [arXiv:1011.1669v3].
- 1532 21. Furgale, P.; Schwesinger, U.; Rufli, M.; Derendarz, W.; Grimmert, H.; Muhlfellner, P.; Wonneberger, S.;
1533 Timpner, J.; Rottmann, S.; Li, B.; Schmidt, B.; Nguyen, T.N.; Cardarelli, E.; Cattani, S.; Bruning, S.;
1534 Horstmann, S.; Stellmacher, M.; Mielenz, H.; Koser, K.; Beermann, M.; Hane, C.; Heng, L.; Lee, G.H.;
1535 Fraundorfer, F.; Iser, R.; Triebel, R.; Posner, I.; Newman, P.; Wolf, L.; Pollefeys, M.; Brosig, S.; Effertz, J.;
1536 Pradalier, C.; Siegwart, R. Toward automated driving in cities using close-to-market sensors: An overview
1537 of the V-Charge Project. *IEEE Intelligent Vehicles Symposium, Proceedings* **2013**, pp. 809–816.
- 1538 22. Fisher, A. GOOGLE'S SELF-DRIVING CARS: A QUEST FOR ACCEPTANCE. [http://www.popsoci.com/
1539 cars/article/2013-09/google-self-driving-car](http://www.popsoci.com/cars/article/2013-09/google-self-driving-car), 2013-09-18.
- 1540 23. Asvadi, A.; Premebida, C.; Peixoto, P.; Nunes, U. 3D Lidar-based static and moving obstacle detection
1541 in driving environments: An approach based on voxels and multi-region ground planes. *Robotics and
1542 Autonomous Systems* **2016**, *83*, 299–311.
- 1543 24. Zhao, G.; Xiao, X.; Yuan, J.; Ng, G.W. Fusion of 3D-LIDAR and camera data for scene parsing. *Journal of
1544 Visual Communication and Image Representation* **2014**, *25*, 165–183.
- 1545 25. Moosmann, F.; Pink, O.; Stiller, C. Segmentation of 3D lidar data in non-flat urban environments using a
1546 local convexity criterion. *Intelligent Vehicles Symposium, 2009 IEEE*. IEEE, 2009, pp. 215–220.
- 1547 26. Sack, D.; Burgard, W. A comparison of methods for line extraction from range data. Proc. of the 5th IFAC
1548 symposium on intelligent autonomous vehicles (IAV), 2004, Vol. 33.
- 1549 27. Oliveira, M.; Santos, V.; Sappa, A.D.; Dias, P. Scene Representations for Autonomous Driving: An
1550 Approach Based on Polygonal Primitives. *Robot 2015: Second Iberian Robotics Conference*. Springer,
1551 2016, pp. 503–515.
- 1552 28. Wang, M.; Tseng, Y.H. Incremental segmentation of lidar point clouds with an octree-structured voxel
1553 space. *The Photogrammetric Record* **2011**, *26*, 32–57.
- 1554 29. Vo, A.V.; Truong-Hong, L.; Laefer, D.F.; Bertolotto, M. Octree-based region growing for point cloud
1555 segmentation. *ISPRS Journal of Photogrammetry and Remote Sensing* **2015**, *104*, 88–100.
- 1556 30. Nguyen, A.; Le, B. 3d point cloud segmentation: a survey. 2013 6th IEEE Conference on Robotics,
1557 Automation and Mechatronics (RAM). IEEE, 2013, pp. 225–230.
- 1558 31. Yao, W.; Deng, Z.; Zhou, L. Road curb detection using 3D lidar and integral laser points for intelligent
1559 vehicles. *Soft Computing and Intelligent Systems (SCIS) and 13th International Symposium on Advanced
1560 Intelligent Systems (ISIS)*, 2012 Joint 6th International Conference on. IEEE, 2012, pp. 100–105.
- 1561 32. Chen, X.; Deng, Z. Detection of Road Obstacles Using 3D Lidar Data via Road Plane Fitting. Proceedings
1562 of the 2015 Chinese Intelligent Automation Conference. Springer, 2015, pp. 441–449.
- 1563 33. Yu, Y.; Li, J.; Guan, H.; Wang, C.; Yu, J. Semiautomated extraction of street light poles from mobile LiDAR
1564 point-clouds. *IEEE Transactions on Geoscience and Remote Sensing* **2015**, *53*, 1374–1386.
- 1565 34. Zhou, Y.; Wang, D.; Xie, X.; Ren, Y.; Li, G.; Deng, Y.; Wang, Z. A fast and accurate segmentation method
1566 for ordered LiDAR point cloud of large-scale scenes. *IEEE Geoscience and Remote Sensing Letters* **2014**,
1567 *11*, 1981–1985.
- 1568 35. Rusu, R.B. Semantic 3D object maps for everyday manipulation in human living environments.
1569 *KI-Künstliche Intelligenz* **2010**, *24*, 345–348.

- 1570 36. Ioannou, Y.; Taati, B.; Harrap, R.; Greenspan, M. Difference of normals as a multi-scale operator in
1571 unorganized point clouds. 2012 Second International Conference on 3D Imaging, Modeling, Processing,
1572 Visualization & Transmission. IEEE, 2012, pp. 501–508.
- 1573 37. Hu, X.; Li, X.; Zhang, Y. Fast filtering of LiDAR point cloud in urban areas based on scan line segmentation
1574 and GPU acceleration. *IEEE Geoscience and Remote Sensing Letters* **2013**, *10*, 308–312.
- 1575 38. Vosselman, G. Point cloud segmentation for urban scene classification. *ISPRS Int. Arch. Photogramm.*
1576 *Remote Sens. Spat. Inf. Sci* **2013**.
- 1577 39. Reddy, S.K.; Pal, P.K. Segmentation of point cloud from a 3D LIDAR using range difference between
1578 neighbouring beams. Proceedings of the 2015 Conference on Advances In Robotics. ACM, 2015, p. 55.
- 1579 40. Burgard, W. Techniques for 3D Mapping. *Slides from SLAM Summer school 2009* **2009**.
- 1580 41. Hähnel, D.; Thrun, S. 3D Laser-based obstacle detection for autonomous driving. *Abstract in intelligent*
1581 *Robots and Systems* **2008**.
- 1582 42. Montemerlo, M.; Becker, J.; Bhat, S.; Dahlkamp, H.; Dolgov, D.; Ettinger, S.; Haehnel, D.; Hilden, T.;
1583 Hoffmann, G.; Huhnke, B.; others. Junior: The stanford entry in the urban challenge. *Journal of field*
1584 *Robotics* **2008**, *25*, 569–597.
- 1585 43. Vieira, M.; Shimada, K. Surface mesh segmentation and smooth surface extraction through region
1586 growing. *Computer aided geometric design* **2005**, *22*, 771–792.
- 1587 44. Rabbani, T.; Van Den Heuvel, F.; Vosselmann, G. Segmentation of point clouds using smoothness
1588 constraint. *International Archives of Photogrammetry, Remote Sensing and Spatial Information Sciences* **2006**,
1589 *36*, 248–253.
- 1590 45. Deschaud, J.E.; Goulette, F. A fast and accurate plane detection algorithm for large noisy point clouds
1591 using filtered normals and voxel growing. Proceedings of 3D Processing, Visualization and Transmission
1592 Conference (3DPVT2010), 2010.
- 1593 46. Biosca, J.M.; Lerma, J.L. Unsupervised robust planar segmentation of terrestrial laser scanner point clouds
1594 based on fuzzy clustering methods. *ISPRS Journal of Photogrammetry and Remote Sensing* **2008**, *63*, 84–98.
- 1595 47. Teboul, O.; Simon, L.; Koutsourakis, P.; Paragios, N. Segmentation of building facades using procedural
1596 shape priors. Computer Vision and Pattern Recognition (CVPR), 2010 IEEE Conference on. IEEE, 2010,
1597 pp. 3105–3112.
- 1598 48. Boulaassal, H.; Landes, T.; Grussenmeyer, P.; Tarsha-Kurdi, F.; others. Automatic segmentation of
1599 building facades using terrestrial laser data. *International Archives of Photogrammetry, Remote Sensing and*
1600 *Spatial Information Sciences* **2007**, *36*, W52.
- 1601 49. Broggi, A.; Cattani, S.; Patander, M.; Sabbatelli, M.; Zani, P. A full-3D voxel-based dynamic obstacle
1602 detection for urban scenario using stereo vision. 16th International IEEE Conference on Intelligent
1603 Transportation Systems (ITSC 2013). IEEE, 2013, pp. 71–76.
- 1604 50. Azim, A.; Aycard, O. Layer-based supervised classification of moving objects in outdoor dynamic
1605 environment using 3D laser scanner. 2014 IEEE Intelligent Vehicles Symposium Proceedings. IEEE,
1606 2014, pp. 1408–1414.
- 1607 51. Asvadi, A.; Peixoto, P.; Nunes, U. Two-Stage Static/Dynamic Environment Modeling Using Voxel
1608 Representation. Robot 2015: Second Iberian Robotics Conference. Springer, 2016, pp. 465–476.
- 1609 52. Oniga, F.; Nedeveschi, S. Processing dense stereo data using elevation maps: Road surface, traffic isle, and
1610 obstacle detection. *IEEE Transactions on Vehicular Technology* **2010**, *59*, 1172–1182.
- 1611 53. Vosselman, G.; Gorte, B.G.; Sithole, G.; Rabbani, T. Recognising structure in laser scanner point clouds.
1612 *International archives of photogrammetry, remote sensing and spatial information sciences* **2004**, *46*, 33–38.
- 1613 54. Tarsha-Kurdi, F.; Landes, T.; Grussenmeyer, P.; others. Hough-transform and extended ransac algorithms
1614 for automatic detection of 3d building roof planes from lidar data. Proceedings of the ISPRS Workshop
1615 on Laser Scanning, 2007, Vol. 36, pp. 407–412.
- 1616 55. Rabbani, T.; Van Den Heuvel, F. Efficient hough transform for automatic detection of cylinders in point
1617 clouds. *ISPRS WG III/3, III/4* **2005**, *3*, 60–65.
- 1618 56. Yang, B.; Dong, Z. A shape-based segmentation method for mobile laser scanning point clouds. *ISPRS*
1619 *journal of photogrammetry and remote sensing* **2013**, *81*, 19–30.
- 1620 57. Chang, C.C.; Lin, C.J. LIBSVM: a library for support vector machines. *ACM Transactions on Intelligent*
1621 *Systems and Technology (TIST)* **2011**, *2*, 27.

- 1622 58. Lafferty, J.; McCallum, A.; Pereira, F. Conditional random fields: Probabilistic models for segmenting
1623 and labeling sequence data. Proceedings of the eighteenth international conference on machine learning,
1624 ICML, 2001, Vol. 1, pp. 282–289.
- 1625 59. Golovinskiy, A.; Funkhouser, T. Min-cut based segmentation of point clouds. Computer Vision
1626 Workshops (ICCV Workshops), 2009 IEEE 12th International Conference on. IEEE, 2009, pp. 39–46.
- 1627 60. Golovinskiy, A.; Kim, V.G.; Funkhouser, T. Shape-based recognition of 3D point clouds in urban
1628 environments. 2009 IEEE 12th International Conference on Computer Vision. IEEE, 2009, pp. 2154–2161.
- 1629 61. Riemenschneider, H.; Bódis-Szomorú, A.; Weissenberg, J.; Van Gool, L. Learning where to classify in
1630 multi-view semantic segmentation. European Conference on Computer Vision. Springer, 2014, pp.
1631 516–532.
- 1632 62. Martinovic, A.; Knopp, J.; Riemenschneider, H.; Van Gool, L. 3d all the way: Semantic segmentation
1633 of urban scenes from start to end in 3d. Proceedings of the IEEE Conference on Computer Vision and
1634 Pattern Recognition, 2015, pp. 4456–4465.
- 1635 63. Riegler, G.; Ulusoy, A.O.; Geiger, A. OctNet: Learning Deep 3D Representations at High Resolutions.
1636 *arXiv preprint arXiv:1611.05009* 2016.
- 1637 64. Zhang, J.; Lin, X.; Ning, X. SVM-based classification of segmented airborne LiDAR point clouds in urban
1638 areas. *Remote Sensing* 2013, 5, 3749–3775.
- 1639 65. Maturana, D.; Scherer, S. Voxnet: A 3d convolutional neural network for real-time object recognition.
1640 Intelligent Robots and Systems (IROS), 2015 IEEE/RSJ International Conference on. IEEE, 2015, pp.
1641 922–928.
- 1642 66. Qi, C.R.; Su, H.; Niessner, M.; Dai, A.; Yan, M.; Guibas, L.J. Volumetric and Multi-View CNNs for Object
1643 Classification on 3D Data. *arXiv preprint arXiv:1604.03265* 2016.
- 1644 67. Wu, Z.; Song, S.; Khosla, A.; Yu, F.; Zhang, L.; Tang, X.; Xiao, J. 3d shapenets: A deep representation for
1645 volumetric shapes. Proceedings of the IEEE Conference on Computer Vision and Pattern Recognition,
1646 2015, pp. 1912–1920.
- 1647 68. Hillel, A.B.; Lerner, R.; Levi, D.; Raz, G. Recent progress in road and lane detection: a survey. *Machine*
1648 *Vision and Applications* 2014, 25, 727–745.
- 1649 69. McCall, J.C.; Trivedi, M.M. Video-based lane estimation and tracking for driver assistance: survey, system,
1650 and evaluation. *Intelligent Transportation Systems, IEEE Transactions on* 2006, 7, 20–37.
- 1651 70. Ranft, B.; Stiller, C. The Role of Machine Vision for Intelligent Vehicles. *IEEE Transactions on Intelligent*
1652 *Vehicles* 2016, 1, 8–19.
- 1653 71. Sivaraman, S.; Trivedi, M.M. Looking at Vehicles on the Road: A Survey of Vision-Based Vehicle
1654 Detection, Tracking, and Behavior Analysis. *IEEE Transactions on Intelligent Transportation Systems* 2013,
1655 14, 1773–1795.
- 1656 72. Mukhtar, A.; Xia, L.; Tang, T.B. Vehicle detection techniques for collision avoidance systems: A review.
1657 *IEEE Transactions on Intelligent Transportation Systems* 2015, 16, 2318–2338.
- 1658 73. Dollar, P.; Wojek, C.; Schiele, B.; Perona, P. Pedestrian detection: An evaluation of the state of the art. *IEEE*
1659 *transactions on pattern analysis and machine intelligence* 2012, 34, 743–761.
- 1660 74. Labayrade, R.; Douret, J.; Aubert, D. A multi-model lane detector that handles road singularities.
1661 Intelligent Transportation Systems Conference, 2006. ITSC'06. IEEE. IEEE, 2006, pp. 1143–1148.
- 1662 75. XINXIN, D. TOWARDS SUSTAINABLE AUTONOMOUS VEHICLES. PhD thesis, 2016.
- 1663 76. Nedeveschi, S.; Schmidt, R.; Graf, T.; Danescu, R.; Frentiu, D.; Marita, T.; Oniga, F.; Pocol, C. 3D lane
1664 detection system based on stereovision. Intelligent Transportation Systems, 2004. Proceedings. The 7th
1665 International IEEE Conference on. IEEE, 2004, pp. 161–166.
- 1666 77. Li, Q.; Zheng, N.; Cheng, H. An adaptive approach to lane markings detection. Intelligent Transportation
1667 Systems, 2003. Proceedings. IEEE, 2003, Vol. 1, pp. 510–514.
- 1668 78. Tapia-Espinoza, R.; Torres-Torriti, M. A comparison of gradient versus color and texture analysis for lane
1669 detection and tracking. Robotics Symposium (LARS), 2009 6th Latin American. IEEE, 2009, pp. 1–6.
- 1670 79. Sun, T.Y.; Tsai, S.J.; Chan, V. HSI color model based lane-marking detection. Intelligent Transportation
1671 Systems Conference, 2006. ITSC'06. IEEE. IEEE, 2006, pp. 1168–1172.
- 1672 80. Kim, Z. Robust lane detection and tracking in challenging scenarios. *Intelligent Transportation Systems,*
1673 *IEEE Transactions on* 2008, 9, 16–26.

- 1674 81. Gopalan, R.; Hong, T.; Shneier, M.; Chellappa, R. A learning approach towards detection and tracking of
1675 lane markings. *Intelligent Transportation Systems, IEEE Transactions on* **2012**, *13*, 1088–1098.
- 1676 82. Fritsch, J.; Kuhn, T.; Kummert, F. Monocular road terrain detection by combining visual and spatial
1677 information. *Intelligent Transportation Systems, IEEE Transactions on* **2014**, *15*, 1586–1596.
- 1678 83. Kang, D.J.; Jung, M.H. Road lane segmentation using dynamic programming for active safety vehicles.
1679 *Pattern Recognition Letters* **2003**, *24*, 3177–3185.
- 1680 84. Kum, C.H.; Cho, D.C.; Ra, M.S.; Kim, W.Y. Lane detection system with around view monitoring for
1681 intelligent vehicle. SoC Design Conference (ISOCC), 2013 International. IEEE, 2013, pp. 215–218.
- 1682 85. Cui, G.; Wang, J.; Li, J. Robust multilane detection and tracking in urban scenarios based on LIDAR and
1683 mono-vision. *Image Processing, IET* **2014**, *8*, 269–279.
- 1684 86. Lu, W.; Seignez, E.; Rodriguez, F.S.A.; Reynaud, R. Lane marking based vehicle localization using
1685 particle filter and multi-kernel estimation. Control Automation Robotics & Vision (ICARCV), 2014 13th
1686 International Conference on. IEEE, 2014, pp. 601–606.
- 1687 87. Sivaraman, S.; Trivedi, M.M. Integrated lane and vehicle detection, localization, and tracking: A
1688 synergistic approach. *Intelligent Transportation Systems, IEEE Transactions on* **2013**, *14*, 906–917.
- 1689 88. Du, X.; Tan, K.K. Vision-based approach towards lane line detection and vehicle localization. *Machine*
1690 *Vision and Applications* **2015**, pp. 1–17.
- 1691 89. Du, X.; Tan, K.K.; Htet, K.K.K. Vision-based lane line detection for autonomous vehicle navigation and
1692 guidance. Control Conference (ASCC), 2015 10th Asian. IEEE, 2015, pp. 3139–3143.
- 1693 90. Du, X.; Tan, K.K. Comprehensive and practical vision system for self-driving vehicle lane-level
1694 localization. *IEEE transactions on image processing* **2016**, *25*, 2075–2088.
- 1695 91. Borkar, A.; Hayes, M.; Smith, M.T. A novel lane detection system with efficient ground truth generation.
1696 *Intelligent Transportation Systems, IEEE Transactions on* **2012**, *13*, 365–374.
- 1697 92. Danescu, R.; Nedevschi, S. Probabilistic lane tracking in difficult road scenarios using stereovision.
1698 *Intelligent Transportation Systems, IEEE Transactions on* **2009**, *10*, 272–282.
- 1699 93. Topfer, D.; Spehr, J.; Effertz, J.; Stiller, C. Efficient Road Scene Understanding for Intelligent Vehicles
1700 Using Compositional Hierarchical Models. *Intelligent Transportation Systems, IEEE Transactions on* **2015**,
1701 *16*, 441–451.
- 1702 94. Yoo, H.; Yang, U.; Sohn, K. Gradient-enhancing conversion for illumination-robust lane detection.
1703 *Intelligent Transportation Systems, IEEE Transactions on* **2013**, *14*, 1083–1094.
- 1704 95. López, A.; Serrat, J.; Canero, C.; Lumbreras, F.; Graf, T. Robust lane markings detection and road geometry
1705 computation. *International Journal of Automotive Technology* **2010**, *11*, 395–407.
- 1706 96. Du, X.; Tan, K.K. Autonomous Reverse Parking System Based on Robust Path Generation and Improved
1707 Sliding Mode Control. *Intelligent Transportation Systems, IEEE Transactions on* **2015**, *16*, 1225–1237.
- 1708 97. Labayrade, R.; Douret, J.; Laneur, J.; Chapuis, R. A reliable and robust lane detection system based on
1709 the parallel use of three algorithms for driving safety assistance. *IEICE transactions on information and*
1710 *systems* **2006**, *89*, 2092–2100.
- 1711 98. Wu, S.J.; Chiang, H.H.; Perng, J.W.; Chen, C.J.; Wu, B.F.; Lee, T.T. The heterogeneous systems integration
1712 design and implementation for lane keeping on a vehicle. *Intelligent Transportation Systems, IEEE*
1713 *Transactions on* **2008**, *9*, 246–263.
- 1714 99. Huang, A.S.; Moore, D.; Antone, M.; Olson, E.; Teller, S. Finding multiple lanes in urban road networks
1715 with vision and lidar. *Autonomous Robots* **2009**, *26*, 103–122.
- 1716 100. Ding, D.; Yoo, J.; Jung, J.; Jin, S.; Kwon, S. Various lane marking detection and classification for
1717 vision-based navigation system? Consumer Electronics (ICCE), 2015 IEEE International Conference on.
1718 IEEE, 2015, pp. 491–492.
- 1719 101. Jiang, Y.; Gao, F.; Xu, G. Computer vision-based multiple-lane detection on straight road and in a curve.
1720 Image Analysis and Signal Processing (IASP), 2010 International Conference on. IEEE, 2010, pp. 114–117.
- 1721 102. Jiang, R.; Klette, R.; Vaudrey, T.; Wang, S. New lane model and distance transform for lane detection and
1722 tracking. *Computer Analysis of Images and Patterns*. Springer, 2009, pp. 1044–1052.
- 1723 103. Ruyi, J.; Reinhard, K.; Tobi, V.; Shigang, W. Lane detection and tracking using a new lane model and
1724 distance transform. *Machine vision and applications* **2011**, *22*, 721–737.
- 1725 104. Liu, G.; Worgotter, F.; Markelic, I. Stochastic lane shape estimation using local image descriptors.
1726 *Intelligent Transportation Systems, IEEE Transactions on* **2013**, *14*, 13–21.

- 1727 105. Wang, Y.; Teoh, E.K.; Shen, D. Lane detection and tracking using B-Snake. *Image and Vision computing*
1728 **2004**, *22*, 269–280.
- 1729 106. Sawano, H.; Okada, M. A road extraction method by an active contour model with inertia and differential
1730 features. *IEICE transactions on information and systems* **2006**, *89*, 2257–2267.
- 1731 107. Borkar, A.; Hayes, M.; Smith, M.T. Robust lane detection and tracking with ransac and Kalman filter.
1732 *ICIP*, 2009, pp. 3261–3264.
- 1733 108. Sach, L.T.; Atsuta, K.; Hamamoto, K.; Kondo, S. A robust road profile estimation method for low texture
1734 stereo images. *Image Processing (ICIP), 2009 16th IEEE International Conference on*. IEEE, 2009, pp.
1735 4273–4276.
- 1736 109. Guo, C.; Mita, S.; McAllester, D. Stereovision-based road boundary detection for intelligent vehicles
1737 in challenging scenarios. *Intelligent Robots and Systems, 2009. IROS 2009. IEEE/RSJ International*
1738 *Conference on*. IEEE, 2009, pp. 1723–1728.
- 1739 110. Wedel, A.; Badino, H.; Rabe, C.; Loose, H.; Franke, U.; Cremers, D. B-spline modeling of road surfaces
1740 with an application to free-space estimation. *IEEE Transactions on Intelligent Transportation Systems* **2009**,
1741 *10*, 572–583.
- 1742 111. Ladický, L.; Sturgess, P.; Russell, C.; Sengupta, S.; Bastanlar, Y.; Clocksin, W.; Torr, P.H. Joint optimization
1743 for object class segmentation and dense stereo reconstruction. *International Journal of Computer Vision* **2012**,
1744 *100*, 122–133.
- 1745 112. Mendes, C.C.T.; Frémont, V.; Wolf, D.F. Vision-Based Road Detection using Contextual Blocks. *arXiv*
1746 *preprint arXiv:1509.01122* **2015**.
- 1747 113. Kühnl, T.; Kummert, F.; Fritsch, J. Spatial ray features for real-time ego-lane extraction. 2012 15th
1748 International IEEE Conference on Intelligent Transportation Systems. IEEE, 2012, pp. 288–293.
- 1749 114. Freund, Y.; Schapire, R.E. A decision-theoretic generalization of on-line learning and an application to
1750 boosting. *European conference on computational learning theory*. Springer, 1995, pp. 23–37.
- 1751 115. Vitor, G.B.; Victorino, A.C.; Ferreira, J.V. A probabilistic distribution approach for the classification of
1752 urban roads in complex environments. *Workshop on IEEE International Conference on Robotics and*
1753 *Automation (ICRA)*, 2014.
- 1754 116. Vitor, G.B.; Victorino, A.C.; Ferreira, J.V. Comprehensive performance analysis of road detection
1755 algorithms using the common urban Kitti-road benchmark. 2014 IEEE Intelligent Vehicles Symposium
1756 Proceedings. IEEE, 2014, pp. 19–24.
- 1757 117. Fritsch, J.; Kuehnl, T.; Geiger, A. A New Performance Measure and Evaluation Benchmark for Road
1758 Detection Algorithms. *International Conference on Intelligent Transportation Systems (ITSC)*, 2013.
- 1759 118. Jia, Y.; Shelhamer, E.; Donahue, J.; Karayev, S.; Long, J.; Girshick, R.; Guadarrama, S.; Darrell, T. Caffe:
1760 Convolutional architecture for fast feature embedding. *Proceedings of the 22nd ACM international*
1761 *conference on Multimedia*. ACM, 2014, pp. 675–678.
- 1762 119. Mendes, C.C.T.; Frémont, V.; Wolf, D.F. Exploiting Fully Convolutional Neural Networks for Fast Road
1763 Detection. *Image*, *16*, 16x15x15.
- 1764 120. Brust, C.A.; Sickert, S.; Simon, M.; Rodner, E.; Denzler, J. Convolutional patch networks with spatial prior
1765 for road detection and urban scene understanding. *arXiv preprint arXiv:1502.06344* **2015**.
- 1766 121. Mohan, R. Deep deconvolutional networks for scene parsing. *arXiv preprint arXiv:1411.4101* **2014**.
- 1767 122. Oliveira, G.L.; Burgard, W.; Brox, T. Efficient deep models for monocular road segmentation. *Intelligent*
1768 *Robots and Systems (IROS)*, 2016 IEEE/RSJ International Conference on. IEEE, 2016, pp. 4885–4891.
- 1769 123. Laddha, A.; Kocamaz, M.K.; Navarro-Serment, L.E.; Hebert, M. Map-supervised road detection.
1770 *Intelligent Vehicles Symposium (IV)*, 2016 IEEE. IEEE, 2016, pp. 118–123.
- 1771 124. Uijlings, J.R.; van de Sande, K.E.; Gevers, T.; Smeulders, A.W. Selective search for object recognition.
1772 *International journal of computer vision* **2013**, *104*, 154–171.
- 1773 125. Zitnick, C.L.; Dollár, P. Edge boxes: Locating object proposals from edges. *European Conference on*
1774 *Computer Vision*. Springer, 2014, pp. 391–405.
- 1775 126. Chen, X.; Kundu, K.; Zhang, Z.; Ma, H.; Fidler, S.; Urtasun, R. Monocular 3d object detection for
1776 autonomous driving. *Proceedings of the IEEE Conference on Computer Vision and Pattern Recognition*,
1777 2016, pp. 2147–2156.
- 1778 127. Ren, S.; He, K.; Girshick, R.; Sun, J. Faster R-CNN: Towards real-time object detection with region proposal
1779 networks. *Advances in neural information processing systems*, 2015, pp. 91–99.

- 1780 128. He, K.; Zhang, X.; Ren, S.; Sun, J. Spatial pyramid pooling in deep convolutional networks for visual
1781 recognition. *European Conference on Computer Vision*. Springer, 2014, pp. 346–361.
- 1782 129. Yang, F.; Choi, W.; Lin, Y. Exploit all the layers: Fast and accurate cnn object detector with scale dependent
1783 pooling and cascaded rejection classifiers. *Proceedings of the IEEE Conference on Computer Vision and
1784 Pattern Recognition*, 2016, pp. 2129–2137.
- 1785 130. Cai, Z.; Fan, Q.; Feris, R.S.; Vasconcelos, N. A unified multi-scale deep convolutional neural network for
1786 fast object detection. *European Conference on Computer Vision*. Springer, 2016, pp. 354–370.
- 1787 131. Xiang, Y.; Choi, W.; Lin, Y.; Savarese, S. Subcategory-aware Convolutional Neural Networks for Object
1788 Proposals and Detection. *arXiv preprint arXiv:1604.04693* **2016**.
- 1789 132. Redmon, J.; Divvala, S.; Girshick, R.; Farhadi, A. You only look once: Unified, real-time object detection.
1790 *arXiv preprint arXiv:1506.02640* **2015**.
- 1791 133. Liu, W.; Anguelov, D.; Erhan, D.; Szegedy, C.; Reed, S. SSD: Single Shot MultiBox Detector. *arXiv preprint
1792 arXiv:1512.02325* **2015**.
- 1793 134. Hall, D.L.; Llinas, J. An introduction to multisensor data fusion. *Proceedings of the IEEE* **1997**, *85*, 6–23.
- 1794 135. Schoenberg, J.R.; Nathan, A.; Campbell, M. Segmentation of dense range information in complex urban
1795 scenes. *Intelligent Robots and Systems (IROS), 2010 IEEE/RSJ International Conference on*. IEEE, 2010,
1796 pp. 2033–2038.
- 1797 136. Xiao, L.; Dai, B.; Liu, D.; Hu, T.; Wu, T. CRF based road detection with multi-sensor fusion. 2015 IEEE
1798 Intelligent Vehicles Symposium (IV). IEEE, 2015, pp. 192–198.
- 1799 137. Premebida, C.; Carreira, J.; Batista, J.; Nunes, U. Pedestrian detection combining rgb and dense lidar data.
1800 2014 IEEE/RSJ International Conference on Intelligent Robots and Systems. IEEE, 2014, pp. 4112–4117.
- 1801 138. Felzenszwalb, P.F.; Girshick, R.B.; McAllester, D.; Ramanan, D. Object detection with discriminatively
1802 trained part-based models. *IEEE transactions on pattern analysis and machine intelligence* **2010**, *32*, 1627–1645.
- 1803 139. Premebida, C.; Monteiro, G.; Nunes, U.; Peixoto, P. A lidar and vision-based approach for pedestrian and
1804 vehicle detection and tracking. 2007 IEEE Intelligent Transportation Systems Conference. IEEE, 2007, pp.
1805 1044–1049.
- 1806 140. Premebida, C.; Nunes, U. A multi-target tracking and GMM-classifier for intelligent vehicles. 2006 IEEE
1807 Intelligent Transportation Systems Conference. IEEE, 2006, pp. 313–318.
- 1808 141. Eitel, A.; Springenberg, J.T.; Spinello, L.; Riedmiller, M.; Burgard, W. Multimodal deep learning for robust
1809 rgb-d object recognition. *Intelligent Robots and Systems (IROS), 2015 IEEE/RSJ International Conference
1810 on*. IEEE, 2015, pp. 681–687.
- 1811 142. Schlosser, J.; Chow, C.K.; Kira, Z. Fusing LIDAR and images for pedestrian detection using convolutional
1812 neural networks. 2016 IEEE International Conference on Robotics and Automation (ICRA). IEEE, 2016,
1813 pp. 2198–2205.
- 1814 143. Kelly, A. *Mobile Robotics*; Cambridge University Press: New York, 2013.
- 1815 144. Najjar, M.E.E. A Road-Matching Method for Precise Vehicle Localization Using Belief Theory and Kalman
1816 Filtering". *Autonomous Robots* **19**(2). *Auton. Robots* **2005**, *19*, 173–191.
- 1817 145. Guivant, J.; Katz, R. Global urban localization based on road maps. In *Proc. of IEEE International
1818 Conference on Intelligent Robots and Systems (IROS, 2007)*.
- 1819 146. Bosse, M.; Newman, P.; Leonard, J.; Soika, M.; Feiten, W.; Teller, S. An Atlas Framework for Scalable
1820 Mapping. in *IEEE International Conference on Robotics and Automation*, 2003, pp. 1899–1906.
- 1821 147. Grisetti, G. Improving grid-based slam with rao-blackwellized particle filters by adaptive proposals and
1822 selective resampling. In *Proc. of the IEEE Int. Conf. on Robotics and Automation (ICRA, 2005)*, pp.
1823 2443–2448.
- 1824 148. Thrun, S.; Fox, D.; Burgard, W.; Dellaert, F. Robust Monte Carlo Localization for Mobile Robots, 2001.
- 1825 149. Walter, M.R.; Eustice, R.M.; Leonard, J.J. Exactly sparse extended information filters for feature-based
1826 SLAM. *Proceedings of the IJCAI Workshop on Reasoning with Uncertainty in Robotics* **2001**, *26*, 17–26.
- 1827 150. Murphy, K. Bayesian Map Learning in Dynamic Environments. In *Neural Info. Proc. Systems (NIPS)*.
1828 MIT Press, pp. 1015–1021.
- 1829 151. Grisetti, G.; Stachniss, C.; Burgard, W. Improved techniques for grid mapping with rao-blackwellized
1830 particle filters. *IEEE Transactions on Robotics* **2007**, *23*, 2007.
- 1831 152. Lu, F.; Milios, E. Globally Consistent Range Scan Alignment for Environment Mapping. *AUTONOMOUS
1832 ROBOTS* **1997**, *4*, 333–349.

- 1833 153. Frese, U. Closing a million-landmarks loop. In: Proceedings of the IEEE/RSJ International Conference
1834 on Intelligent Robots and Systems, Beijing. submitted, 2006, pp. 5032–5039.
- 1835 154. Grisetti, G.; Stachniss, C.; Burgard, W. Non-linear constraint network optimization for efficient map
1836 learning. *IEEE Transactions on Intelligent Transportation Systems*, p. 2009.
- 1837 155. Kaess, M.; Ranganathan, A.; Dellaert, F. iSAM: Incremental Smoothing and Mapping. *Robotics, IEEE
1838 Transactions on* **2008**, *24*, 1365–1378.
- 1839 156. Kaess, M.; Johannsson, H.; Roberts, R.; Ila, V.; Leonard, J.; Dellaert, F. iSAM2: Incremental Smoothing and
1840 Mapping Using the Bayes Tree. *Intl. J. of Robotics Research, IJRR* **2012**, *31*, 217–236.
- 1841 157. Kummerle, R.; Grisetti, G.; Strasdat, H.; Konolige, K.; Burgard, W. G2o: A general framework for
1842 graph optimization. Robotics and Automation (ICRA), 2011 IEEE International Conference on, 2011,
1843 pp. 3607–3613.
- 1844 158. Grisetti, G.; Kümmerle, R.; Stachniss, C.; Burgard, W. A Tutorial on Graph-Based SLAM.
- 1845 159. Callmer, J.; Ramos, F.; Nieto, J. Learning to detect loop closure from range data. Proceedings of 2009 IEEE
1846 International Conference on Robotics and Automation, 2009, pp. 15–22.
- 1847 160. Newman, P.; Cole, D.; Ho, K. Outdoor slam using visual appearance and laser ranging. Proceedings of
1848 2006 IEEE International Conference on Robotics and Automation, 2006, p. 1180–1187.
- 1849 161. Sünderhauf, N.; Protzel, P. Switchable Constraints for Robust Pose Graph SLAM. In Proc. of IEEE
1850 International Conference on Intelligent Robots and Systems (IROS, 2012).
- 1851 162. Olson, E.; Agarwal, P. Inference on Networks of Mixtures for Robust Robot Mapping, 2013.
- 1852 163. Latif, Y.; Cadena, C.; Neira, J. Robust loop closing over time. Proc. of Robotics: Science and Systems (RSS,
1853 2012).
- 1854 164. Belongie, S.; Malik, J.; Puzicha, J. Shape Matching and Object Recognition Using Shape Contexts. *IEEE
1855 Transactions on Pattern Analysis and Machine Intelligence* **2001**, *24*, 509–522.
- 1856 165. Steder, B.; Grisetti, G.; Burgard, W. Robust place recognition for 3D range data based on point features.
1857 In Proc. of the IEEE Int. Conf. on Robotics and Automation (ICRA, 2010).
- 1858 166. Huber, D.; Hebert, M. Fully Automatic Registration Of Multiple 3D Data Sets, 2001.
- 1859 167. Magnusson, M.; Andreasson, H.; Nuchter, A.; Lilienthal, A.J. Appearance-based loop detection from 3D
1860 laser data using the normal distributions transform. 2009 IEEE International Conference on Robotics and
1861 Automation, 2009, pp. 23–28.
- 1862 168. Mozos, O.M.; Stachniss, C.; Burgard, W. Supervised Learning of Places from Range Data using AdaBoost.
1863 Proceedings of the 2005 IEEE International Conference on Robotics and Automation, 2005, pp. 1730–1735.
- 1864 169. Óscar Martínez Mozos.; Rottmann, A.; Triebel, R.; Jensfelt, P.; Burgard, W. Supervised semantic labeling of
1865 places using information extracted from sensor data. *Robotics and Autonomous Systems* **2007**, *55*, 391–402.
- 1866 170. Posner, I.; Schroeter, D.; Newman, P. Online generation of scene descriptions in urban environments,
1867 2008.
- 1868 171. Sengupta, S.; Sturgess, P.; Ladický, L.; Torr, P.H.S. Automatic dense visual semantic mapping from
1869 street-level imagery. 2012 IEEE/RSJ International Conference on Intelligent Robots and Systems, 2012,
1870 pp. 857–862.
- 1871 172. Nüchter, A.; Hertzberg, J. Towards semantic maps for mobile robots, 2008.
- 1872 173. Galindo, C.; Saffiotti, A.; Coradeschi, S.; Buschka, P.; Fernandez-Madrigan, J.A.; Gonzalez, J.
1873 Multi-hierarchical semantic maps for mobile robotics. 2005 IEEE/RSJ International Conference on
1874 Intelligent Robots and Systems, 2005, pp. 2278–2283.
- 1875 174. Vasudevan, S.; Siegwart, R. Bayesian space conceptualization and place classification for semantic maps
1876 in mobile robotics, 2008.
- 1877 175. Xie, D.; Todorovic, S.; Zhu, S.C. Inferring Dark Matter and Dark Energy from Videos. 2013 IEEE
1878 International Conference on Computer Vision, 2013, pp. 2224–2231.
- 1879 176. Sukanuma, N.; Uozumi, T. Precise position estimation of autonomous vehicle based on map-matching.
1880 2011 IEEE Intelligent Vehicles Symposium (IV), 2011, pp. 296–301.
- 1881 177. Hentschel, M.; Wagner, B. Autonomous robot navigation based on OpenStreetMap geodata. 13th
1882 International IEEE Conference on Intelligent Transportation Systems, 2010, pp. 1645–1650.
- 1883 178. Wulf, O.; Arras, K.O.; Christensen, H.I.; Wagner, B. 2D Mapping of Cluttered Indoor Environments by
1884 Means of 3D Perception. Institute of Computer Science University of Osnabrück, 2004.

- 1885 179. Levinson, J.; Thrun, S. Robust Vehicle Localization in Urban Environments Using Probabilistic Maps. In
1886 Proceedings of the IEEE International Conference on Robotics and Automation, 2010, pp. 4372–4378.
- 1887 180. Baldwin, I.; Newman, P. Road vehicle localization with 2D push-broom LIDAR and 3D priors. 2012 IEEE
1888 International Conference on Robotics and Automation, 2012, pp. 2611–2617.
- 1889 181. Wulf, O.; Lecking, D.; Wagner, B. Robust Self-Localization in Industrial Environments Based on 3D
1890 Ceiling Structures. 2006 IEEE/RSJ International Conference on Intelligent Robots and Systems, 2006,
1891 pp. 8–8.
- 1892 182. Lecking, D.; Wulf, O.; Wagner, B. Localization in a wide range of industrial environments using
1893 relative 3D ceiling features. 2008 IEEE International Conference on Emerging Technologies and Factory
1894 Automation, 2008, pp. 333–337.
- 1895 183. Ozguner, U.; Acarman, T.; Redmill, K. *Autonomous ground vehicles*; Artech House, 2011.
- 1896 184. Buehler, M.; Iagnemma, K.; Singh, S. *The DARPA urban challenge: autonomous vehicles in city traffic*; Vol. 56,
1897 springer, 2009.
- 1898 185. Montemerlo, M.; Becker, J.; Bhat, S.; Dahlkamp, H.; Dolgov, D.; Ettinger, S.; Haehnel, D.; Hilden, T.;
1899 Hoffmann, G.; Huhnke, B.; others. Junior: The stanford entry in the urban challenge. *Journal of field*
1900 *Robotics* **2008**, *25*, 569–597.
- 1901 186. Bacha, A.; Bauman, C.; Faruque, R.; Fleming, M.; Terwelp, C.; Reinholtz, C.; Hong, D.; Wicks, A.; Alberi,
1902 T.; Anderson, D.; others. Odin: Team victorTango’s entry in the DARPA urban challenge. *Journal of Field*
1903 *Robotics* **2008**, *25*, 467–492.
- 1904 187. Kuwata, Y.; Teo, J.; Fiore, G.; Karaman, S.; Frazzoli, E.; How, J.P. Real-time motion planning with
1905 applications to autonomous urban driving. *IEEE Transactions on Control Systems Technology* **2009**,
1906 *17*, 1105–1118.
- 1907 188. Bohren, J.; Foote, T.; Keller, J.; Kushleyev, A.; Lee, D.; Stewart, A.; Vernaza, P.; Derenick, J.; Spletzer, J.;
1908 Satterfield, B. Little Ben: the Ben Franklin racing team’s entry in the 2007 DARPA urban challenge. *Journal*
1909 *of Field Robotics* **2008**, *25*, 598–614.
- 1910 189. Miller, I.; Campbell, M.; Huttenlocher, D.; Kline, F.R.; Nathan, A.; Lupashin, S.; Catlin, J.; Schimpf,
1911 B.; Moran, P.; Zych, N.; others. Team Cornell’s Skynet: Robust perception and planning in an urban
1912 environment. *Journal of Field Robotics* **2008**, *25*, 493–527.
- 1913 190. Campbell, M.; Egerstedt, M.; How, J.P.; Murray, R.M. Autonomous driving in urban environments:
1914 approaches, lessons and challenges. *Philosophical Transactions of the Royal Society of London A: Mathematical,*
1915 *Physical and Engineering Sciences* **2010**, *368*, 4649–4672.
- 1916 191. Leonard, J.; How, J.; Teller, S.; Berger, M.; Campbell, S.; Fiore, G.; Fletcher, L.; Frazzoli, E.; Huang, A.;
1917 Karaman, S.; others. A perception-driven autonomous urban vehicle. *Journal of Field Robotics* **2008**,
1918 *25*, 727–774.
- 1919 192. Challenge, D.U. “Route Network Definition File (RNDF) and Mission Data File(MDF) formats, 2007.
- 1920 193. Qin, B.; Chong, Z.J.; Bandyopadhyay, T.; Ang, M.H. Metric mapping and topo-metric graph learning of
1921 urban road network. 2013 6th IEEE Conference on Robotics, Automation and Mechatronics (RAM). IEEE,
1922 2013, pp. 119–123.
- 1923 194. Liu, W.; Kim, S.W.; Ang, M.H. Probabilistic road context inference for autonomous vehicles. 2015 IEEE
1924 International Conference on Robotics and Automation (ICRA). IEEE, 2015, pp. 1640–1647.
- 1925 195. Dijkstra, E.W. A note on two problems in connexion with graphs. *Numerische mathematik* **1959**, *1*, 269–271.
- 1926 196. Hart, P.E.; Nilsson, N.J.; Raphael, B. A formal basis for the heuristic determination of minimum cost
1927 paths. *IEEE transactions on Systems Science and Cybernetics* **1968**, *4*, 100–107.
- 1928 197. Bast, H.; Dellinger, D.; Goldberg, A.; Müller-Hannemann, M.; Pajor, T.; Sanders, P.; Wagner, D.; Werneck,
1929 R.F. Route planning in transportation networks. *arXiv preprint arXiv:1504.05140* **2015**.
- 1930 198. Baker, C.R.; Dolan, J.M. Traffic interaction in the urban challenge: Putting boss on its best behavior. 2008
1931 IEEE/RSJ International Conference on Intelligent Robots and Systems. IEEE, 2008, pp. 1752–1758.
- 1932 199. Broggi, A.; Debattisti, S.; Panciroli, M.; Porta, P.P. Moving from analog to digital driving. *Intelligent*
1933 *Vehicles Symposium (IV)*, 2013 IEEE. IEEE, 2013, pp. 1113–1118.
- 1934 200. Furda, A.; Vlacic, L. Towards increased road safety: Real-time decision making for driverless city vehicles.
1935 *Systems, Man and Cybernetics*, 2009. SMC 2009. IEEE International Conference on. IEEE, 2009, pp.
1936 2421–2426.

- 1937 201. Furda, A.; Vlacic, L. Enabling safe autonomous driving in real-world city traffic using multiple criteria
1938 decision making. *IEEE Intelligent Transportation Systems Magazine* **2011**, *3*, 4–17.
- 1939 202. Wongpiromsarn, T.; Karaman, S.; Frazzoli, E. Synthesis of provably correct controllers for autonomous
1940 vehicles in urban environments. 2011 14th International IEEE Conference on Intelligent Transportation
1941 Systems (ITSC). IEEE, 2011, pp. 1168–1173.
- 1942 203. Chaudhari, P.; Wongpiromsarn, T.; Frazzoli, E. Incremental minimum-violation control synthesis for
1943 robots interacting with external agents. 2014 American Control Conference. IEEE, 2014, pp. 1761–1768.
- 1944 204. Castro, L.I.R.; Chaudhari, P.; Tumova, J.; Karaman, S.; Frazzoli, E.; Rus, D. Incremental sampling-based
1945 algorithm for minimum-violation motion planning. 52nd IEEE Conference on Decision and Control.
1946 IEEE, 2013, pp. 3217–3224.
- 1947 205. Latombe, J.C. *Robot motion planning*; Vol. 124, Springer Science & Business Media, 2012.
- 1948 206. Reif, J.H. Complexity of the mover's problem and generalizations. *Foundations of Computer Science*,
1949 1979., 20th Annual Symposium on. IEEE, 1979, pp. 421–427.
- 1950 207. LaValle, S.M. *Planning algorithms*; Cambridge university press, 2006.
- 1951 208. Karaman, S.; Frazzoli, E. Sampling-based algorithms for optimal motion planning. *Int. J. Robotics Research*
1952 **2011**, *30*, 846–894.
- 1953 209. LaValle, S.M.; Kuffner, J.J. Randomized kinodynamic planning. *The International Journal of Robotics*
1954 *Research* **2001**, *20*, 378–400.
- 1955 210. Kavraki, L.; Latombe, J.C. Randomized preprocessing of configuration for fast path planning. *Robotics*
1956 *and Automation*, 1994. Proceedings., 1994 IEEE International Conference on. IEEE, 1994, pp. 2138–2145.
- 1957 211. Xu, W.; Wei, J.; Dolan, J.M.; Zhao, H.; Zha, H. A real-time motion planner with trajectory optimization for
1958 autonomous vehicles. *Robotics and Automation (ICRA)*, 2012 IEEE International Conference on. IEEE,
1959 2012, pp. 2061–2067.
- 1960 212. Wongpiromsarn, T.; Topcu, U.; Murray, R.M. Receding horizon control for temporal logic specifications.
1961 Proceedings of the 13th ACM international conference on Hybrid systems: computation and control.
1962 ACM, 2010, pp. 101–110.
- 1963 213. Tumova, J.; Hall, G.C.; Karaman, S.; Frazzoli, E.; Rus, D. Least-violating control strategy synthesis with
1964 safety rules. Proceedings of the 16th international conference on Hybrid systems: computation and
1965 control. ACM, 2013, pp. 1–10.
- 1966 214. Bandyopadhyay, T.; Won, K.S.; Frazzoli, E.; Hsu, D.; Lee, W.S.; Rus, D. Intention-aware motion planning.
1967 In *Algorithmic Foundations of Robotics X*; Springer, 2013; pp. 475–491.
- 1968 215. Bandyopadhyay, T.; Jie, C.Z.; Hsu, D.; Ang Jr, M.H.; Rus, D.; Frazzoli, E. Intention-aware pedestrian
1969 avoidance. *Experimental Robotics*. Springer, 2013, pp. 963–977.
- 1970 216. Ong, S.C.; Png, S.W.; Hsu, D.; Lee, W.S. Planning under uncertainty for robotic tasks with mixed
1971 observability. *The International Journal of Robotics Research* **2010**, *29*, 1053–1068.
- 1972 217. Kurniawati, H.; Hsu, D.; Lee, W.S. SARSOP: Efficient Point-Based POMDP Planning by Approximating
1973 Optimally Reachable Belief Spaces. *Robotics: Science and Systems*. Zurich, Switzerland, 2008, Vol. 2008.
- 1974 218. Kaelbling, L.P.; Littman, M.L.; Cassandra, A.R. Planning and acting in partially observable stochastic
1975 domains. *Artificial intelligence* **1998**, *101*, 99–134.
- 1976 219. Bai, H.; Hsu, D.; Lee, W.S. Integrated perception and planning in the continuous space: A POMDP
1977 approach. *The International Journal of Robotics Research* **2014**, *33*, 1288–1302.
- 1978 220. Kavraki, L.E.; Svestka, P.; Latombe, J.C.; Overmars, M.H. Probabilistic roadmaps for path planning in
1979 high-dimensional configuration spaces. *IEEE transactions on Robotics and Automation* **1996**, *12*, 566–580.
- 1980 221. LaValle, S.M. Rapidly-exploring random trees: A new tool for path planning **1998**.
- 1981 222. Kuffner, J.J.; LaValle, S.M. RRT-connect: An efficient approach to single-query path planning. *Robotics*
1982 *and Automation*, 2000. Proceedings. ICRA'00. IEEE International Conference on. IEEE, 2000, Vol. 2, pp.
1983 995–1001.
- 1984 223. Urmson, C.; Simmons, R.G. Approaches for heuristically biasing RRT growth. *IROS*, 2003, Vol. 2, pp.
1985 1178–1183.
- 1986 224. Janson, L.; Schmerling, E.; Clark, A.; Pavone, M. Fast marching tree: A fast marching sampling-based
1987 method for optimal motion planning in many dimensions. *The International journal of robotics research*
1988 **2015**, p. 0278364915577958.

- 1989 225. Li, Y.; Littlefield, Z.; Bekris, K.E. Sparse methods for efficient asymptotically optimal kinodynamic
1990 planning. In *Algorithmic Foundations of Robotics XI*; Springer, 2015; pp. 263–282.
- 1991 226. Blackmore, L.; Ono, M.; Williams, B.C. Chance-constrained optimal path planning with obstacles. *IEEE*
1992 *Transactions on Robotics* **2011**, *27*, 1080–1094.
- 1993 227. Huynh, V.A.; Frazzoli, E. Probabilistically-sound and asymptotically-optimal algorithm for stochastic
1994 control with trajectory constraints. 2012 IEEE 51st IEEE Conference on Decision and Control (CDC).
1995 IEEE, 2012, pp. 1486–1493.
- 1996 228. Roy, N.; Burgard, W.; Fox, D.; Thrun, S. Coastal navigation-mobile robot navigation with uncertainty
1997 in dynamic environments. *Robotics and Automation*, 1999. Proceedings. 1999 IEEE International
1998 Conference on. IEEE, 1999, Vol. 1, pp. 35–40.
- 1999 229. Auode, G.S.; Luders, B.D.; Levine, D.S.; How, J.P. Threat-aware path planning in uncertain urban
2000 environments. *Intelligent Robots and Systems (IROS)*, 2010 IEEE/RSJ International Conference on. IEEE,
2001 2010, pp. 6058–6063.
- 2002 230. Luders, B.D.; Auode, G.S.; Joseph, J.M.; Roy, N.; How, J.P. Probabilistically safe avoidance of dynamic
2003 obstacles with uncertain motion patterns **2011**.
- 2004 231. Levinson, J.; Askeland, J.; Becker, J.; Dolson, J.; Held, D.; Kammel, S.; Kolter, J.Z.; Langer, D.; Pink,
2005 O.; Pratt, V.; others. Towards fully autonomous driving: Systems and algorithms. *Intelligent Vehicles*
2006 *Symposium (IV)*, 2011 IEEE. IEEE, 2011, pp. 163–168.
- 2007 232. Van Den Berg, J.; Abbeel, P.; Goldberg, K. LQG-MP: Optimized path planning for robots with motion
2008 uncertainty and imperfect state information. *The International Journal of Robotics Research* **2011**, *30*, 895–913.
- 2009 233. Du Toit, N.E.; Burdick, J.W. Robotic motion planning in dynamic, cluttered, uncertain environments.
2010 *Robotics and Automation (ICRA)*, 2010 IEEE International Conference on. IEEE, 2010, pp. 966–973.
- 2011 234. Ferguson, D.; Howard, T.M.; Likhachev, M. Motion planning in urban environments. *Journal of Field*
2012 *Robotics* **2008**, *25*, 939–960.
- 2013 235. Van Den Berg, J.; Overmars, M. Planning time-minimal safe paths amidst unpredictably moving
2014 obstacles. *The International Journal of Robotics Research* **2008**, *27*, 1274–1294.
- 2015 236. Zucker, M.; Kuffner, J.; Branicky, M. Multipartite RRTs for rapid replanning in dynamic environments.
2016 Proceedings 2007 IEEE International Conference on Robotics and Automation. IEEE, 2007, pp. 1603–1609.
- 2017 237. Fiorini, P.; Shiller, Z. Motion planning in dynamic environments using velocity obstacles. *The International*
2018 *Journal of Robotics Research* **1998**, *17*, 760–772.
- 2019 238. Van den Berg, J.; Lin, M.; Manocha, D. Reciprocal velocity obstacles for real-time multi-agent navigation.
2020 *Robotics and Automation*, 2008. ICRA 2008. IEEE International Conference on. IEEE, 2008, pp. 1928–1935.
- 2021 239. Van Den Berg, J.; Snape, J.; Guy, S.J.; Manocha, D. Reciprocal collision avoidance with
2022 acceleration-velocity obstacles. *Robotics and Automation (ICRA)*, 2011 IEEE International Conference
2023 on. IEEE, 2011, pp. 3475–3482.
- 2024 240. Alonso-Mora, J.; Breitenmoser, A.; Rufli, M.; Beardsley, P.; Siegwart, R. Optimal reciprocal collision
2025 avoidance for multiple non-holonomic robots. In *Distributed Autonomous Robotic Systems*; Springer, 2013;
2026 pp. 203–216.
- 2027 241. Hsu, D.; Kindel, R.; Latombe, J.C.; Rock, S. Randomized kinodynamic motion planning with moving
2028 obstacles. *The International Journal of Robotics Research* **2002**, *21*, 233–255.
- 2029 242. Kant, K.; Zucker, S.W. Toward efficient trajectory planning: The path-velocity decomposition. *The*
2030 *International Journal of Robotics Research* **1986**, *5*, 72–89.
- 2031 243. Liu, W.; Weng, Z.; Chong, Z.; Shen, X.; Pendleton, S.; Qin, B.; Fu, G.M.J.; Ang, M.H. Autonomous
2032 vehicle planning system design under perception limitation in pedestrian environment. *2015 IEEE*
2033 *7th International Conference on Cybernetics and Intelligent Systems (CIS) and IEEE Conference on Robotics,*
2034 *Automation and Mechatronics (RAM)* **2015**, pp. 159–166.
- 2035 244. Karaman, S.; Frazzoli, E. Sampling-based optimal motion planning for non-holonomic dynamical
2036 systems. *Robotics and Automation (ICRA)*, 2013 IEEE International Conference on. IEEE, 2013, pp.
2037 5041–5047.
- 2038 245. Webb, D.J.; van den Berg, J. Kinodynamic RRT*: Asymptotically optimal motion planning for robots with
2039 linear dynamics. *Robotics and Automation (ICRA)*, 2013 IEEE International Conference on. IEEE, 2013,
2040 pp. 5054–5061.

- 2041 246. Schmerling, E.; Janson, L.; Pavone, M. Optimal sampling-based motion planning under differential
2042 constraints: the driftless case. *Robotics and Automation (ICRA), 2015 IEEE International Conference*
2043 *on. IEEE, 2015*, pp. 2368–2375.
- 2044 247. Dubins, L.E. On curves of minimal length with a constraint on average curvature, and with prescribed
2045 initial and terminal positions and tangents. *American Journal of mathematics* **1957**, *79*, 497–516.
- 2046 248. Reeds, J.; Shepp, L. Optimal paths for a car that goes both forwards and backwards. *Pacific Journal of*
2047 *Mathematics* **1990**, *145*, 367–393.
- 2048 249. Jeon, J.H.; Karaman, S.; Frazzoli, E. Optimal sampling-based Feedback Motion Trees among obstacles
2049 for controllable linear systems with linear constraints. *Robotics and Automation (ICRA), 2015 IEEE*
2050 *International Conference on. IEEE, 2015*, pp. 4195–4201.
- 2051 250. Allen, R.E.; Clark, A.A.; Starek, J.A.; Pavone, M. A machine learning approach for real-time reachability
2052 analysis. *Intelligent Robots and Systems (IROS 2014), 2014 IEEE/RSJ International Conference on. IEEE,*
2053 *2014*, pp. 2202–2208.
- 2054 251. Shkolnik, A.; Walter, M.; Tedrake, R. Reachability-guided sampling for planning under differential
2055 constraints. *Robotics and Automation, 2009. ICRA'09. IEEE International Conference on. IEEE, 2009,*
2056 *pp. 2859–2865.*
- 2057 252. Chen, C.; Rickert, M.; Knoll, A. Kinodynamic motion planning with Space-Time Exploration Guided
2058 Heuristic Search for car-like robots in dynamic environments. *Intelligent Robots and Systems (IROS),*
2059 *2015 IEEE/RSJ International Conference on. IEEE, 2015*, pp. 2666–2671.
- 2060 253. Narayanan, V.; Phillips, M.; Likhachev, M. Anytime safe interval path planning for dynamic
2061 environments. *2012 IEEE/RSJ International Conference on Intelligent Robots and Systems. IEEE, 2012,*
2062 *pp. 4708–4715.*
- 2063 254. Gonzalez, J.P.; Dornbush, A.; Likhachev, M. Using state dominance for path planning in dynamic
2064 environments with moving obstacles. *Robotics and Automation (ICRA), 2012 IEEE International*
2065 *Conference on. IEEE, 2012*, pp. 4009–4015.
- 2066 255. Bouraine, S.; Fraichard, T.; Azouaoui, O.; Salhi, H. Passively safe partial motion planning for mobile
2067 robots with limited field-of-views in unknown dynamic environments. *2014 IEEE International*
2068 *Conference on Robotics and Automation (ICRA). IEEE, 2014*, pp. 3576–3582.
- 2069 256. Bruce, J.; Veloso, M. Real-time randomized path planning for robot navigation. *Intelligent Robots and*
2070 *Systems, 2002. IEEE/RSJ International Conference on. IEEE, 2002, Vol. 3*, pp. 2383–2388.
- 2071 257. Ferguson, D.; Kalra, N.; Stentz, A. Replanning with rrts. *Proceedings 2006 IEEE International Conference*
2072 *on Robotics and Automation, 2006. ICRA 2006. IEEE, 2006*, pp. 1243–1248.
- 2073 258. Otte, M.; Frazzoli, E. $\{\mathrm{RRT}^{\mathrm{X}}\}$: Real-Time Motion Planning/Replanning for Environments
2074 with Unpredictable Obstacles. In *Algorithmic Foundations of Robotics XI*; Springer, 2015; pp. 461–478.
- 2075 259. Pendleton, S.; Uthacharoenpong, T.; Chong, Z.J.; Ming, G.; Fu, J.; Qin, B.; Liu, W.; Shen, X.; Weng, Z.;
2076 Kamin, C.; Ang, M.A.; Kuwae, L.T.; Marczuk, K.A.; Andersen, H.; Feng, M.; Butron, G.; Chong, Z.Z.;
2077 Ang, M.H.; Frazzoli, E.; Rus, D. Autonomous Golf Cars for Public Trial of Mobility-on-Demand Service.
2078 *IEEE/RSJ International Conference on Intelligent Robots and Systems (IROS), 2015*, pp. 1164–1171.
- 2079 260. Martinez-Gomez, L.; Fraichard, T. Benchmarking Collision Avoidance Schemes for Dynamic
2080 Environments. *ICRA Workshop on Safe Navigation in Open and Dynamic Environments, 2009.*
- 2081 261. Martinez-Gomez, L.; Fraichard, T. Collision avoidance in dynamic environments: an ics-based solution
2082 and its comparative evaluation. *Robotics and Automation, 2009. ICRA'09. IEEE International Conference*
2083 *on. IEEE, 2009*, pp. 100–105.
- 2084 262. Large, F.; Laugier, C.; Shiller, Z. Navigation among moving obstacles using the NLVO: Principles and
2085 applications to intelligent vehicles. *Autonomous Robots* **2005**, *19*, 159–171.
- 2086 263. Seder, M.; Petrovic, I. Dynamic window based approach to mobile robot motion control in the presence of
2087 moving obstacles. *Proceedings 2007 IEEE International Conference on Robotics and Automation. IEEE,*
2088 *2007*, pp. 1986–1991.
- 2089 264. Mayne, D.Q. Model predictive control: Recent developments and future promise. *Automatica* **2014**,
2090 *50*, 2967–2986.
- 2091 265. Hrovat, D.; Di Cairano, S.; Tseng, H.; Kolmanovsky, I. The development of Model Predictive Control
2092 in automotive industry: A survey. *2012 IEEE International Conference on Control Applications* **2012**, pp.
2093 295–302.

- 2094 266. Borrelli, F.; Bemporad, A.; Fodor, M.; Hrovat, D. An MPC/hybrid system approach to traction control.
2095 *IEEE Transactions on Control Systems Technology* **2006**, *14*, 541–552.
- 2096 267. Falcone, P.; Borrelli, F. A model predictive control approach for combined braking and steering in
2097 autonomous vehicles. *Proceedings of the IEEE 2007 Mediterranean Conference on Control & Automation*
2098 *(MED'07)* **2007**, pp. 1–6.
- 2099 268. Falcone, P.; Borrelli, F.; Asgari, J.; Tseng, H.E.; Hrovat, D. Predictive Active Steering Control for
2100 Autonomous Vehicle Systems. *Control* **2007**, *15*, 566–580.
- 2101 269. Liu, C.; Carvalho, A.; Schildbach, G.; Hedrick, J.K. Stochastic Predictive Control for Lane Keeping
2102 Assistance Systems Using A Linear Time-Varying Model **2015**. pp. 3355–3360.
- 2103 270. Salazar, M.; Alessandretti, A.; Aguiar, A.P.; Jones, C.N. An Energy Efficient Trajectory Tracking Control
2104 of Car-like Vehicles **2015**. *1*, 3675–3680.
- 2105 271. Faulwasser, T.; Findeisen, R. Nonlinear Model Predictive Control for Constrained Output Path Following.
2106 *IEEE Transactions on Automatic Control* **2015**, *9286*, 1–1, [[1502.02468](#)].
- 2107 272. Raffo, G.; Gomes, G.; Normey-Rico, J.; Kelber, C.; Becker, L. A Predictive Controller for Autonomous
2108 Vehicle Path Tracking. *IEEE Transactions on Intelligent Transportation Systems* **2009**, *10*, 92–102.
- 2109 273. Howard, T.M.; Green, C.; Kelly, A. Receding horizon model-predictive control for mobile robot navigation
2110 of intricate paths. *Proceedings of the 7th International Conferences on Field and Service Robotics* **2010**, pp. 69–78.
- 2111 274. Berntorp, K.; Magnusson, F. Hierarchical predictive control for ground-vehicle maneuvering. *Proceedings*
2112 *of the American Control Conference* **2015**, 2015-July, 2771–2776.
- 2113 275. Verschuere, R.; Bruyne, S.D.; Zanon, M.; Janick, V.F.; Moritz, D. Towards Time-Optimal Race Car Driving
2114 using Nonlinear MPC in Real-Time. *Scl.Hanyang.Ac.Kr* **2014**, pp. 2505–2510.
- 2115 276. Hespanha, J.P. Trajectory-tracking and path-following of underactuated autonomous vehicles with
2116 parametric modeling uncertainty. *Automatic Control, IEEE Transactions on* **2007**, *52*, 1362–1379.
- 2117 277. Kunz, T.; Stilman, M. Time-Optimal Trajectory Generation for Path Following with Bounded Acceleration
2118 and Velocity. *MIT Press* **2013**.
- 2119 278. Talvala, K.L.R.; Kritayakirana, K.; Gerdes, J.C. Pushing the limits: From lanekeeping to autonomous
2120 racing. *Annual Reviews in Control* **2011**, *35*, 137–148.
- 2121 279. Funke, J.; Brown, M.; Erlien, S.M.; Gerdes, J.C. Prioritizing collision avoidance and vehicle stabilization
2122 for autonomous vehicles. *IEEE Intelligent Vehicles Symposium, Proceedings* **2015**, 2015-August, 1134–1139.
- 2123 280. Erlien, S.M.; Funke, J.; Gerdes, J.C. Incorporating non-linear tire dynamics into a convex approach to
2124 shared steering control. *Proceedings of the American Control Conference* **2014**, pp. 3468–3473.
- 2125 281. Subosits, J.; Gerdes, J.C. Autonomous vehicle control for emergency maneuvers: The effect of topography.
2126 *Proceedings of the American Control Conference* **2015**, 2015-July, 1405–1410.
- 2127 282. Park, M.W.; Lee, S.W.; Han, W.Y. Development of Lateral Control System for Autonomous Vehicle Based
2128 on Adaptive Pure Pursuit Algorithm. *International Conference on Control, Automation and Systems*,
2129 2014, number 14th, pp. 1443–1447.
- 2130 283. Wit, J.S.. Vector Pursuit Path Tracking for Autonomous Ground Vehicles. PhD thesis, University of
2131 Florida, 2000.
- 2132 284. Campbell, S.F. Steering Control of an Autonomous Ground Vehicle with Application to the DARPA Urban
2133 Challenge. PhD thesis, Massachusetts Institute of Technology, 2005.
- 2134 285. Kuwata, Y.; Teo, J.; Karaman, S. Motion planning in complex environments using closed-loop prediction.
2135 *Proc. AIAA Guidance, ...* **2008**.
- 2136 286. Ollero, A.; Heredia, G.; Mercedes, A.R. Stability analysis of mobile robot path tracking. *IEEE/RSJ*
2137 *International Conference on Intelligent Robots and Systems (IROS)*, 1995, Vol. 3, pp. 461–466.
- 2138 287. Hoffmann, G.M.; Tomlin, C.J.; Montemerlo, M.; Thrun, S. Autonomous automobile trajectory tracking
2139 for off-road driving: Controller design, experimental validation and racing. *Proceedings of the American*
2140 *Control Conference* **2007**, pp. 2296–2301.
- 2141 288. Snider, J.M. Automatic Steering Methods for Autonomous Automobile Path Tracking. Technical report,
2142 2009.
- 2143 289. De Luca, A.; Oriolo, G.; Samson, C. Feedback Control of a Nonholonomic Car-like Robot. In *Robot Motion*
2144 *Planning and Control*; Laumond, J.P., Ed.; Springer, 1998; chapter 4, pp. 171–253.
- 2145 290. Murray, R.; Sastry, S. Steering nonholonomic systems in chained form. [1991] *Proceedings of the 30th IEEE*
2146 *Conference on Decision and Control* **1991**, pp. 1121–1126.

- 2147 291. Kim, E.; Kim, J.; Sunwoo, M. Model predictive control strategy for smooth path tracking of
2148 autonomous vehicles with steering actuator dynamics. *International Journal of Automotive Technology* **2014**,
2149 *15*, 1155–1164.
- 2150 292. Falcone, P.; Borrelli, F.; Tseng, H.E.; Asgari, J.; Hrovat, D. Linear time-varying model predictive control
2151 and its application to active steering systems: Stability analysis and experimental validation. *International*
2152 *Journal of Robust and Nonlinear Control* **2008**, *18*, 862–875.
- 2153 293. Gerla, M.; Kleinrock, L. Vehicular networks and the future of the mobile internet. *Computer Networks*
2154 **2011**, *55*, 457–469.
- 2155 294. Kim, S.W.; Chong, Z.J.; Qin, B.; Shen, X.; Cheng, Z.; Liu, W.; Ang, M.H. Cooperative perception for
2156 autonomous vehicle control on the road: Motivation and experimental results. Intelligent Robots and
2157 Systems (IROS), 2013 IEEE/RSJ International Conference on. IEEE, 2013, pp. 5059–5066.
- 2158 295. Kim, S.W.; Qin, B.; Chong, Z.J.; Shen, X.; Liu, W.; Ang, M.H.; Frazzoli, E.; Rus, D. Multivehicle
2159 Cooperative Driving Using Cooperative Perception: Design and Experimental Validation. *Intelligent*
2160 *Transportation Systems, IEEE Transactions on* **2015**, *16*, 663–680.
- 2161 296. Shen, X.; Chong, Z.; Pendleton, S.; James Fu, G.; Qin, B.; Frazzoli, E.; Ang, MarceloH., J. Teleoperation of
2162 On-Road Vehicles via Immersive Telepresence Using Off-the-shelf Components. In *Intelligent Autonomous*
2163 *Systems 13*; Springer International Publishing, 2016; Vol. 302, *Advances in Intelligent Systems and Computing*,
2164 pp. 1419–1433.
- 2165 297. Tachet, R.; Santi, P.; Sobolevsky, S.; Reyes-Castro, L.I.; Frazzoli, E.; Helbing, D.; Ratti, C. Revisiting street
2166 intersections using slot-based systems. *PLoS one* **2016**, *11*, e0149607.
- 2167 298. Knuth, J.; Barooah, P. Distributed collaborative localization of multiple vehicles from relative pose
2168 measurements. Communication, Control, and Computing, 2009. Allerton 2009. 47th Annual Allerton
2169 Conference on. IEEE, 2009, pp. 314–321.
- 2170 299. Rekleitis, I.M.; Dudek, G.; Milios, E.E. Multi-robot cooperative localization: a study of trade-offs between
2171 efficiency and accuracy. Intelligent Robots and Systems, 2002. IEEE/RSJ International Conference on.
2172 IEEE, 2002, Vol. 3, pp. 2690–2695.
- 2173 300. Madhavan, R.; Fregene, K.; Parker, L.E. Distributed heterogeneous outdoor multi-robot localization.
2174 Robotics and Automation, 2002. Proceedings. ICRA'02. IEEE International Conference on. IEEE, 2002,
2175 Vol. 1, pp. 374–381.
- 2176 301. Fox, D.; Burgard, W.; Kruppa, H.; Thrun, S. Collaborative multi-robot localization. In *Mustererkennung*
2177 *1999*; Springer, 1999; pp. 15–26.
- 2178 302. Martinelli, A.; Pont, F.; Siegwart, R. Multi-Robot Localization Using Relative Observations. Robotics
2179 and Automation, 2005. ICRA 2005. Proceedings of the 2005 IEEE International Conference on, 2005, pp.
2180 2797–2802.
- 2181 303. Fox, D.; Burgard, W.; Kruppa, H.; Thrun, S. A probabilistic approach to collaborative multi-robot
2182 localization. *Autonomous robots* **2000**, *8*, 325–344.
- 2183 304. Walls, J.; Cunningham, A.; Eustice, R. Cooperative localization by factor composition over a faulty
2184 low-bandwidth communication channel. Robotics and Automation (ICRA), 2015 IEEE International
2185 Conference on, 2015, pp. 401–408.
- 2186 305. Webster, S.; Walls, J.; Whitcomb, L.; Eustice, R. Decentralized Extended Information Filter for
2187 Single-Beacon Cooperative Acoustic Navigation: Theory and Experiments. *Robotics, IEEE Transactions*
2188 *on* **2013**, *29*, 957–974.
- 2189 306. Paull, L.; Seto, M.; Leonard, J. Decentralized cooperative trajectory estimation for autonomous
2190 underwater vehicles. Intelligent Robots and Systems (IROS 2014), 2014 IEEE/RSJ International
2191 Conference on, 2014, pp. 184–191.
- 2192 307. Li, H.; Nashashibi, F. Multi-vehicle cooperative localization using indirect vehicle-to-vehicle relative pose
2193 estimation. Vehicular Electronics and Safety (ICVES), 2012 IEEE International Conference on, 2012, pp.
2194 267–272.
- 2195 308. Shen, X.; Pendleton, S.; Ang, M.H. Efficient L-shape fitting of laser scanner data for vehicle pose
2196 estimation. 2015 IEEE 7th International Conference on Cybernetics and Intelligent Systems (CIS) and
2197 IEEE Conference on Robotics, Automation and Mechatronics (RAM). IEEE, 2015, pp. 173–178.
- 2198 309. Shen, X.; Pendleton, S.; Ang Jr, M.H. Scalable Cooperative Localization with Minimal Sensor
2199 Configuration. In *Distributed Autonomous Robotic Systems*; Springer, 2016; pp. 89–104.

- 2200 310. Switkes, J.P.; Gerdes, J.C.; Berdichevsky, G.; Berdichevsky, E. Systems and Methods for Semi-Autonomous
2201 Vehicular Convoys, 2012. US Patent App. 13/542,622.
- 2202 311. Durrant-Whyte, H. A Beginner's Guide to Decentralised Data Fusion. *Technical Document of Australian*
2203 *Centre for Field Robotics, University of Sydney, Australia* **2000**, pp. 1–27.
- 2204 312. Leung, K.; Barfoot, T.; Liu, H. Decentralized Localization of Sparsely-Communicating Robot Networks:
2205 A Centralized-Equivalent Approach. *Robotics, IEEE Transactions on* **2010**, *26*, 62–77.
- 2206 313. Li, H.; Nashashibi, F. Cooperative Multi-Vehicle Localization Using Split Covariance Intersection Filter.
2207 *Intelligent Transportation Systems Magazine, IEEE* **2013**, *5*, 33–44.
- 2208 314. Shen, X.; Andersen, H.; Leong, W.; Kong, H.; Jr., M.H.A.; Rus, D. A General Framework for Multi-vehicle
2209 Cooperative Localization Using Pose Graph. *Intelligent Transportation Systems, IEEE Transactions on*.
2210 submitted.
- 2211 315. Clark, C.M.; Rock, S.M.; Latombe, J.C. Motion planning for multiple mobile robots using dynamic
2212 networks. *Robotics and Automation, 2003. Proceedings. ICRA'03. IEEE International Conference on*.
2213 *IEEE, 2003, Vol. 3, pp. 4222–4227.*
- 2214 316. Bennewitz, M.; Burgard, W.; Thrun, S. Optimizing schedules for prioritized path planning of multi-robot
2215 systems. *Robotics and Automation, 2001. Proceedings 2001 ICRA. IEEE International Conference on*.
2216 *IEEE, 2001, Vol. 1, pp. 271–276.*
- 2217 317. Van Den Berg, J.P.; Overmars, M.H. Prioritized motion planning for multiple robots. *Intelligent Robots*
2218 *and Systems, 2005.(IROS 2005). 2005 IEEE/RSJ International Conference on. IEEE, 2005, pp. 430–435.*
- 2219 318. Velagapudi, P.; Sycara, K.; Scerri, P. Decentralized prioritized planning in large multirobot teams.
2220 *Intelligent Robots and Systems (IROS), 2010 IEEE/RSJ International Conference on. IEEE, 2010, pp.*
2221 *4603–4609.*
- 2222 319. LaValle, S.M.; Hutchinson, S.A. Optimal motion planning for multiple robots having independent goals.
2223 *Robotics and Automation, IEEE Transactions on* **1998**, *14*, 912–925.
- 2224 320. Guo, Y.; Parker, L.E. A distributed and optimal motion planning approach for multiple mobile robots.
2225 *Robotics and Automation, 2002. Proceedings. ICRA'02. IEEE International Conference on. IEEE, 2002,*
2226 *Vol. 3, pp. 2612–2619.*
- 2227 321. Shen, X.; Chong, Z.J.; Pendleton, S.; Liu, W.; Qin, B.; Fu, G.M.J.; Ang, M.H. Multi-vehicle motion
2228 coordination using v2v communication. *2015 IEEE Intelligent Vehicles Symposium (IV). IEEE, 2015,*
2229 *pp. 1334–1341.*

2230 © 2017 by the authors. Submitted to *Machines* for possible open access publication
2231 under the terms and conditions of the Creative Commons Attribution (CC-BY) license
2232 (<http://creativecommons.org/licenses/by/4.0/>).